From soil to water

Assessing the effect of soil diversity on the hydrology of a complex landscape, a case study in Gordon Gulch Valley, Colorado Front Range of the Rocky Mountains.

Sanne Diek
February, 2013

From soil to water
Assessing the effect of soil diversity on the hydrology of a complex landscape, a case study in Gordon Gulch Valley, Colorado Front Range of the Rocky Mountains.

MSc Thesis

Sanne Diek

Master's thesis submitted to Wageningen University in partial fulfilment of the Master of Science: Earth and Environment, specialisation Soil Geography and Landscape

Wageningen, January 2013

Sanne Diek
sanne.diek@wur.nl
880304 181 120

Supervisor
dr. ir. A.J.A.M. (Arnaud) Temme
Soil Geography and Landscape Group
Wageningen University, Netherlands

dr. ir. A.J. (Ryan) Teuling
Hydrology and Quantitative Water Management Group
Wageningen University, Netherlands

Acknowledgements

Although I'm the author of this thesis, several people helped me the last eight months in finishing this thesis successfully:

Arnaud Temme for the many hours in the INSTAAR lab, for his feedback, for sharing his apartment for a month, for the fieldwork in Gordon Gulch, for digging the soil pits, for keeping me motivated, for the valuable discussions, for showing us around in Boulder, and for taking us to the FOP trip.

Ryan Teuling for his valuable hydrological and general feedback, for becoming my second supervisor, and for his enthusiasm.

Joost Iwema for helping me with R, and for writing a script to run SWAP.

Jos van Dam for introducing me to the basics of SWAP, and for helping me to start up with SWAP.

Suzanne Anderson for the warm welcome, and for arranging all our wishes for the fieldwork.

Greg Tucker for the warm welcome at the campus, for letting us join the CZO seminar, and for using his office on our days at the campus.

Eric Perish for all my questions related to the CZO website.

Albert Kettner for arranging that I could use the lab during the weekend.

Wendy Roth for letting us use the INSTAAR lab.

Martijn Schwering for the fieldwork in Gordon Gulch, and for being my traveling companion for two months.

David Dethier for sharing his data.

Eve Hinckley for sharing her data.

Abigail Langston for sharing her data.

Melissa Foster for joining us during a fieldwork day.

Harm Bartholomeus for providing me a way to calculate LAI.

Paul Torfs for all valuable comments related to R, and for being the R oracle for Joost.

Jo Kolk Studiefonds for the financial support for my trip to Boulder.

Table of contents

1. Introduction 1
1.1 Background 1
1.2 Objectives and research questions 2
1.3 Outline 2
2 Study area 3
2.1 Topographic setting 3
2.2 Landscape characteristics 4
2.3 Geology, geomorphology and pedology 5
2.4 Land use 5
2.5 Climate 5
3 Methods and Materials 7
3.1 Methods 7
3.2 Materials 18
4 Results 21
4.1 Landscape characteristics 21
4.2 Soil characteristics 28
4.3 Hydrological analysis 36
5 Discussion 51
5.1 Soil properties 51
5.2 Hydrological properties 53
5.3 A complex landscape 56
6 Conclusion 63
7 References 65

Appendix A – Hydraulic properties I
Appendix B – SWAP input V
Appendix C – Cross tables field characteristics VII
Appendix D – Cross tables soil properties IX
Appendix E – Hydrological processes XIII
Appendix F – Discharge XXI
Appendix X – References XXIII

List of figures

Figure 1: Schematic representation of the topography of the Front Range 3
Figure 2: Study area - Gordon Gulch Valley 4
Figure 3: Daily maximum and minimum temperatures and average precipitation and snowfall. 6
Figure 4: General methodological overview 8
Figure 5: Main window of the user-interface of rosetta 13
Figure 6: Comparison between the measured snow depth data of the CZO and the modelled data used as input for swap. 15
Figure 7: Landscape characteristics 21
Figure 8: Profile graph of the Gordon Gulch Valley 22
Figure 9: Maps of the landscape characteristics of the study area 26
Figure 10: Field observations 28
Figure 11: Maps of a selection of soil properties 32
Figure 12: Schematic overview of the most important hydrological processes. 36
Figure 13: Boxplots of the monthly evolution of the hydrological fluxes. 40
Figure 14: Boxplot for each characterising area of the three-year total of the hydrological characteristics. 44
Figure 15: Monthly evolution of the hydrological characteristics for each characterising area. 46
Figure 16: Hydrological properties of the Gordon Gulch Valley. 53
Figure 17: Measured discharge data compared to the net bottom outflux. 53
Figure 18: Measured discharge data compared to the precipitation input (rain and snowmelt). 54
Figure 19: Change of water storage in soil profile for three accumulation positions. 56
Figure 20: Location of the transect of the CZO and the corresponding fieldpoints from our dataset used as subset to compare our data to the data of the CZO. 58
Figure 21: Hydrological properties of a subset of the field points, corresponding to the location of the CZO transect, compared to the hydrological properties of the whole area subdivided into the five characterising areas. 60

List of Tables

Table 1: Landscape characteristics of the study area 5
Table 2: Field work - landscape characteristics 9
Table 3: Field work - soil and horizon properties 10
Table 4: Landscape characteristics derived from available data 17
Table 5: Field and laboratory equipment 18
Table 6: Input data 19
Table 7: Site characteristics for all characterising areas 25
Table 8: Summary of the continuous soil properties 29
Table 9: Summary of the categorical soil properties 29
Table 10: Soil properties per horizon 30
Table 11: Categorical soil properties per horizon 31
Table 12: Soil properties, differences between the five characterising areas 33
Table 13: Categorical soil properties of the top horizons, differences between the five characterising areas 34
Table 14: Hydrological processes (summary of appendix E) 37
Table 15: Hydrological properties per month for all locations. 39
Table 16: Hydrological properties, cumulative for the whole simulation period (Nov-2009 till Sep-2012) 43
Table 17: Soil properties of the horizons and general soil properties, differences between the north and south facing slopes 56
Table 18: Categorical soil properties of the top horizon, differences between the north and south facing slopes 57

Introduction 1.

1.1 Background

When considering that 26% of the world's population lives within the mountains or at the foothills of the mountains (Meybeck et al., 2001), that mountain-based resources indirectly provides sustenance for more than half of the world's population and moreover, that 40% of the global population lives in the watersheds of rivers originating in the planet's different mountain ranges (Beniston, 2006), the mountain areas become interesting study areas. According to Van Tol et al. (2011) the demand of water doubles every 20 years, which is more than twice the rate of the world's population growth.

Specific for the Colorado Mountain Range the water supply is limited, because of its semi-arid environment (Murphy, 2006). In these areas snowmelt in the spring is the major hydrological event and is critical for recharging soil moisture reserves, for vegetation and for feeding stream networks (Hinckley et al., 2012). Lower elevation systems - which are located at the rain-snow transition and where snowpacks can be intermittent in winter and spring - are especially sensitive to climate shifts in this context (Hinckley et al., 2012). Climate shifts, resulting in altered precipitation patterns and increasing temperatures could change the snowpack, the amount and timing of the snow accumulation and the melt water inputs and subsequently the hydrological response of the area. Hinckley et al. (2012) mention that this can result in higher risks of prolonged droughts and secondary effects, for example fire risks.

The seasonal variability of water supply and the demand for year-round water availability calls for protection and management of surface and groundwater resources, which requires accurate analysis of hydrological processes (van Tol et al., 2011). This analysis includes the identification, definition and quantification of the pathways, connectivities, thresholds and residence times of components of the various water bodies, and the residence flow of water through the landscape (van Tol et al., 2011). However, hydrological methodologies to estimate these processes are expensive and time consuming (Wösten et al., 2001; Pachepsky et al., 2006; van Tol et al., 2011).

Soils play a key role in hydrology (Terribile et al., 2011; van Tol et al., 2011), because of the integration of their soil forming (environmental) factors, (i) climate, (ii) organisms, (iii) topography, (iv) parent material, (v) time, and (vi) human influence (Jenny, 1941; Völkel et al., 2011). In this way the soils reflect the catchment's geology, topography, and vegetation and subsequently the hydrological response of a catchment.
Soils are especially important indicators of, and more importantly, can even control the partitioning of the hydrological flow paths (including infiltration and runoff), residence time distributions, water storage, filtering, and furthermore the physical and chemical support to vegetation (Soulsby et al., 2006; van Tol et al., 2010). Furthermore, soil properties are relatively easy to measure in contrast to hydrological characteristics.

This integral understanding of complex landscapes fits perfectly into the present research executed as part of the Critical Zone Observatory (CZO). The CZO research focusses on increasing the understanding of the integration and coupling of processes operating and shaping the Earth's surface dynamic environment (Anderson et al., 2008). One strategy to reach this goal is to look at environmental gradients. One of these gradients is the Boulder Creek CZO which covers the gradient from the Continental Divide to the foot of the Rocky Mountains. The overarching goal of the Boulder Creek CZO is to understand how erosion and weathering processes form the dynamics of the Critical Zone and how these different dynamics control the biological and hydrological function of the Critical Zone (Anderson et al., 2008). This research contributes to this goal.

1.2 Objectives and research questions

This study aims to provide information about hydrological characteristics based on relatively easy to measure soil properties, resulting in the following objective:

To determine how relatively easy to measure soil properties and their variation over space can be used to determine hydrological characteristics in a mountainous watershed.

This objective can be reached by finding an answer to the following research questions:

(i) Which soil properties influence hydrological characteristics?
(ii) What are the soil properties and landscape characteristics of the Gordon Gulch Valley?
(iii) How do these soil properties relate to the landscape characteristics in the Gordon Gulch Valley?
(iv) What are the current hydrological characteristics of the Gordon Gulch Valley?
(v) How do these hydrological characteristics relate to the landscape characteristics in the Gordon Gulch Valley?

1.3 Outline

Chapter 2 will describe the study area (Gordon Gulch Valley, located in the Front Range of the Rocky Mountains, Colorado) more in depth. Chapter 3 will clarify the used methodology for this research and the used materials. In chapter 4 the results will be described. These will be explained and discussed in chapter 5 and concluded in chapter 6.

Study area 2.

2.1 Topographic setting

The Gordon Gulch Valley is located in the upper montane zone of the Front Range. The Front Range is a range of roughly 50 km wide and is characterised by the Flatirons in the East and the Continental Divide in the West (Figure 1 shows a schematic representation of the Front Range). In the East, the Front Range is bordered by the Great Plains, a flat floor at around 1500 m. Here, a number of low-gradient smooth surfaces (pediments, pediments buried by alluvium, and more narrow fingers of alluvium) protruded from the Front Range (Anderson et al., 2006). From the Great Plains, the range starts with the Flatirons and rises abruptly by 800 m. The surface between the Flatirons and the spine of the range is characterised by a rolling surface (2300-3000 m) and is called the subsummit surface or the Rocky Mountain surface. The spine of the range is only a few kilometres wide, here the topography rises another 1000 m, this is called the Continental Divide.

Several rivers drain the Front Range, flowing through it in an easterly or north-easterly direction (Birkeland et al., 2003). To the south is Coal Creek, this river heads 28 km east of the Continental Divide. Its headwaters were never glaciated. North of Coal Creek is Boulder Creek with several tributaries (the North, Middle and South Boulder Creek). Boulder Creek heads just east from the Continental Divide. Its headwaters were extensively glaciated during the Pleistocene. To the north is Left Hand Creek, just like Boulder Creek the heads are located just east form the Continental Divide and its headwaters were glaciated during the Pleistocene. The canyons of these rivers are steep-sided (Birkeland et al., 2003), are (from east to west) at first quite narrow and steep, into the subsummit surface the rivers are less deeply incised, above the end moraines from the glaciers the profile of the canyons is characterised by major steps and flats (Anderson et al., 2006).

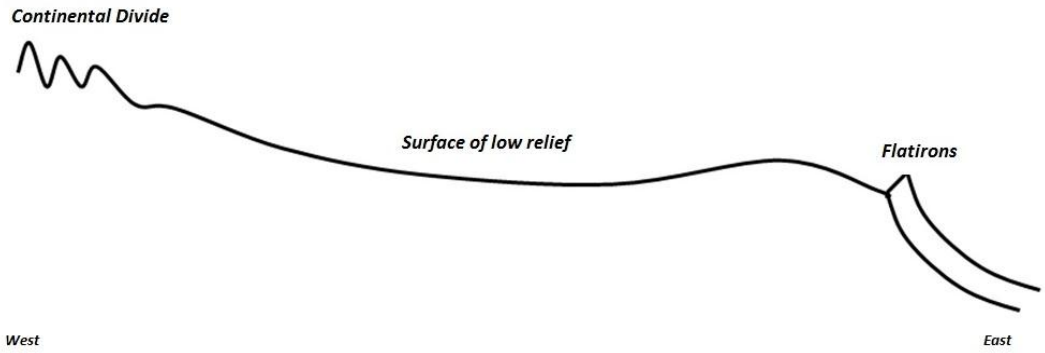

Figure 1: Schematic representation of the topography of the Front Range
Source: based on a figure from Bubel (2008), in Buraas (2009)

The climate of the Front Range can be characterised as a continental climate with pronounced seasonal variations in temperature (Buraas, 2009). With the change in topography and elevation from the Great Plains towards the Continental Divide the Front Range can be divided in different climatic zones (Birkeland et al., 2003), (i) plains (< 1710 m), (ii) lower montane (1830-2350 m), (iii) upper montane (2440-2740 m), (iv) subalpine (2840-3350 m), and (v) alpine tundra (> 3450 m). Temperatures decrease with elevation (10.6 °C in the plains zone and -3.8 °C in the alpine tundra zone (mean annual temperature)) and the difference between minimum and maximum temperatures increases with decreasing elevation. Precipitation increases with elevation (461 mm in the plains zone and 1021 mm in the alpine tundra zone (mean annual precipitation)) and mainly falls as snow in the upper basin.

The geology of the upper basin of the Front Range is composed of Precambrian siliceous metamorphic and granitic rocks, consisting of gneiss and schist which where intruded by granodiorite and granite (Birkeland et al., 2003), furthermore intrusive dikes and sills with deposits of metallic ores can be found (which were mined from 1858 till 1945). The lower basin is underlain by Paleozoic and Mesozoic sedimentary rocks. Younger deposits of shale, sandstone, limestone and conglomerate have

been tilted during mountain-building events and have formed easterly-dipping hogbacks, ridges, and valleys at the edge of the mountain front. The rivers and its tributaries are characterised by Quaternary alluvium (Murphy et al., 2003).
Vegetation and land use is in the upper basin characterised by forest and shrubs and above the tree line by sparsely low-growing tundra vegetation. The lower basin consists of grassland, agriculture (mainly pasture, alfalfa, wheat, corn and barley) and built-up areas (Murphy et al., 2003; Murphy, 2006).

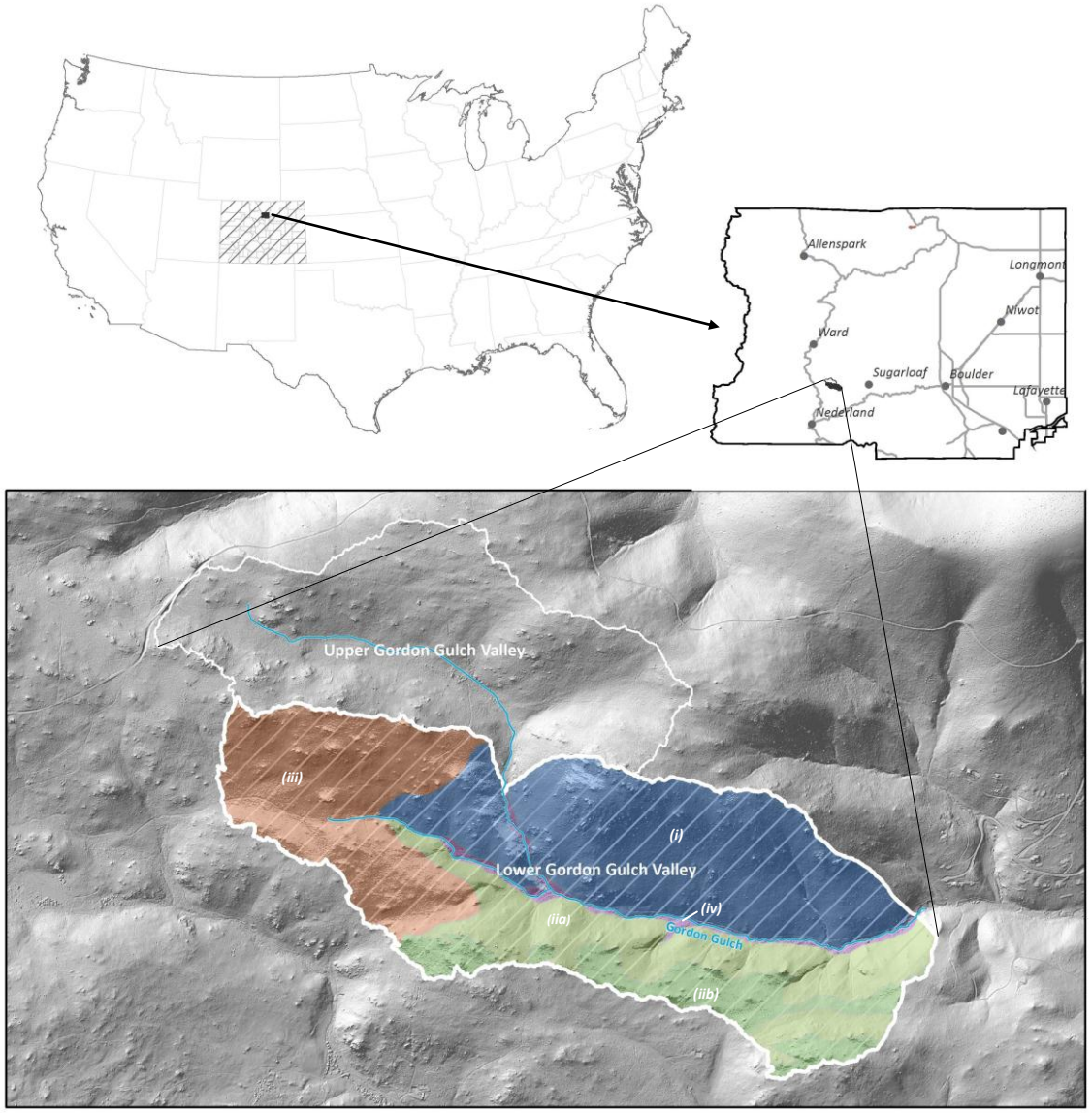

Figure 2: Study area - Gordon Gulch Valley
Where the study area, the Lower Gordon Gulch Valley, is shaded with diagonal stripes. The colours indicate the five characterising areas of the study area, (i) the south facing slopes, (iia) the flat north facing slopes, (iib) the steep north facing slopes, (iii) the smooth area in the west of the study area and (iv) the Gordon Gulch and its small terraces.

2.2 Landscape characteristics

The Gordon Gulch Valley can be divided in the Upper en Lower Gordon Gulch Valley. The valley is carved by the Gordon Gulch, a stream which is partly intermittent and partly permanent. The Gordon Gulch joins the north Boulder Creek about 16 km downstream from the Continental Divide. The area of the Lower Gordon Gulch Valley is around 1.68 km^2, and is characterised by an average elevation of 2584 m (with a minimum and a maximum of respectively 2436 m and 2726 m) and by steep slopes, an average slope of 16.6° (see Table 1). The valley is part of the Arapahoe National Forest and not surprisingly the valley is largely covered by forest. The forests on the north facing slopes are more

dense and consist mainly of Lodgepole Pines (*Pinus contorta*), while the south facing slopes have fewer trees, mainly Ponderosa Pines (*Pinus ponderosa*) and have more undergrowth (Boulder Creek CZO).

The valley can be divided into five characterising areas, with each its own landscape characteristics (these will be discussed in detail in section 4.1), (i) the south facing slopes, (iia) the steep north facing slopes, (iib) the flat north facing slopes, (iii) the smooth area in the west of the study area and (iv) the Gordon Gulch and its small terraces (Figure 2).

Table 1: Landscape characteristics of the study area

	mean	min.	max.	sd.
elevation [m]	2584	2436	2726	63.58
slope [°]	16.6	0.0	79.7	8.43
plan curvature	0.35	-759.98	1171.14	18.55
profile curvature	0.35	-989.62	767.62	21.06
aspect	145.5	-1.0	360.0	91.71
vegetation height [m]	4.82	0.04	17.05	2.55
tree cover [%]	37.1	0.0	90.0	23.91
undergrowth cover [%]	34.8	0.0	100.0	30.03
annual global radiation [Wh m^{-2}]	$1.6\ 10^6$	$4.8\ 10^5$	$1.9\ 10^6$	$2.0\ 10^5$
LAI [-]	5.62	4.77	6.06	0.18
LAI_{tree} [-]	5.09	0.00	5.95	1.05
TWI [-]	5.62	-0.27	16.60	1.49
erosion [m]	-0.10	-18.05	0.38	0.59

2.3 Geology, geomorphology and pedology

The valley is mainly underlain by Precambrium gneisses with some outcrops of Precambrium granite, Precambrium quartz monzonite and dikes of Cretaceous quartz monzonite. Close to the streams Quartenary alluvium can be found (USGS, 2005; Buraas, 2009).

The pedology of the valley can be described by the following characteristics[1] (USDA-NRCS., 1999; USDA-NCRS., 2008). On the slopes, shallow and more or less freely drained, dry soils that formed in slope alluvium over residuum from granitic rocks, gneiss, and schist can be found (*Loamy-skeletal, paramicaceous, shallow Ustic Dystrocryepts*). They support a sparse coniferous forest with widely spaced trees. The soils near the creek can be characterised by soils with shallow ground water at some time during the year. Therefore these soils have a low chroma and commonly show faint redoximorphic features (*Aquic Argiudolls*). These soils support chiefly tall grasses. The steep north and south facing slopes have moderately deep, freely drained soils that have a dark coloured, humus-rich surface horizon less than 50 cm thick and a higher percentage of clay in the lower part of the epipedon (*Typic Haplustolls*). The flat north facing slopes have shallow, freely drained soils with a dark coloured, humus-rich surface horizon less than 50 cm thick and a higher percentage of clay in the lower part of the epipedon formed from the residuum from granitic rocks, gneiss, and schist (*Loamy-skeletal, paramicaceous, shallow Typic Haplustolls*). Most of these soils support grasses and shrubs, the soils in the mountains support trees or grass and widely spaced trees.

2.4 Land use

Although the Gordon Gulch Valley was not heavily mined, prospect pits can be found all over the valley. Trees of the valley were used to satisfy the heavy demands for timber (fuel, mine timbers, and town construction). As a consequence the area was almost completely stripped during the late 19th century and early 20th century (Buraas, 2009). Nowadays, only a small area is subject to logging, because of fire prevention. The present use of the valley is mainly for recreation purposes.

2.5 Climate

The Gordon Gulch Valley has a continental climate and is located in the montane climatic zone. This results in large seasonal temperature differences. There is little precipitation, around 550 mm a year. From this precipitation, a maximum is received in May and a minimum during the winter.

[1] The soil description is based on the USDA Soil Taxonomy developed by United States Department of Agriculture and the National Cooperative Soil Survey (USDA-NCRS).

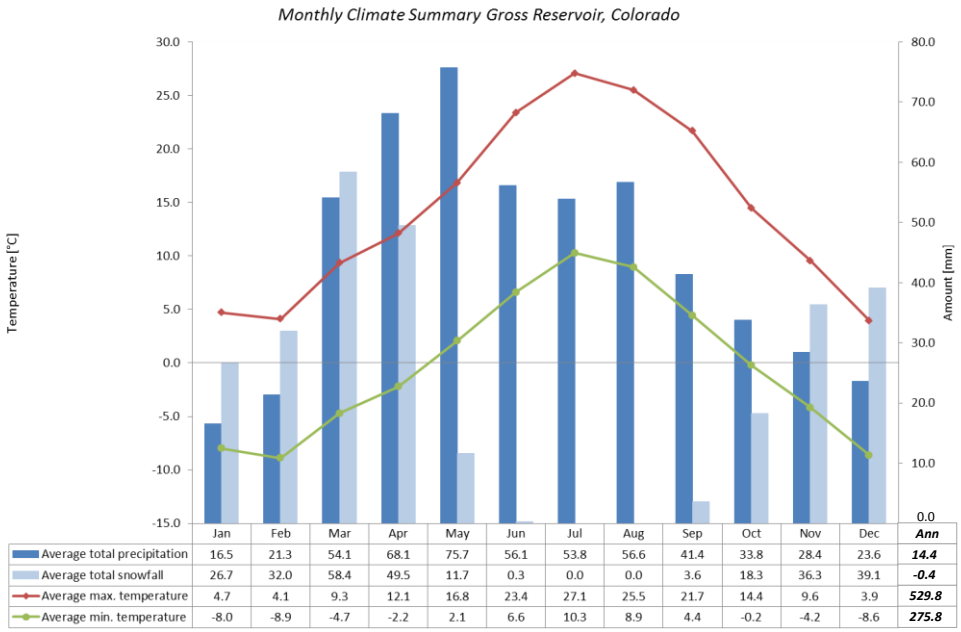

	Jan	Feb	Mar	Apr	May	Jun	Jul	Aug	Sep	Oct	Nov	Dec	Ann
Average total precipitation	16.5	21.3	54.1	68.1	75.7	56.1	53.8	56.6	41.4	33.8	28.4	23.6	***14.4***
Average total snowfall	26.7	32.0	58.4	49.5	11.7	0.3	0.0	0.0	3.6	18.3	36.3	39.1	***-0.4***
Average max. temperature	4.7	4.1	9.3	12.1	16.8	23.4	27.1	25.5	21.7	14.4	9.6	3.9	***529.8***
Average min. temperature	-8.0	-8.9	-4.7	-2.2	2.1	6.6	10.3	8.9	4.4	-0.2	-4.2	-8.6	***275.8***

Figure 3: Daily maximum and minimum temperatures and average precipitation and snowfall.
Source: based on meteorological data collected from May 1978 to September 2012 at the Gross Reservoir meteorological station at 2423 m (Western Regional Climate Center, 2012).

Methods and Materials 3.

3.1 Methods

This study has two main parts: (i) the analysis of the soil properties of the Gordon Gulch Valley and (ii) the analysis of the hydrological characteristics of the Gordon Gulch Valley. Although the soil properties were in the first place analysed in order to derive the hydrological characteristics from these properties, the soil properties themselves are valuable data. The dataset of soil properties reflects a wider variety of soil properties than accounted for in recent literature of the area. Previous research mainly focused on the transect which disclose the differences between the north facing and south facing slopes. Analysis of the soil properties therefore offers the opportunity to look in more detail at the relation between soil properties and landscape characteristics, this applies for the hydrological characteristics as well. Figure 4 shows a general overview of the methodology used for this research.

Fieldwork was done on 100 locations in the Gordon Gulch Valley. This fieldwork and subsequent laboratory measurements resulted in a dataset describing the soil and horizon properties of these locations.

We explored the hydrological processes though a literature study. The output of this literature study was used in the choice for the pedotransfer functions and in describing the hydrological characteristics based on the soil and landscape characteristics of the valley.

For all locations, and for the different soil horizons, soil hydraulic parameters were estimated based on measured texture percentages and bulk density using the ROSETTA pedotransfer functions (Schaap et al., 2001).

With available meteorological data, the soil dataset and the estimated hydraulic parameters as input, the hydrological model SWAP was used to model hydrological behaviour of the 100 points, and by implication of the watershed.

In order to get more insight in the relation of these soil properties and hydrological characteristics with the landscape position, both soil properties and hydrological characteristics were correlated to landscape characteristics.

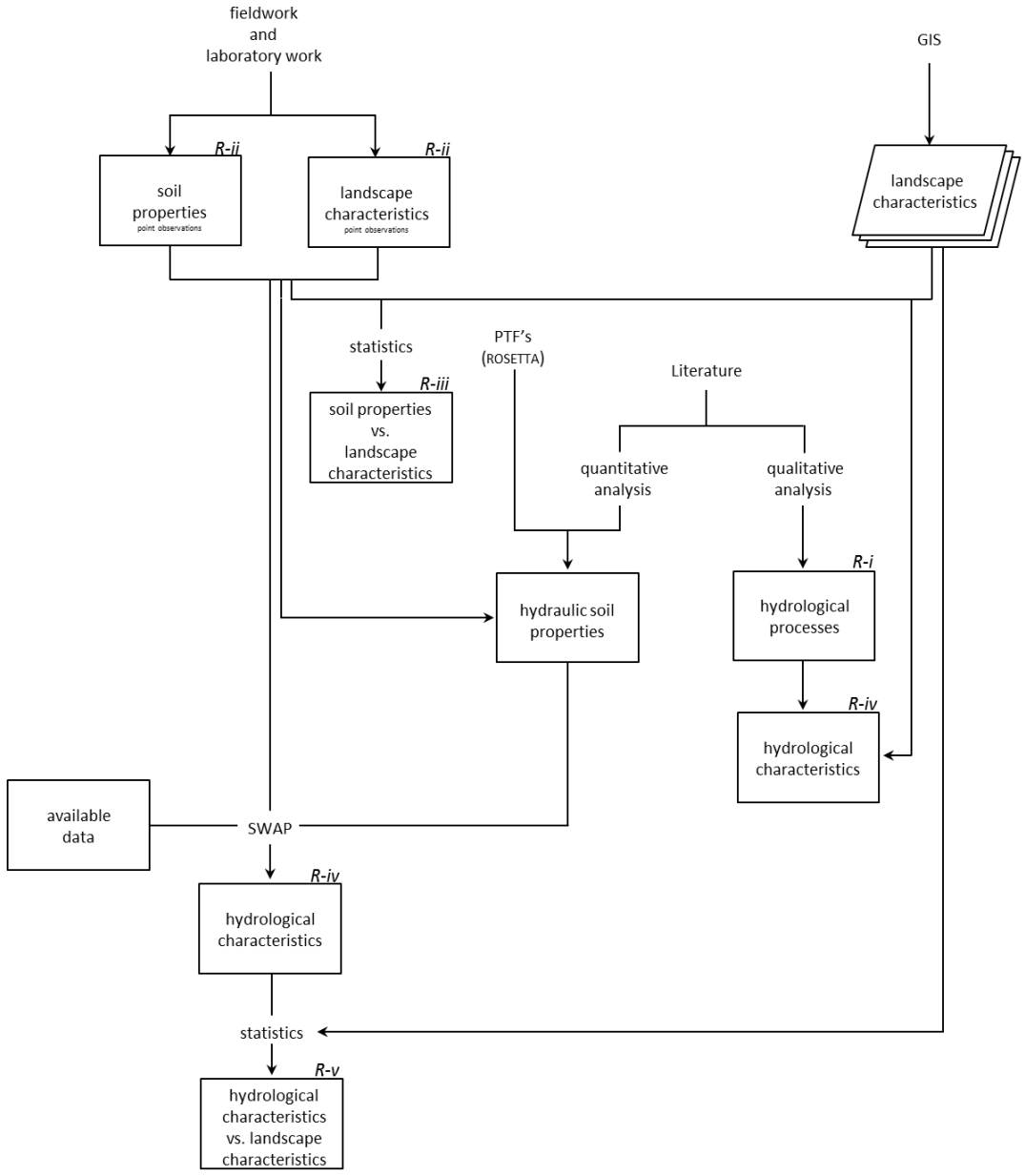

Figure 4: General methodological overview
The square boxes indicate input and outputs of a certain step, the boxes without a line indicate the used methodology and the boxes with an 'R-...' in the right corner indicate an output that answers the specified research question.

3.1.1 Fieldwork

Fieldwork took place between the end of August and half September. During fieldwork 100 locations were visited and general observations of the Gordon Gulch Valley were made.

For every location a site description was made. This description contained the measurement of the slope, aspect and curvature, an estimation of the vegetation cover (type and cover percentage, distinction in tree and undergrowth coverage) and the surface stoniness (size and cover percentage) and a description of the parent material and runoff features and exposed bedrock (distance and direction) when present (Table 2). In addition, for every location the soil properties were described. Therefore a soil pit was made up to the hard rock, as a consequence the focus of the soil description was on the upper 40 cm of the soil. The upper 40 cm were sufficient, since top soils in combination with the vegetation play a major role in distributing important components of the hydrological cycle (transpiration, evaporation, runoff and groundwater recharge) and in this way, top soils and the vegetation type strongly determine the hydrological response (van Dam, 2000). For each soil pit the

Master Soil Horizons were distinguished and described. Structure, stoniness, roots, mottles and concretions were estimated according the classification of the FAO soil description guidelines (FAO, 1990). Soil colour was estimated based on the Munsell colour charts (Munsell Color, 2009).
Bulk density, soil moisture content, soil porosity, texture, pH and organic carbon content were measured in the laboratory. Two sets of samples were collected at every soil pit, one bulk density sample and one sample of every soil horizon. To collect the bulk density sample a plastic corer was used to assemble a constant volume of soil.

Table 2: Field work - landscape characteristics

soil property	data type	unit	methodology
slope	continuous, ratio	[°]	measured in the field with an inclinometer
aspect	continuous, interval	[-]	measured in the field with a compass
vegetation cover			estimated in the field
tree cover	continuous, ratio	[%]	
undergrowth cover	continuous, ratio	[%]	
vegetation type			description of the dominant vegetation types
tree type	discrete, nominal	[-]	
undergrowth type	discrete, nominal	[-]	
parent material/geology	discrete, nominal	[-]	description of the dominant parent material
curvature	continuous, interval	[-]	estimated in the field
surface stoniness	continuous, ratio	[%]	estimated in the field
distance to exposed bedrock	continuous, ratio	[m]	estimated in the field

3.1.2 Laboratory work

Both the horizon samples and the bulk density samples were processed in the laboratory in order to measure several soil properties (Table 3). All samples were dried in the oven (three hours at 105 °C), weighted before and after drying. After this the horizon samples were ground in a mortar and sieved with a 2 mm sieve to remove all stones from the sample. Then the sample was split into three subsamples in order to measure the texture percentages, the organic carbon and the pH.
In order to measure the texture percentages the subsample was sieved with a 0.63 mm sieve to separate the sand from the silt/clay, both were weighted. To separate the clay from the silt, 15-20 ml of the silt/clay subsample was mixed with water and soap in a tube with a millimetre scale. After several days the silt and clay were both deposited with a clear boundary between the two. The amount was measured with a 10-4 meter ruler.
pH was measured by mixing the subsample with distilled water in a 1:2 ratio. The pH of this mixture was measured with a calibrated pH measurer (YSI 63 pH instrument).
In order to measure the organic carbon content of the soil a subsample of around 5 gram was measured at 0.0001 gram precision. This subsample was dried for two hours in the oven at 550 °C. After drying the subsample was weighted again to calculate the loss of organic carbon.

Table 3a: Field work - soil and horizon properties

soil property	data type	unit	methodology	lab
horizons			description based on the FAO soil description guidelines	
OM	continuous, ratio	[%]	calculating the percentage based on loss on ignition	x
texture			measurement of the amount by separation based on sieving and sedimentation	x
sand	continuous, ratio	[%]		
silt	continuous, ratio	[%]		
clay	continuous, ratio	[%]		
moisture content	continuous, ratio	[mass%]		x
soil colour			estimation based on Munsell colour charts	
HUE	discrete, ordinal	[-]		
value	discrete, ordinal	[-]		
chroma	discrete, ordinal	[-]		
pH	continuous, interval	[-]	measurement in a mixture of soil and distilled water (1:2 ratio) with a pH measurer	x
structure	discrete, nominal	[-]	estimation for each soil horizon according the classification of the FAO soil description guidelines (pp. 44-46)	
root			estimation for each horizon according the classification of the FAO soil description guidelines (p. 60)	
density	continuous, ratio	[%]		
size	discrete, ordinal	Very fine, Fine, Medium, Coarse		
stoniness			estimation for each soil horizon according the classification of the FAO soil description guidelines (pp. 29-30)	
density	continuous, ratio	[%]		
size	discrete, ordinal	Very fine gravels, Fine gravels, Medium gravels, Course gravels, Stones, Boulders		
bulk density[2]	continuous, ratio	[g cm^{-3}]	calculation by dividing the (dried) weight of the soil sample by the volume of the soil sample the soil sample was taken according to the core method	x
soil porosity[1]	continuous, ratio	[%]	calculation by subtracting the division of bulk density by particle density (generally taken 2.65 mg m^{-3}) from one the soil sample was taken according to the core method	x
moisture content[1]	continuous, ratio	[mass%]	calculation of the percentage by the division of the difference between the wet weight and dried weight of the soil sample by the dried weight of the soil sample the soil sample was taken according to the core method	x
volumetric water content[1]	continuous, ratio	[volume%]	calculation of the percentage by the division of the difference between the wet weight and dried weight of the soil sample by the volume of the soil sample the soil sample was taken according to the core method.	x
soil water-filled pore space[1]	continuous, ratio	[%]	calculation of the percentage by the division of the volumetric water content by the soil porosity the soil sample was taken according to the core method	x

[2] In contrast to the other characteristics, these characteristics were not measured for each horizon, but were measured for the upper 7 cm of the soil.

Table 3b: Field work - soil and horizon properties

soil property	data type	unit	methodology	lab
thickness Oi/Oh[3]	continuous, ratio	[cm]	measurement in the field with a tape measure	
thickness top layer[2]	continuous, ratio	[cm]	measurement in the field with a tape measure	
thickness mid layer[2]	continuous, ratio	[cm]	measurement in the field with a tape measure	
starting depth C layer[2]	continuous, ratio	[cm]	measurement in the field with a tape measure	

3.1.3 Pedotransfer functions

The estimation of the water content and the hydraulic conductivity are needed to describe the hydrological characteristics of the study area. The hydraulic conductivity is a property of the soil which describes the ease with which water can move through pore spaces or fractures. This depends on the permeability of the material and on the degree of saturation. Saturated hydraulic conductivity (K_{sat}) describes water movement through saturated soils under a unit gradient. The water content (moisture content or soil moisture) can be described as the quantity of water contained by the soil. The residual water content (θ_r) describes the water content in extreme dry conditions, the saturated water content (θ_s) in extreme wet conditions and is therefore equal to the porosity of the soil.

Measurement of these soil hydraulic properties is time consuming (Vereecken et al., 1989; Schaap et al., 2001; Wösten et al., 2001; McBratney et al., 2002; Pachepsky et al., 2006) and luckily good predictions instead of direct measurement are accurate enough for many applications (Wösten et al., 2001). Pedotransfer functions were developed for this purpose and are defined as functions that relate soil hydraulic parameters to the easier measurable soil properties usually available from soil surveys (Bouma, 1989 cited in: Pachepsky et al., 2006).

Several types of pedotransfer functions have been developed. Wösten et al. (2001) divide them in three categories:

(i) The first category pedotransfer functions predicts soil hydraulic characteristics based on soil structure models. This model make use of the similarity in shape between the water retention curve and the cumulative particle-size distribution (Wösten et al., 2001). Water retention characteristics are predicted based on particle-size distribution, bulk density and particle density. A well-known example of this category is the Arya and Paris model (Arya and Paris, 1981).

(ii) The second category pedotransfer functions contains the prediction of specific points of interest of the water retention curve. Regression equations are used to predict these specific points. Advantages of these category of pedotransfer functions are (i) the ability to make fairly accurate predictions and (ii) the possibility to have insight in which soil properties are relevant for predicting specific points at the water retention curve. A disadvantage is that it is necessary to have many regression equations to predict the complete water retention curve.

(iii) The third category pedotransfer functions contains the prediction of parameters of soil hydraulic functions in order to predict continuous soil hydraulic properties. In contrast to the other categories, this category of pedotransfer functions predict the parameters of specific soil hydraulic functions. An advantage of this method is that the complete curve of the soil water content and the hydraulic conductivity can be predicted.

For this study the third category pedotransfer functions is most appropriate. A more recent form of this category are pedotransfer functions which are based on artificial neural networks. An artificial neural network consists of many interconnected simple computational elements (Wösten et al., 2001). The advantage of this method is its ability to predict the behaviour of complex systems. Therefore, when the number of inputs is large enough, pedotransfer functions which make use of artifical neural networks perform better than pedotransfer functions using regression techniques (Wösten et al., 2001).

[3] In contrast to the other characteristics, these characteristics were only measured for each soil pit and not for every layer.

Soil hydraulic functions

There exist many different functions which describe both water content and hydraulic conductivity (an overview of commonly used equations is given in Wösten (2001)).

In this study we will use the well-known and commonly used equations of Van Genuchten (1980). These equations are described in Wösten (1997; Sonneveld et al., 2003) and include equations for the soil water content (θ [m^3 m^{-3}]) and the hydraulic conductivity (K [m s^{-1}]), both as a function of the pressure head (h [hPa]):

$$\theta(h) = \theta_r + \frac{\theta_s - \theta_r}{(1+|\alpha h|^n)^{1-\frac{1}{n}}} \qquad \textbf{[1]}$$

$$K(h) = K_s \frac{[(1+|\alpha h|^n)^{1-\frac{1}{n}} - |\alpha h|^{n-1}]^2}{(1-|\alpha h|^n)^{(1-\frac{1}{n})\cdot(l+2)}} \qquad \textbf{[2]}$$

where the subscripts r and s refer to residual and saturated values of the soil water content and a, n and l are parameters that determine the shape of the water retention curve (θ against h) and the hydraulic conductivity curve (K against h).

ROSETTA

Although a lot of pedotransfer functions were created, for example the pedotransfer functions based on the HYPRES soil database (a European soil database) described by Wösten et al. (2001), and the continuous pedotransfer function for soils in the Netherlands based on linear regression from Wösten (1997), the most appropriate pedotransfer functions for this study area is the model ROSETTA , since this model is based partly on a North American soil database.

ROSETTA (Figure 5) is a model which makes use of artificial neural networks and compares input data of soil parameters (i.e. texture, bulk density) with three different databases with soil hydraulic data and corresponding soil properties. In total 2,134 soil samples for water retention with a total of 20,574 $\theta(h)$ points, a subset of 1,306 soil samples for saturated hydraulic conductivity, and a subset for 235 soil samples for unsaturated hydraulic conductivity with a total of 4,117 $K(h)$ points. Most of the samples were derived from soils in temperate to subtropical climates of North America and Europe (Schaap et al., 2001).

The output depends on the input data and can result in five different pedotransfer functions, increasing in complexity. The first function is based on the USDA textural classes only, the second on the texture percentages of sand, silt, and clay, the third adds bulk density, the fourth adds one point of the retention function ($\theta_{2.5}$) and the last adds two point of the water retention function ($\theta_{2.5}$ and $\theta_{4.2}$) (Schaap et al., 2001; Stumpp et al., 2009).

Since we measured texture percentages and bulk density we will use the third pedotransfer functions based on sand, silt and clay percentages and bulk density.

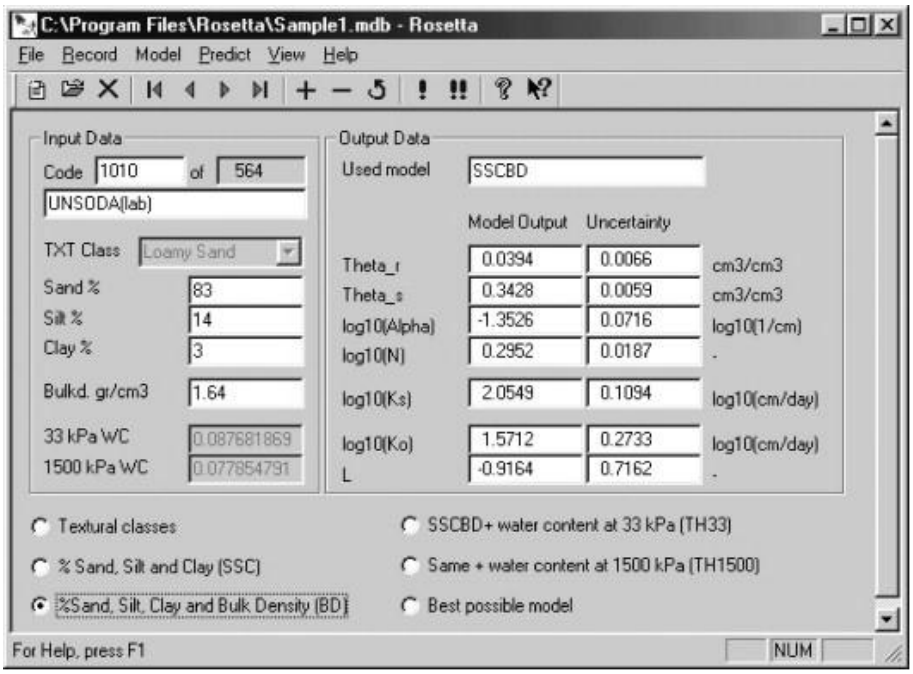

Figure 5: Main window of the user-interface of rosetta
Source: Based on figure 3 in the article of Schaap et al. (2005)

Assumptions

Several assumptions had to be made in order to estimate the pedotransfer functions. Bulk density was only available for the upper 7 cm of the soil, therefore it was assumed that bulk density was constant within the whole soil profile. Two soils (GGL001 and GGL011) had a bulk density below 0.5 g m^{-3}. ROSETTA cannot deal with a bulk density below 0.5 g m^{-3}, therefore we calculated the pedotransfer functions for these soils for a bulk density from 0.55 to 0.50 g m^{-3} with an interval of 0.01 and linearly extrapolated to the actual value of bulk density. Data were missing for two soil horizons (GGL001AC and GGL014Ah). Silt and clay percentages were missing for GGL001AC, these were calculated in the same ratio as for the upper soil horizon of this soil. GGL014Ah was missing all texture percentages. A comparable soil (in terms of landscape position, organic matter content, pH, colour and bulk density) was found (GGL004Ah) and the texture percentages of this soil were used for GGL014Ah.

The output of ROSETTA and the validation of the Van Genuchten parameters, with measured Van Genuchten parameters from Hinckley et al. (2012), can be found in Appendix A.

3.1.4 Hydrological model

SWAP

In order to simulate the hydrological characteristics of the Gordon Gulch Valley we used the Soil Water Atmosphere Plant (or SWAP) model (van Dam, 2000). This model simulates transport of water, solutes and heat in the vadose zone in interaction with vegetation development. The model uses the Richards' equation (Richards, 1931) to simulate the soil moisture movement (Kroes et al., 2008). SWAP is a one dimensional model with an upper boundary just above the canopy and a lower boundary in the top of the groundwater system, since in this zone transport processes are predominantly vertical (van Dam, 2000; Kroes et al., 2008). Simulation focusses on the vertical water movement of the soil (e.g. soil water storage, runoff, net bottom flux, and soil evaporation) and in addition on the hydrological processes considering the vegetation cover (e.g. transpiration and interception).

Within the model, the soil column is divided in compartments, for which the transport and balance equations of water, solutes and heat are solved. Interaction between residence and movement of water, solute and heat is calculated for small time steps (ranging between seconds and hours).

Interaction with plant growth processes is calculated for larger time steps (daily). SWAP makes a distinction between soil evaporation and plant transpiration. Soil heterogeneity is taken into account by providing options for, inter alia, soil layering (van Dam, 2000).

Parameterisation and assumptions

Since we want to simulate the hydrological characteristics of the Gordon Gulch Valley, we focussed the simulation on the calculation of the transport and balance equations of the movement of water. For the results we used the *.bal* and *.inc* files which gives respectively the short yearly water and solute balance and the monthly incremental water balance. Within these files precipitation, interception, runoff, transpiration, net bottom flux, soil evaporation, and the soil water storage are the values which were used in the analysis of the SWAP output.

The model was run for the period 22 September 2009 till 7 October 2012. For this period daily meteorological data and detailed rain data were available. We analysed the output for the period November 2009 till September 2012. September and October of the first year were used as a start-up period to adapt the initial conditions of the model.

Several assumptions were made and parameters were set in order to run the model properly, these are discussed below. This section is divided in three sections representing the three important input files for SWAP, (i) atmospheric forcing (meteorological file (*[][4].YYY* file) and detailed rain file (*betasso[].YYY* file)), (ii) soil parameterisation (*[].swp* file) and (iii) crop parameterisation (*[].crp* file).

(i) Atmospheric forcing

Daily meteorological data consist of minimum and maximum air temperature [°C] at 10m, wind speed [m s^{-1}] at 10 m, humidity [kPa], and rain [mm], the detailed rain data consist of hourly rain data [mm], both were collected from the nearby meteorological station, Betasso (1960m, 40.0N, -105.3W). Some data were missing in the daily meteorological data for 2012, for temperature, wind speed and humidity these missing data were replaced by the average of the three previous years. For rain these missing data were replaced by zero. In the detailed rain data some data was missing for the year 2009 and 2012, the data of 2009 could be completed based on daily rain data. For 2012 these missing data were replaced by zero.

Daily global radiation [kJ m^{-2}] was calculated with the tool Area Solar Radiation (Spatial Analyst) in ArcMap. However, for some days the daily global radiation was not or incorrectly calculated. For these days the daily global radiation was linear interpolated.

Air temperature was differentiated per location. Assumed was that temperature is affected by elevation and the daily global radiation. For the relation between temperature and altitude we used the lapse rate from International Standard Atmosphere (ISA), defined by the International Civil Aviation Organization (ICAO) of 6.49 °C/1,000 m. For the relation between daily global radiation and temperature no factor was found, therefore we assumed that temperature was dependent on the difference between the daily global radiation of the location and the maximum daily global radiation in the area times the maximum temperature difference caused by the elevation differences. For each location air temperature was calculated with:

$$T_i = T_{betasso} + \left(\alpha \cdot (E_i - E_{betasso})\right) + \left(\frac{R_i - R_{\min}}{R_{\max} - R_{\min}} \cdot \left(\frac{E_{\max}}{E_{\min}} \cdot -\alpha \right) \right) \qquad \textbf{[3]}$$

where T is the temperature [°C], E is the elevation [m], R is the daily global radiation [W/m^2], α is -0.00649 °C/m, $E_{betasso}$ is 1960m, the index $_i$ indicates the location, $_{min}$ indicates the minimum value and $_{max}$ indicates the maximum value.

Since no data were available on the heat flow of the soil, snow could not be calculated based on the simple snow module in SWAP. The occurrence of snow was therefore calculated based on the available temperature and (detailed) rain data. Assumed was that rain changes into snow when the average air temperature is below -2 °C. In this case it was assumed that there is no input from precipitation (rain

[4] *[]* indicates the considered field location.

is zero). When the temperature will be above 0 °C the snow (or accumulated rain) will melt. The speed of this snow melt is affected by temperature and global daily radiation, and is assumed to be a simple function of temperature and daily global radiation (Kustas et al., 1994):

$$M = a_r T_d + m_Q R_n \qquad \textbf{[4]}$$

where a_r is a restricted degree-day factor, m_Q is the conversion factor for energy flux density to snowmelt depth (cm d^{-1} (W m^{-2})$^{-1}$), T_d is the difference between the daily temperature and the base temperature (in this case 0 °C), and R_n is the net radiation [W m^{-2}]. The value of m_Q is approximately 0.26, so each W m^{-2} of daily average energy input results in a daily snowmelt depth of about 0.3 mm water equivalent. Kustas et al. (1994) proposes, based on an article of Martinec (1989), a degree-day factor ranging between 2.0 and 2.5 mm °C^{-1}.
This equation, however, does not include the negative affect of shadow beneath the trees on snowmelt. Since available snow data of the CZO show that this is an important factor, we included this shadow effect in the equation. No full coverage data on tree cover was available, therefore we used the vegetation height (resolution 1 m) as an indicator of tree cover. All areas with a vegetation height smaller than 1.5 m were assumed to be without trees, all areas with a vegetation height higher than 1.5 m were assumed to be with trees. The Leaf Area Index (LAI) raster (calculation of the LAI is described in the section *Crop parameterisation*, p.16) was corrected with this binary raster. For each cell of the LAI-raster (resolution 30 m) the number of tree cells was counted and divided by 900 (30 x 30 cells). This percentage was then multiplied by the cell value of the LAI-raster and resulted in a LAI_{tree}. The LAI_{tree} was linear interpolated between the five available dates.
Based on available snow depth data of the CZO we calibrated the equation and corrected the degree-day factor with a factor 10, which improved the modelled snowmelt considerably (Figure 6). These steps resulted in the following equation for snowmelt:

$$M = 0.25 \cdot T_d + 0.26 \cdot e^{-0.5 \cdot LAI_{tree} \cdot R_n} \qquad \textbf{[5]}$$

The snowmelt was added to the rain which was already considered.

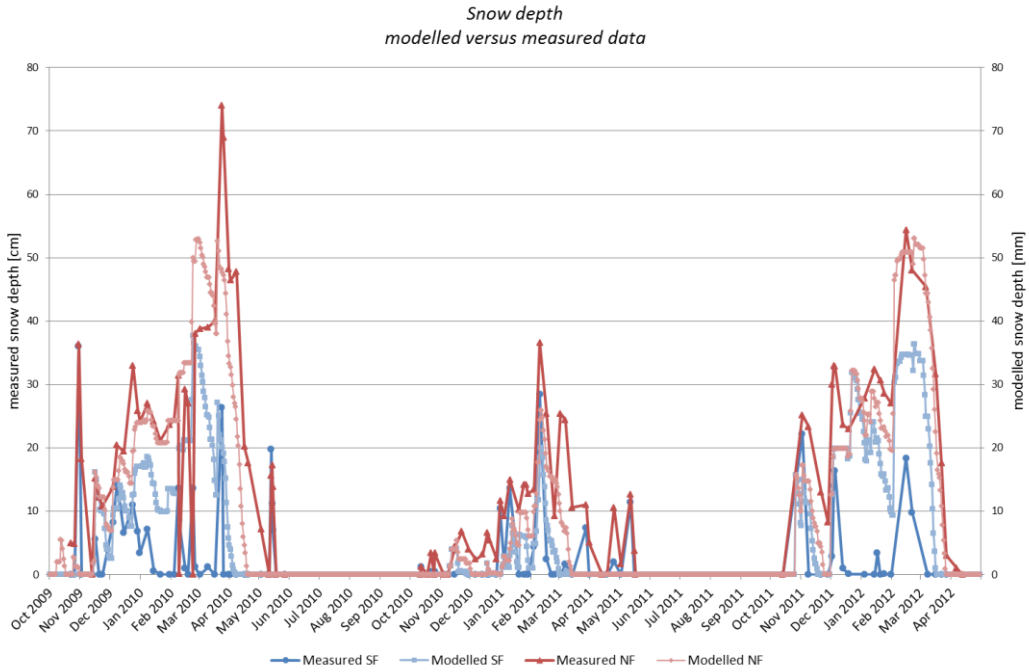

Figure 6: Comparison between the measured snow depth data of the CZO and the modelled data used as input for swap.

(ii) Soil parameterisation

The profile compositions of each site with their corresponding Van Genuchten parameters were used as inputs for the model. The height of the compartments were set to 2 cm, therefore the height of the layers was rounded to the above lying even number. For the hydraulic parameters the air entry pressure head was set to zero. Since limited hydraulic data was available for the C-horizons, only the top horizons (A and B horizons and a few C horizons) were used as input for the model. The depth of the bottom horizon was assumed to be equal to the rooting depth.

For the initial soil moisture condition it was assumed that the initial soil water pressure head was constant over the depth and was set to -300 cm. For runoff it was assumed that ponds could get a maximum depth of 0.1 cm before running off. The drainage resistance for surface runoff was set to 0.5 d and the exponent set to 1.0.

Furthermore no irrigation was applied, no runon, no hysteresis, no macropore flow and no lateral drainage were assumed and no heat transport and no solute transport were simulated. The bottom boundary condition was assumed to be free drainage of the soil profile.

(iii) Crop parameterisation

Leaf area index (LAI) was empirically determined for January, March, June, September and December. The determination was based on the relation between LAI and the Weighted Difference Vegetation Index (WDVI) from Clevers and Verhoef (1993):

$$LAI = -\frac{1}{\alpha} \cdot \ln\left(1 - \frac{WDVI}{WDVI_{\infty}}\right) \qquad \textbf{[6]}$$

with α = 0.3 and $WDVI_{\infty}$ = 35 for forest. WDVI was calculated from Landsat 4-5TM images for 12 January, 17 March, 21 June and 25 September 2010 and 19 December 2006. All images had a resolution of 30 m, a cloud cover less than 10% and a quality of at least 9 (on a scale from 1 (bad) to 10 (good)). The calculation was done according the following equation:

$$WDVI = \mathrm{Refl}(NIR) - C \cdot \mathrm{Refl}(\mathrm{Red}) \qquad \textbf{[7]}$$

Where *Refl(NIR)* is the reflectance of near infrared (band 4), *Refl(Red)* is the reflectance of red (band 3) and C is the correction for the bare ground reflection. C can be calculated by dividing the bare ground reflection in band 4 by the bare ground reflection in band 3. C was calculated based on data from Condit (1970) for a soil from the Garden of the Gods in Colorado, and resulted in a C of 1.4.
The crop height was calculated based on the difference between the Digital Surface Model and the Digitial Terrain Model. We assumed the vegetation height constant over the year.
Since the C horizon often consists of mobile regolith, saprolite or saprock we assumed that the rooting depth was 20 cm deeper than the start of the C horizon. For soils were no C horizon was reached we assumed that the roots would reach to 150 cm depth for terrace soils and soils in accumulation positions and 70 cm for other deep soils (GGL020 and GGL030). Soil depth in the SWAP file was set equal to this rooting depth. Fieldwork observations were used for rooting density, the rooting density was variable over the rooting depth.
Interception values were based on values from the Dutch Nationaal Hydrologisch Instrumentarium (NHI, 2008). Values were available for deciduous trees (oak (*Quercus*)), coniferous trees (Scots Pine (*Pinus sylvestris*)) and for undergrowth (natural grasland/Calluna (*Calluna vulgaris*)). The vegetation types of all locations were categorised in these three types. The interception values were assumed to be constant over the year.

Albedo, minimum canopy resistance and canopy resistance of intercepted water were assumed to be constant over the year and for each vegetation type. They were set as 0.23, 150.0 s m^{-1}, and 0.0 s m^{-1} respectively. For soil water extraction no limitations were assumed, this resulted in HLIM1 is 100.0 cm, HLIM2U 100.0 cm, HLIM2L is 100.0 cm, HLIM3H is -1000.0 cm, HLIM3L is -2000.0 cm, HLIM4 is -16000.0 cm, ADCRH is 0.5 cm d^{-1} and ADCRL is 0.1 cm d^{-1}.

Furthermore no irrigation was applied and no salt stress was assumed.

SWAP warnings

Running the SWAP model entailed some modelling warnings (for fieldpoints 005, 007, 009, 010, 014, 015, 017, 029, 031, 050, 054, 088, 090, 092, 094, 096, 097, and 099). These warnings were related to the convergence of the Richards Equation and is often related to extremely non-linear soil physics or inconsistent preconditions. Because we were not able to correct this we decided to exclude locations of which the net bottom flux or the groundwater level show inexplicable jumps. This resulted in the exclusion for analysis of the fieldpoints 007, 015, 031, 092, 096, and 099. Furthermore three fieldpoints had a water balance unequal to zero (012, 023, and 029). This deviation from zero was very small (-0.01 in all cases) and we decided to include these fieldpoints in further analysis. The other fieldpoints which gave a warning during running showed no unexpected values and were included in further analysis.

The graphical representation of the SWAP inputs precipitation (rain and snowmelt), LAI, global monthly radiation, minimum and maximum daily average temperature can be found in Appendix B.

3.1.5 Statistics

Both the soil properties and the hydrological characteristics were analysed for the landscape characteristics of the Gordon Gulch Valley using statistics.

In the first place we looked at the correlation of the soil properties and the landscape characteristics (see Table 4) with the use of correlation matrices (Pearson's correlation coefficients). The correlation matrices indicate the correlation between variables (ranging from -1 to 1, values close to -1 or 1 indicating a large negative or positive correlation and values close to zero indicating little or no correlation).

Table 4a: Landscape characteristics derived from available data

soil property	data type	unit	methodology
elevation	continuous, ratio	[m]	available Light Detection And Ranging (LiDAR) Digital Elevation Model (DEM) data
slope	continuous, ratio	[°]	derivative from the LiDAR DEM data, calculated with ArcGIS
aspect	continuous, interval	[°]	derivative from the LiDAR DEM data, calculated with ArcGIS
plan curvature	continuous, ratio	[-]	derivative from the LiDAR DEM data, calculated with ArcGIS
profile curvature	continuous, ratio	[-]	derivative from the LiDAR DEM data, calculated with ArcGIS
erosion	continuous, ratio	[m]	calculated with LandscApe ProcesS modelling at mUlti-dimensions and Scales (LAPSUS)
multiple flow accumulation	continuous, ratio	[-]	calculated with LAPSUS
global annual radiation	continuous, ratio	[Wh m^{-2}]	calculated based on the LiDAR DEM data with ArcGIS
vegetation height	continuous, ratio	[m]	calculated based on the difference between the LiDAR Digital Surface Model (DSM) and LiDAR DEM data
topographic Wetness Index (TWI)	continuous, ratio	[-]	calculated based on the natural logarithm of the division of the specific contributing area (in this case the multiple flow accumulation times the area of each pixel of this raster [m^2]) by the tangents of the slope
distance to streams	continuous, ratio	[m]	calculated with ArcGIS

Table 4b: Landscape characteristics derived from available data

soil property	data type	unit	methodology
Weighted Difference Vegetation Index (WDVI)	continuous, ratio	[-]	calculated based on Landsat 4-5 TM data by the subtraction of reflectance of the red band times the reflectance of the bare soil from the reflectance of the near infrared band (Clevers and Verhoef, 1993) for January, March, June, September and December the reflectance of the bare soil (1.4) was derived from Condit (1970) for a comparable soil from the Garden of the Gods, Colorado
Leaf Area Index (LAI)	continuous, ratio	[-]	calculated based on the empirical relation between LAI and WDVI of Clevers and Verhoef (1993) for January, March, June, September and December

In the second place we looked at the correlation of the soil properties and hydrological characteristics of Gordon Gulch Valley with the use of ANOVA and Pearson's chi-square test. The ANOVA and Chi-square test were executed for the differences of soil properties and hydrological characteristics between the five characterising areas.

ANOVA was used for the continuous data to test the hypothesis that three or more samples have the same mean. The amount of variance explained by the model is quantified with η^2. This value is between 0 and 1, where 1 explains the whole variance of the model and 0 explains nothing of the variance. The Pearson's chi-square test was used for the categorical data to tests the association of two categorical variables based on the idea of comparing the frequencies observed in certain categories with the frequencies expect in certain categories by chance. Cramer's V was used to quantify the strength of the association between the two categories. This value is between 0 and 1, where 0 indicates a very weak association between the two categories and 1 a very strong association.

3.2 Materials

This section contains an enumeration of the materials which are needed for this study. The materials are divided in (i) the materials which were needed during field and laboratory work, (ii) the already available input data, and (iii) the software used to process the data.

3.2.1 Field and laboratory materials

Table 5 shows a list of the needed materials in the field and in the laboratory.

Table 5: Field and laboratory equipment

field	laboratory
GPS	sieve 2 mm
geological hammer	sieve 0.63 mm
sample bags	porcelain crucibles
compass	pH measurer
inclinometer	mortar and pestle
lineal	scale (one, two and four decimals)
tape measure	tube with ml scale
sand ruler	oven (550 °C and 105 °C)
munsell colour chart	porcelain dishes
FAO soil description guide lines	100 ml graduated cylinder
corer (bulk density)	10-4 meter ruler

3.2.2 Input data

Table 6 gives a list of used input data, furthermore the data are shortly described in the table.

Table 6: Input data

data	description	year	source
LiDAR Digital Elevation Model (DEM)	Boulder Creek Critical Zone Observatory Snow-Off LiDAR Survey the map has a resolution of 1 m	2010	National Science Foundation et al. (2010)
LiDAR Digital Surface Model (DSM)	Boulder Creek Critical Zone Observatory Snow-Off LiDAR Survey the map has a resolution of 1 m	2010	National Science Foundation et al. (2010)
digital aerial pictures	aerial pictures by the USDA/FSA of the year 2004, 2005, 2006 and 2009 the resolution of these aerial pictures is respectively 2 m, 1 m, 2 m and 1 m	2004, 2005, 2006, 2009	USDA-NCRS. (2011)
Landsat 4-5 TM data	Landsat 4-5 TM data by the USGS of the dates January 2010, March 2010, June 2010, September 2010, December 2006 the maps have a resolution of 30 m, a cloud cover less than 10% and a quality of 9 (out of 10)	2006, 2010	USGS (2012)
meteorological data	meteorological data from 22 September 2009 till 7 October 2012, including: (i) daily data of minimum, maximum and average air temperature [°C] at 2 and 10m, minimum, maximum and average relative humidity [-] at 2 and 10m, minimum, maximum and average wind speed [m/s] and wind direction [°] at 10m, maximum wind speed [m/s] and wind direction [°] at 2m, minimum, maximum, average [W/m^2] and total solar radiation [MJ/m^2], netto radiation [W/m^2], soil heat flux [W/m^2], soil temperature [°C] at -15cm, soil volumetric water content [%] at -15cm, barometric pressure [Mbar] and total rain gage [mm] and (ii) hourly data of total rain gage [mm] location: Betasso Meteorological Station, 1960m, 40.0N, -105.3W	2012	Boulder Creek CZO (2013a)
bulk density	for three locations (south facing slope, north facing slope, valley floor) in Gordon Gulch Valley, bulk density was measured the parameters were measured at two depths (0 – 10 cm and 10 – 25 cm)	2012	Hinckley et al. (2012)
hydraulic soil properties	for three locations (south facing slope, north facing slope, valley floor) in Gordon Gulch Valley, Van Genuchten parameters were measured the parameters were measured for two depths (0 – 10 cm and 10 – 25 cm)	2012	Hinckley et al. (2012)
snow data	for ten locations (south facing slope, north facing slope, valley floor) in Gordon Gulch Valley, snow depth was measured data were available for the period October 2009 to April 2012	2013	Boulder Creek CZO (2013b, c)
discharge	for the outlet of the Lower Gordon Gulch valley discharge was measured half hourly data were available for the period March 2010 to December 2011	2013	Boulder Creek CZO (2013b)
geology	geological map of the USGS, map for whole the United States the map has a scale of 1:100,000	2005	USGS (2005)
soil	Soil Survey Geographic (SSURGO) database for Arapaho-Roosevelt National Forest Area, Colorado, Parts of Boulder, Clear Creek, Gilpin, Grand, Park, and Larimer Counties the map has a scale of 1:24,000	2008	USDA-NCRS. (2008)

3.2.3 Software

Maps were edited with ArcGIS 10.0 (ESRI). Computations were done with R (http://www.R-project.org), this will be assessed via RStudio (http://rstudio.org). Tables and graphics were made with R or Microsoft Excel 2007. The hydrological model was executed by swap.exe (http://www.swap.alterra.nl/) and automation was done with R as well.

Results 4.

4.1 Landscape characteristics

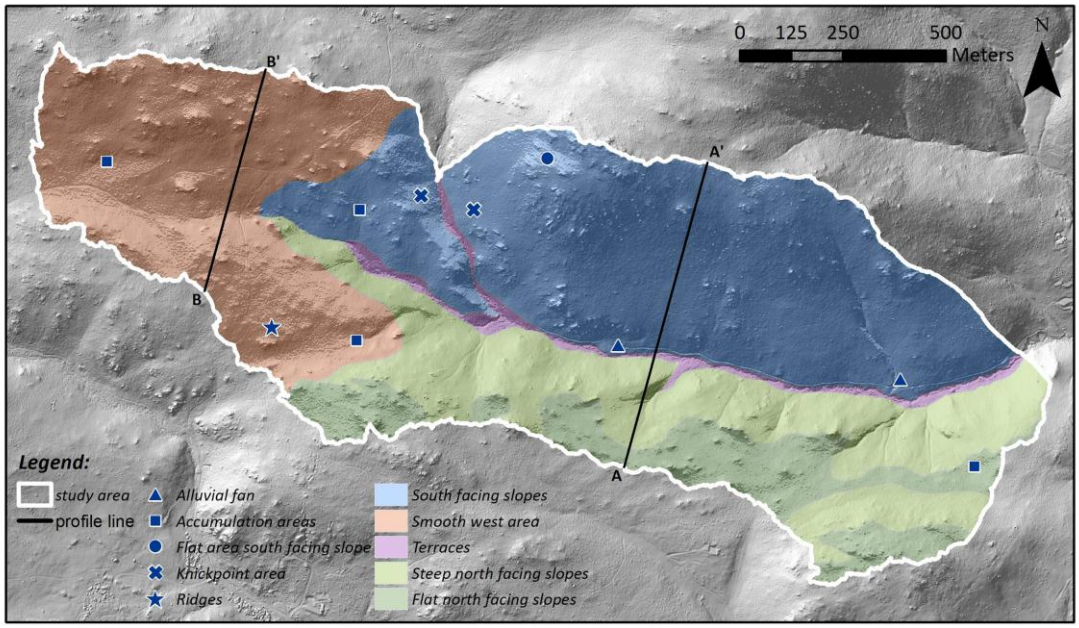

Figure 7: Landscape characteristics

4.1.1 Characterising areas of the study area

The Lower Gordon Gulch Valley can be categorised in different landscape characteristics. These are illustrated by Figure 7. The Lower Gordon Gulch Valley can be divided in three characterising areas, (i) the south facing slopes (*blue area*), (ii) the north facing slopes (*green area*, two subcategories can be distinguished, (iia) the steep north facing slopes (*light green area)* and (iib) the flat north facing slopes *(dark green area))* and (iii) the flatter and smoother area at the west side of the valley (*orange area*). Beside these characterising areas the area is characterised by the Gordon Gulch river and its small alluvial terraces (*purple area*). Site characteristics of these five landscape categories can be found in Table 7. Figure 9 shows maps of 18 site characteristics of the study area.

North and south facing slopes

The clear differences between the north facing and south facing slopes are indicated by differences in slope, density of exposed bedrock, vegetation density, and exposure. The area with the south facing slopes is higher in elevation (with a maximum elevation of 2711 m versus 2635 m) and the slopes are, on average, steeper than the north facing side (21.0° versus 16.4°). The north facing slopes are characterised by steep straight slopes close to the stream (slope of 20.2°, plan curvature of 0.08 and profile curvature of 0.05) and flatter slopes (on average 9.4°) closer to the edge of the watershed (*light green vs. dark green areas*). These differences are shown in Figure 8, which gives a profile graph of three profile lines in the Lower Gordon Gulch Valley (*Figure 7 indicates the position of the profile lines*). Although not as prominent as on the north facing slopes, the south facing slope contains a flatter area as well (●).

Beside these differences there are clear differences between these landscape categories in vegetation type and density, probably as a consequence of the higher exposure of the south facing slopes (1.8 10^6 Wh m^{-2} $year^{-1}$ versus 1.4 10^6 Wh m^{-2} $year^{-1}$). Vegetation at the south facing slopes contains a lower tree density (on average 25.4%), mostly consisting of coniferous trees (*Pinus ponderosa*) and a higher density of undergrowth (on average 47.5%), which consists mostly out of herbaceous and deciduous shrubs and grasses. The north facing slopes on the contrary have a high density (on average 50.6%) of

coniferous trees (*Pinus contorta*) and a lower density (on average 20.3%) of undergrowth, which often consists of pine shrubs, groundcover shrubs, grasses and some mosses.
Runoff features[5] are most dominant on the south facing slopes (58.5% of the fieldpoints on the south facing slopes show runoff features), especially little terraces behind the undergrowth vegetation can be found. This dominance corresponds to the steep slopes and the high erosion value (-0.08 m). Striking is that on the steep north facing slopes the erosion value is higher (-0.09 m), though little runoff features are found (only 17.4% of the fieldpoints on the steep north facing slopes show runoff features). On the contrary the flat north facing slopes, which are showing a very small erosion value (-0.01 m), has more dominant runoff features (33.3% of the fieldpoints on the flat north facing slopes show runoff features), mainly patches were the litter layer has flushed away, the surface stoniness is very high.

Looking at the geology of the north and south facing slopes, at the south facing slopes granite, biotite gneiss and a mixture can be found (respectively 33.3%, 35.9%, and 25.6%). The north facing slopes are more dominated by granite (at the steep slopes 63.6% and 50.0% at the flat slopes) and to a lesser extent some biotite gneiss (at the steep slopes 22.7%) or a mixture of granite and biotite gneiss (at the steep slopes 9.1% and 37.5% at the flat slopes).

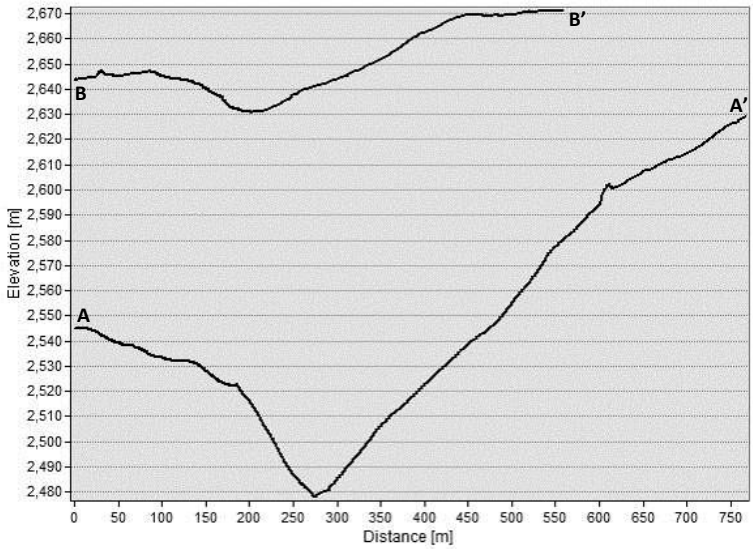

Figure 8: Profile graph of the Gordon Gulch Valley

The south facing slope is furthermore characterised by an area with a high density of exposed bedrock, steep slopes and a high surface stoniness (✖). This area is located at the boundary between the Upper and Lower Gordon Gulch Valley, where the stream enters the Lower Valley and is also known as a knickpoint. This knickpoint is the result of a drop in base level that happened between 7 to 3 Ma BP (Dethier, 2011).

Smooth west area

The smooth west area is very flat compared to the average of the study area (16.6°) and has an average slope of 10.6°. Since the study area descends from west to east, the smooth west area is located at high elevation (2650.8 m). The smooth west area is covered by a moderate density (41.7%) of coniferous trees (*Pinus ponderosa*) and some undergrowth (20.7%), mainly pine shrubs, groundcover shrubs and grasses. The geology of this part of the study area contains granite, biotite gneiss and a mixture of these both, respectively 42.1%, 15.8% and 31.6%. Little runoff features can be found (21.1% of the fieldpoints in the smooth west area show runoff features), which corresponds to the moderate erosion value (-0.05 m).

[5] These include locations were the litter layer has flushed away, the surface stoniness is very high, terraces have formed behind vegetation patches and/or accumulation of soil materials or needles.

In the south of this part ridges can be found in the landscape (★). These ridges are probably caused by the differences in weathering speed of the underlying materials. This results in ridges, where the higher ridges possibly contain more granite and the lower more biotite gneiss (more weathered). Although this was not confirmed by field observations.

Terraces

The terraces can be defined as a moist area with deep soils which are covered by a mixture of coniferous (*Pinus ponderosa* and *Pinus contorta*) and deciduous trees (*Populus tremuloides*) and deciduous shrubs and grasses (86.7%). The soils can be defined as fluvial sedimentary. The slopes are flat (on average 12.4°), although the edges of the creek can be steep. Furthermore, the profile curvature is on average concave, since this is the valley bottom.
Beside this, close to the river the toes of alluvial fans can be found (▲), appearing most clearly at the north side of the river. The deep soils of accumulated materials are covered by deciduous trees (*Populus tremuloides*) and deciduous shrubs and grasses.

Other characteristics

Beside the characteristics of the five landscape categories, another characteristic of the Lower Gordon Gulch valley is the presence of exposed bedrock or tors (*these are visible in the hillshade*). The tors can be found over the whole area, but the density is higher at the south facing slopes.
Furthermore the valley contains some phenomena that indicate the presence of overland flow and the presence of infiltration at certain areas. The presence of overland flow is indicated by areas of which the litter layer is removed. These areas are characterised by a high density of surface stones (often medium or coarse gravels, sometimes grus). Some areas even display a flow pattern or have the shape of a puddle. At places with more vegetation, little terraces have formed behind the vegetation. These runoff features are most present on the steep south facing slopes. Strikingly, runoff features are missing on the lower steep north facing slopes.
The presence of infiltration is indicated by areas located in flatter and accumulating (concave/concave) positions at a slope (■). The accumulation of upslope materials and the infiltration of water results in deeper and moist soils. As a consequence these areas are covered by deciduous trees (*Populus tremuloides*) and deciduous shrubs and grasses.

4.1.2 Cross tables of the landscape characteristics

To give an indication of the positive or negative correlations between the landscape characteristics, and the degree of these correlations we made a cross table. In the table the Pearsons correlation coefficients (r) are showed, the values of r larger than 0.4 and smaller than -0.4 have been highlighted in grey. Furthermore the significance of these correlations has been checked. Because this cross table is large, the table can be found in Appendix (C).

Table C1 shows the correlations between the field characteristics. Obvious correlations are the correlation between somehow related field characteristics. For example, the correlations between flow accumulation, erosion and TWI which give all an indication of the flow path of water in the study area. Furthermore, all vegetation related field characteristics are correlated (vegetation height, LAI, LAI_{tree}, tree cover and undergrowth cover). Striking is that undergrowth cover is negatively correlated to the other vegetation related landscape characteristics, this means that when undergrowth cover increases the other vegetation characteristics will decrease. Global annual radiation is strongly correlated to the vegetation related landscape characteristics, where an increase in global annual radiation result in a decrease in tree cover, LAI, LAI_{tree}, and vegetation height and an increase in undergrowth cover. Since aspect and global annual radiation are strongly correlated, the vegetation related landscape characteristics are strongly correlated to aspect as well. Parent material is strongly correlated to erosion, TWI and flow accumulation.
Other strong correlations are the negative correlation between TWI and slope, the positive correlation of global annual radiation and distance to streams with elevation, the negative correlation of flow accumulation and undergrowth cover with elevation, the positive correlation between of flow accumulation and parent material with undergrowth cover, the positive correlation of erosion and flow accumulation to distance to streams and the negative correlation between distance to streams and vegetation height.

Aspect north/south is strongly correlated to aspect, global annual radiation, vegetation height, tree cover and to the characterising areas. The characterising areas are only correlated to global annual radiation.

Table 7: Site characteristics for all characterising areas

		Elevation [m]	plan curvature {-]	profile curvature [-]	Slope [°]	Erosion [m]	vegetation height [m]	annual global radiation [Wh m^{-2}]	TWI [-]	LAI [-]	LAI_{tree} [-]	tree cover[1] [%]	under-growth cover[1] [%]	distance to exposed bedrock[1] [m]	runoff features[1*]	geology[1*]
(i) south facing slopes	mean	2577.70	0.32	0.21	21.04	-0.08	3.93	$1.8\ 10^6$	5.45	5.64	4.66	25.39	47.49	64.05	*n=41* 0 41.5% 1 58.5%	*n=39* 1 33.3% 5 0.0% 2 35.9% 6 0.0% 3 25.6% 7 2.6% 4 2.6%
	min.	2436.32	-759.98	-989.62	0.00	-17.95	0.04	$5.1\ 10^5$	-0.27	5.11	0.00	0.00	2.00	1.00		
	max.	2711.45	1171.14	767.62	79.69	0.00	17.05	$1.9\ 10^6$	14.88	6.06	5.92	70.00	100.00	100.00		
	sd.	59.37	22.20	25.95	7.52	0.36	2.45	$9.5\ 10^4$	1.17	0.13	1.34	22.73	28.29	43.61		
(iia) steep north facing slopes	mean	2535.65	0.08	0.05	20.24	-0.09	7.08	$1.3\ 10^6$	5.27	5.72	5.69	52.71	12.52	69.26	*n=24* 0 83.3% 1 16.7%	*n=23* 1 65.2% 5 0.0% 2 21.7% 6 0.0% 3 8.7% 7 0.0% 4 4.3%
	min.	2436.25	-176.33	-246.35	0.00	-14.79	0.39	$4.8\ 10^5$	0.89	5.44	2.63	15.00	3.00	1.00		
	max.	2625.82	199.49	227.38	60.09	0.00	15.7	$1.9\ 10^6$	15.59	5.94	5.94	80.00	70.00	100.00		
	sd.	42.75	15.66	16.07	6.34	0.55	2.24	$1.6\ 10^5$	1.16	0.09	0.22	20.64	14.81	43.39		
(iib) flat north facing slopes	mean	2560.75	0.64	0.48	9.39	-0.01	4.81	$1.6\ 10^6$	5.63	5.64	5.44	42.22	28.33	79.00	*n=9* 0 66.6% 1 33.3%	*n=8* 1 50.0% 5 12.5% 2 0.0% 6 0.0% 3 37.5% 7 0.0% 4 0.0%
	min.	2499.35	-159.07	-164.41	0.00	-0.74	0.04	$7.4\ 10^5$	0.87	4.77	0.02	30.00	0.00	3.00		
	max.	2635.60	206.74	192.65	53.32	0.00	10.65	$1.9\ 10^6$	13.34	5.89	5.89	75.00	85.00	100.00		
	sd.	36.87	13.33	13.9	5.01	0.02	1.79	$9.9\ 10^4$	1.43	0.14	0.77	17.70	24.75	41.69		
(iii) smooth west area	mean	2650.81	0.59	0.55	10.64	-0.05	4.20	$1.7\ 10^6$	5.95	5.48	5.06	40.25	21.50	69.60	*n=18* 0 77.8% 1 22.2%	*n=18* 1 38.9% 5 0.0% 2 16.7% 6 0.0% 3 33.3% 7 5.6% 4 5.6%
	min.	2578.93	-451.89	-694.23	0.00	-9.88	0.05	$5.7\ 10^5$	0.07	4.98	1.56	10.00	5.00	5.00		
	max.	2726.17	729.94	638.98	75.44	0.02	12.93	$1.9\ 10^6$	17.83	5.95	5.95	90.00	80.00	100.00		
	sd.	28.46	16.38	18.76	6.32	0.37	1.95	$1.0\ 10^5$	1.59	0.22	0.75	22.68	21.47	42.82		
(iv) terraces	mean	2513.49	-0.53	2.27	12.40	-1.18	6.50	$1.6\ 10^6$	7.70	5.69	5.56	35.83	86.67	100.00	*n=6* 0 100.0% 1 0.0%	*n=6* 1 0.0% 5 33.3% 2 0.0% 6 66.7% 3 0.0% 7 0.0% 4 0.0%
	min.	2435.53	-312.87	-248.99	0.00	-18.05	0.14	$6.1\ 10^5$	0.81	5.46	3.1	0.00	70.00	100.00		
	max.	2590.35	257.23	281.66	56.68	0.38	15.32	$1.8\ 10^6$	20.19	5.87	5.88	70.00	100.00	100.00		
	sd.	46.20	18.93	21.12	6.42	2.41	2.73	$1.4\ 10^5$	3.55	0.09	0.33	22.45	12.11	0.00		

[1]these landscape characteristics were only measured for the 100 field locations.
*geology and runoff features are categorical data, therefore the percentage of observation in each category are showed. The categories for runoff features are present (1) and not present (0), the categories for geology are granite (1), biotite gneiss (2), mixture of biotite gneiss/granite (3), mixture of biotite gneiss/granite/schist (4), alluvial material (5), fluvial sedimentary (6), and accumulated materials (7).

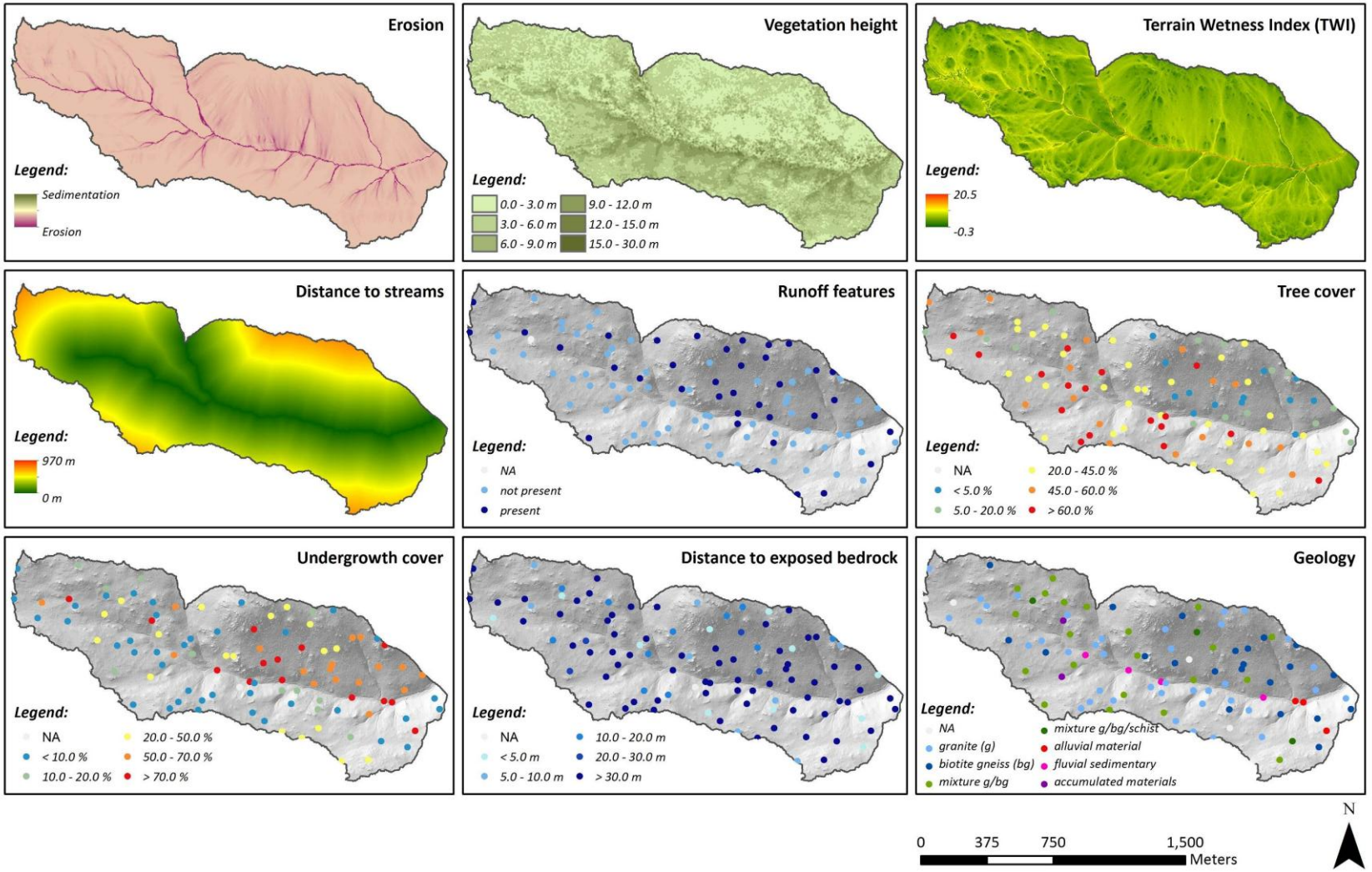

Figure 9a: Maps of the landscape characteristics of the study area

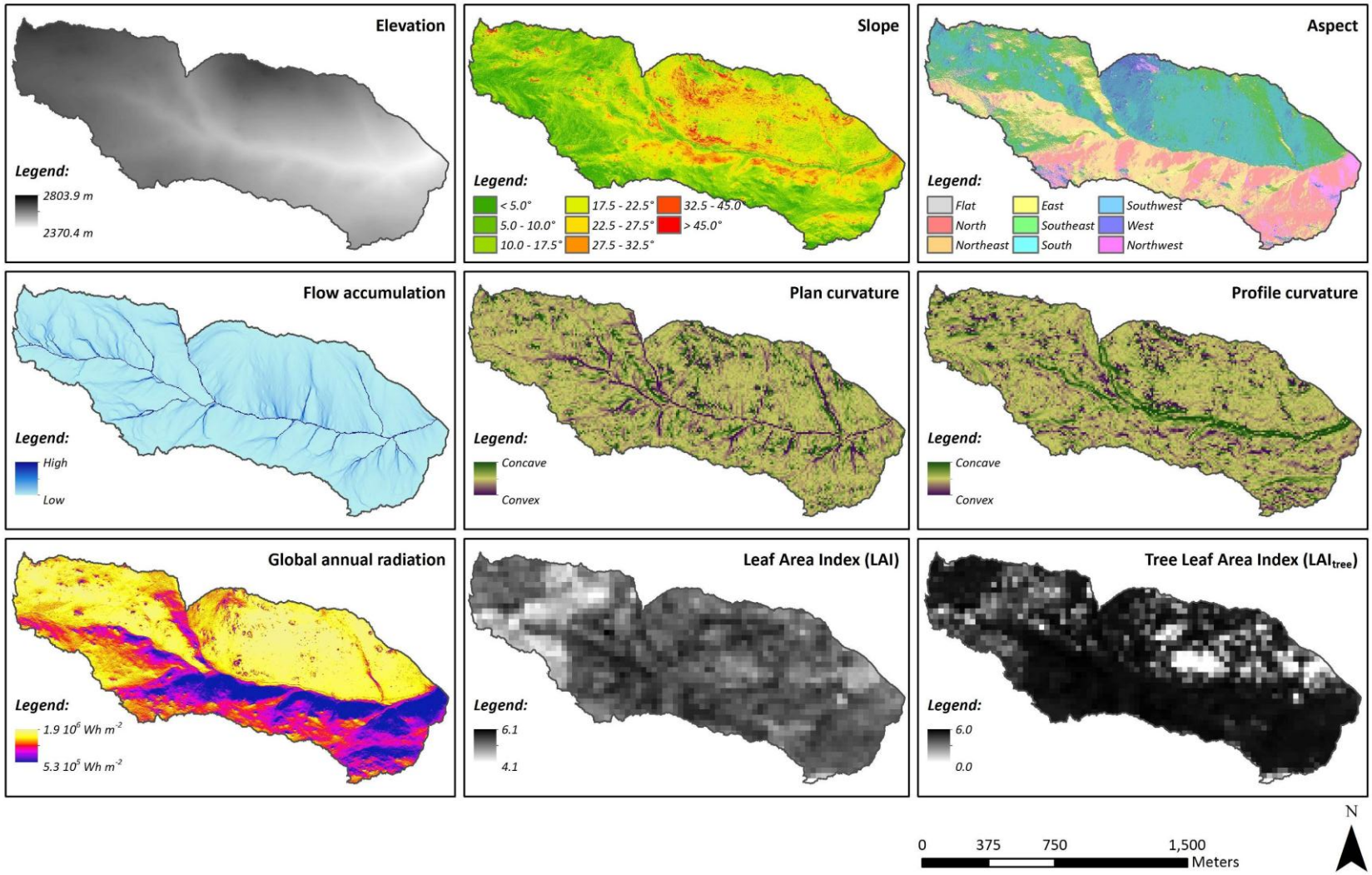

Figure 9b: Maps of the landscape characteristics of the study area

4.2 Soil characteristics

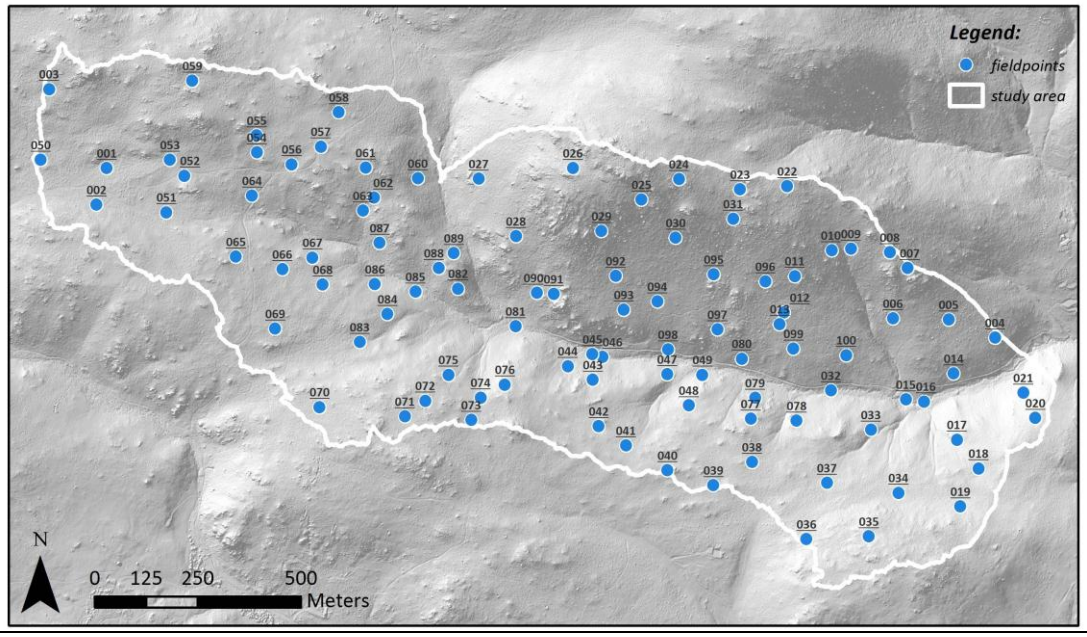

Figure 10: Field observations

This section will shortly discuss the field observations. This is supported by Table 8, Table 9 and Figure 10. Besides, Figure 11 shows a selection of the spatial variability of these properties. The texture of the soils in the Gordon Gulch valley can be categorised as loamy sand (70-85% sand, 0-30% silt and 0-15% of clay) or sand (85-100% sand, 0-15% silt and 0-10% of clay). The organic matter content is on average 6.40%, however, the standard deviation (5.23%) indicate that the organic matter content varies much around the mean. This is confirmed in Table 10, which show the range and variation of the OM percentages between the soil horizons. The pH of the soils in the area can be characterised as moderate acid soils (pH between 5.1 and 6.0), the minimum and maximum in Table 8 (respectively 3.87 and 7.05) show, however, that there are samples which are more acidic or more alkaline than this range. Just like the standard deviation of the organic matter content, the standard deviations of the other characteristics are quite large, indicating a large variation of the values of these characteristics, Table 10 and the next section will emphasise this.

Nevertheless the soils of the Gordon Gulch Valley can be described as generally shallow soils with a high stoniness, a weak granular structure and with a large variation in the thickness and presence of the litter/duff layer. Charcoal is present in about 40 % of all soil pits. The average of the bulk density of the soils is quite low, because the bulk density of sandy soils typically lies between 1.5 and 1.7 g cm^{-3}. There are even several soils (soil pits: 001, 008, 011, 018, 030, 032, 033, 040, 042, 043, 045, 053, 057, 060, 064, 080, 081, 083, 085, and 100) with a bulk density below 1.0 g cm^{-3}. Three of these soil pits have a bulk density even below the 0.7 g cm^{-3}, soil pits 001, 011, and 040, with a bulk density of respectively 0.47, 0.44 and 0.66 g cm^{-3}. Soil pits 011 and 040 probably contain a lot of duff. Soil pit 001 is located at an accumulation position at the toe of a slope. As a consequence the soils are deep (C horizon starts at 36 cm), very moist (volumetric water content of 42.35% and groundwater at 40 cm), contain little stones and have a high amount of organic matter (41.86% in the upper 13 cm). Beside soil pit 001, there are a few other accumulation positions in the study area (section 4.1 and Figure 7 (■)), these involve soil pits 018, 063, and 083. These soil pits, except for 083, are just like, however not as prominent as soil pit 001, deep, moist, contain quite high amounts of organic matter in the whole soil profile, and contain little stones. Although soil pit 083 is located at an accumulation position, especially the lower part of the soil profile does not suit the characteristics of this position, the organic matter content is low (3.08%), the C horizon starts at 8 cm and contains a lot of stones (25%). Nevertheless the upper part of the soil pit is moist (moisture content 38.05%) and contain a high organic matter content (13.38%), and suits the characteristics of an accumulation position better.

Other notable soil pits are 032 and 033. Both soil pits are be palaeosols, which is indicated by the horizon beneath the Bw horizon which contain a higher content of organic matter (respectively 8.62%

versus 3.33% and 12.87% versus 6.19%). Soil pit 032 is located along the river, the 2Ah horizon is probably a former terrace level. The Bw horizon on top of this 2Ah horizon contains more sand (94.79% versus 84.43%), which could indicate a flood event. Soil pit 033 is located at a higher position, on the slope along a gully were water from upslope accumulates and drains towards the Gordon Gulch creek. The former soil probable is buried by soil materials from upslope by a flood event.
Another interesting soil pit is located at the terrace level, namely 045. The soil profile is an alternation of layers with gravels (up to 50%) and more clayey layers. These layers can indicate the amount of water in the Gordon Gulch creek and the speed of the water. Furthermore this profile contains a lot of charcoal at 25, 50, 80, and 110 cm.

The soil properties are not all normally distributed. When the skewedness and kurtosis highly deviate from zero, this indicated that these soil properties differ from the normal distribution. Table 8 show that the organic matter content, the moisture content, the moisture content of the upper 7 cm, the volumetric water content, the thickness of the litter layer, the thickness of the top horizon and the thickness of the mid horizon are not normally distributed.

Table 8: Summary of the continuous soil properties

	n	min.	max.	mean	sd.	skewedness	kurtosis
OM [%]	177	1.34	41.86	6.40	5.23	3.68	18.63
pH [-]	175	3.87	7.05	5.49	0.59	0.11	-0.36
sand [%]	176	74.65	96.85	88.67	3.99	-0.33	-0.08
silt [%]	175	2.76	23.71	10.43	3.80	0.41	-0.06
clay [%]	175	0.00	2.99	0.88	0.57	1.05	1.18
moisture content [mass%]	177	0.00	84.42	7.55	8.16	5.27	43.26
roots [%]	235	0.00	40.00	11.67	7.45	0.93	1.11
stoniness [%]	250	0.00	100.00	28.05	18.62	1.24	2.32
bulk density [g cm^{-3}][6]	100	0.44	1.68	1.17	0.23	-0.50	0.47
soil porosity [%][6]	100	36.78	83.54	55.76	8.74	0.51	0.48
moisture content [mass%][6]	100	0.00	90.60	8.96	9.47	6.46	52.47
soil water-filled pore space [%][6]	100	0.00	51.43	16.62	8.59	1.09	1.60
volumetric water content [volume%][6]	100	0.00	42.35	9.35	5.56	2.33	10.70
thickness Oi/Oh [cm][7]	78	0.50	24.00	2.78	3.15	4.20	24.09
thickness top horizon [cm][7]	100	0.50	43.00	9.43	8.10	1.70	3.43
thickness mid horizon [cm] [7]	55	2.50	68.00	17.21	12.69	1.78	3.86
starting depth C horizon [cm][7]	100	0.50	52.00	15.61	11.09	0.96	0.75

Table 9: Summary of the categorical soil properties

	n	observations
structure	223	
SG		34
WE/GR		171
MO/GR		16
ST/GR		2
duff	177	
not present		154
present		23
charcoal	178	
not present		125
present		53

The results of the one-way ANOVA (F-test) and the Chi-square test (Table 10 and Table 11) show that the differences between the horizons are all significant with a $p < 0.05$, except for the pH and the presence of charcoal. The pH varies only little between the horizons. The organic matter content logically decreases with the depth of the soil. The upper horizons of the soils are sandier than the lower horizons and the percentages of silt and clay increase in the lower horizons. Just like the organic matter content, the moisture content and the amount of roots decrease with the depth of the

[6] *These properties are not available for each soil horizon, but are only measured for the upper 7.0 cm of the soil for each soil pit*
[7] *These properties are not available for each soil horizon, but are only available for each soil pit*

soil. The decrease of the moisture content however, is less significant. Stoniness increases with depth, with a high mean in the C horizon, which often consist of mobile regolith, saprolite or saprock. The structure in the top horizons is dominated by single grain and weak granular, this shifts to weak and moderate granular in the mid horizons and towards weak granular again in the C horizons. Duff is logically only present in the top horizon, where the distinction between duff, litter and Ah horizon was sometimes hard to make. Although the presence of charcoal decreases with the depth (respectively 35%, 26% and 11% in the top, mid an C horizons), this difference is not statistically significant.

Table 10: Soil properties per horizon

		OM [%]	pH [-]	sand [%]	silt [%]	clay [%]	moisture content [mass%]	roots [%]	stoniness [%]
top horizon	n	100	100	99	99	99	100	100	99
	min.	1.56	4.11	79.41	2.76	0	0.5	0	0
	max.	41.86	6.79	96.85	19.58	2	84.42	40	70
	mean	8.28	5.51	89.18	10.09	0.72	9.41	13.61	19.33
mid horizon	n	58	57	58	57	57	58	58	57
	min.	1.96	3.87	80.09	3.7	0	1.25	2	0
	max.	12.96	6.69	96.14	19.09	2.99	14.29	35	70
	mean	4.16	5.52	88.55	10.38	1.01	5.43	13.17	24.7
C horizon	n	19	18	19	19	19	19	75	92
	min.	1.34	4.44	74.65	7.04	0.27	0	2	0
	max.	11.48	7.05	92.5	23.71	2.83	22.8	25	100
	mean	3.33	5.27	86.38	12.34	1.28	4.20	7.89	39.84
η^2		*0.069*	*0.015*	*0.044*	*0.032*	*0.080*	*0.032*	*0.121*	*0.243*
p(equal means)		*$4.32\ 10^{-4}$*	*0.1080*	*$5.35\ 10^{-3}$*	*0.0108*	*$1.47\ 10^{-4}$*	*0.0178*	*$4.35\ 10^{-8}$*	*$<2.00\ 10^{-16}$*

The black values indicate that the considered property is statistical significant with $p < 0.05$

Table 11: Categorical soil properties per horizon

	top horizon		mid horizon		C horizon		*Cramer's V*	*p(no association)*
	n	observations	n	observations	n	observations		
structure	97		56		68		*0.26*	*4.38 10^{-4}*
SG		26		2		4		
WE/GR		63		46		62		
MO/GR		7		8		1		
ST/GR		1		0		1		
duff	100		58		19		*0.31*	*2.58 10^{-4}*
not		78		58		19		
present		22		0		0		
present								
charcoal	100		58		19		*0.17*	*0.077*
not		65		43		17		
present		35		15		2		
present								

The black values indicate that the considered property is statistical significant with $p < 0.05$

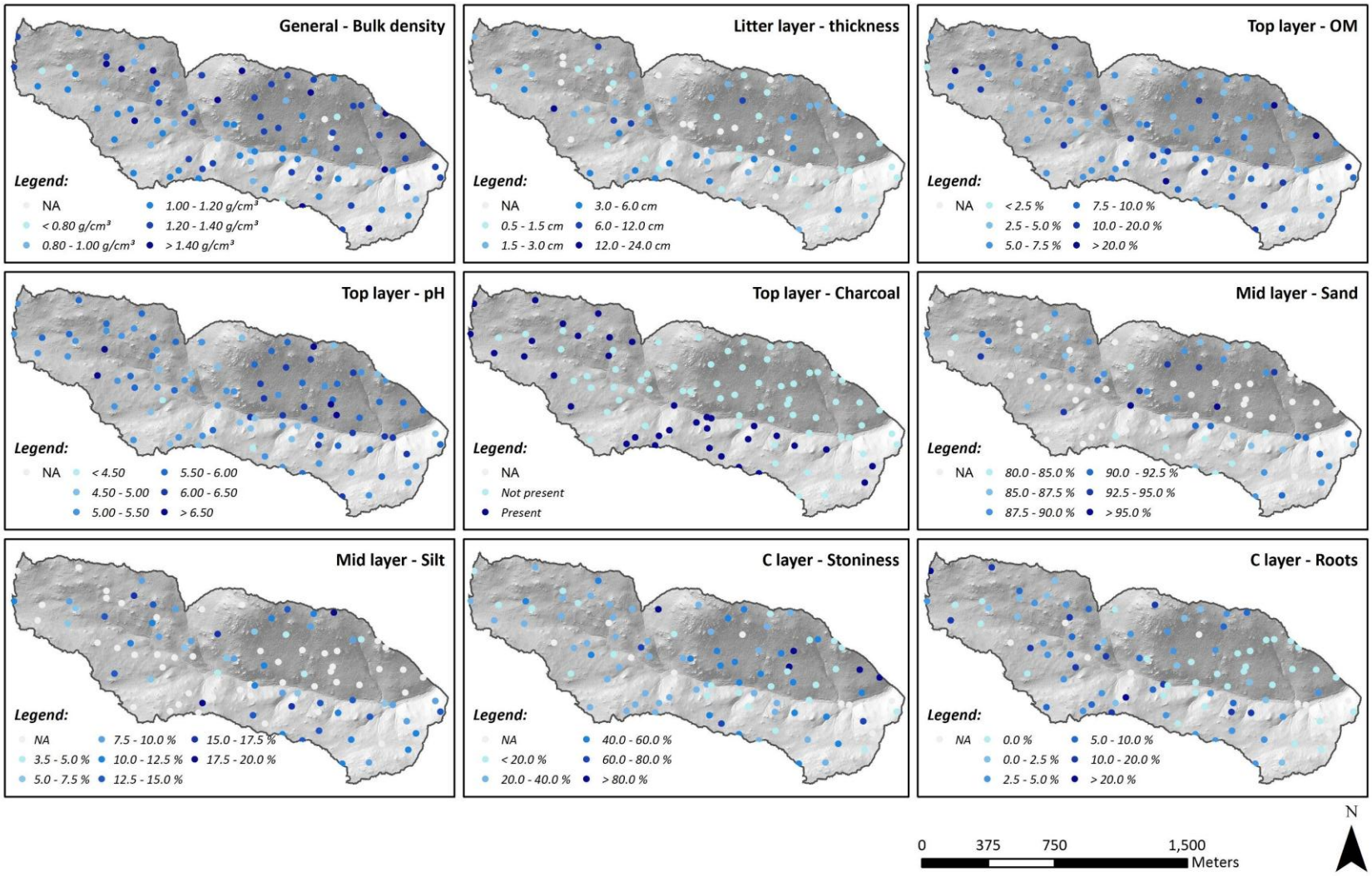

Figure 11: Maps of a selection of soil properties

4.2.1 Differences between the landscape characteristics

Table 12 shows the results of the one-way ANOVA (F-test) for the differences in mean of the soil properties between the (i) south facing slopes, (iia) the steep north facing slopes, (iib) the flat north facing slopes, (iii) the smooth west area and (iv) the terraces.

Table 12: Soil properties, differences between the five characterising areas

		(i) south facing slopes	(iia) steep north facing slopes	(iib) flat north facing slopes	(iii) smooth west area	(iv) ter-races	η^2	p(equal means)
general upper 7 cm of the soil	bulk density [g/cm³]	1.24	1.17	1.09	1.13	1.05	0.032	0.0757
	soil porosity [%]	53.39	55.99	58.97	55.52	56.40	0.032	0.0768
	soil water-filled pore space [%]	15.35	15.98	14.88	18.88	22.96	0.000	0.9224
	moisture content [mass%]	7.17	7.75	8.22	12.76	14.48	0.000	0.8353
	volumetric water content [volume%]	8.16	8.91	8.50	11.27	14.11	0.002	0.6778
	thickness Oi/Oh horizon [cm]	2.12	2.77	2.29	4.33	2.67	0.000	0.8485
	thickness top horizon [cm]	**11.71**	**5.08**	**5.56**	**6.25**	**27.67**	**0.065**	**0.0103**
	thickness mid horizon [cm]	16.75	17.79	17.71	11.95	29.75	0.007	0.5458
	starting depth C horizon [cm]	18.18	13.78	16.75	11.55	25.00	0.010	0.3412
top horizon	OM [%]	6.85	9.00	10.75	9.37	7.81	0.033	0.0719
	pH [-]	**5.64**	**5.36**	**5.22**	**5.45**	**5.92**	**0.053**	**0.0216**
	sand [%]	**90.74**	**87.22**	**86.21**	**89.00**	**91.68**	**0.154**	**$5.76\ 10^{-5}$**
	silt [%]	**8.60**	**11.97**	**13.20**	**10.18**	**7.63**	**0.161**	**$3.88\ 10^{-5}$**
	clay [%]	0.66	0.81	0.59	0.82	0.69	0.002	0.1864
	moisture content [mass%]	6.24	10.12	9.02	14.86	10.62	0.013	0.2622
	roots [%]	14.80	10.58	10.56	13.50	22.50	0.038	0.0529
	stoniness [%]	**23.59**	**19.17**	**12.75**	**18.00**	**4.17**	**0.059**	**0.0155**
mid horizon	OM [%]	3.22	4.76	3.80	4.67	5.40	0.037	0.1480
	pH [-]	5.66	5.29	5.40	5.39	6.12	0.030	0.2000
	sand [%]	89.18	87.36	86.59	88.68	91.96	0.050	0.0903
	silt [%]	9.74	11.44	12.41	10.08	7.52	0.058	0.0718
	clay [%]	1.08	1.20	1.00	0.81	0.52	0.001	0.0700
	moisture content [mass%]	4.15	6.26	4.76	6.22	7.67	0.028	0.2086
	roots [%]	15.48	12.80	10.00	12.00	11.40	0.058	0.0678
	stoniness [%]	28.57	32.00	21.67	17.00	5.60	0.000	0.9343
C horizon	OM [%]	2.30	3.63	2.70	2.54	8.19	0.104	0.1779
	pH [-]	**4.99**	**5.62**	**5.95**	**4.72**	**5.90**	**0.270**	**0.0271**
	sand [%]	84.43	86.83	86.36	87.14	91.95	0.092	0.2069
	silt [%]	13.93	11.86	13.37	11.93	7.23	0.065	0.2916
	clay [%]	1.64	1.31	0.27	0.93	0.81	0.141	0.1129
	moisture content [mass%]	2.57	2.52	3.67	2.81	17.28	0.025	0.1587
	roots [%]	7.79	8.74	5.70	8.25	8.50	0.002	0.1568
	stoniness [%]	49.72	40.91	39.38	26.25	15.00	0.019	0.1900

The black values indicate that the considered property is statistical significant with $p < 0.05$

The differences between the characterising areas are statistically significant ($p < 0.05$) for the thickness of the top horizon, for pH, sand, silt and stoniness in the top horizon, and for pH in the C horizon. Not surprisingly the deep and moist terrace soils have a thick top horizon (27.7 cm), on the contrary the west smooth area has a very thin top horizon (4.9 cm), followed by the thin top horizon at the flat and steep north facing slopes (5.6 cm and 6.4 cm respectively), the south facing slopes have moderately thick top horizons (11.7 cm).

The values for the pH of the top horizon for the five characterising areas are close together, nevertheless these small differences proved to be statistically significant. The north facing slopes have a low pH (respectively 5.4 and 5.2), the pH is highest at the terraces, and the smooth west area is more acid than the south facing slopes. The pH in the C horizon shows a completely different pattern. Here the pH is highest at the flat north facing slopes (6.0), followed by the terraces (5.9) and the steep

north facing slopes (5.6), and lowest at the south facing slopes and the smooth west area (respectively 5.0 and 4.7). Striking is that the pH decreases with the depth at the smooth west area (5.5-5.4-4.7), increases with the depth at the flat north facing slopes (5.2-5.4-5.9), is almost constantly high at the terraces (5.9-6.1-5.9), and is variable at the steep north facing slopes (5.4-5.3-5.6), and the south facing slopes (5.6-5.6-5.0).
Sand is more dominantly present at the terraces (91.7 %), which indicate the influence of the creek. The south facing slopes and the smooth west area have a high amount of sand as well (respectively 90.7 % and 89.0 %). The north facing slopes a smaller percentage sand (87.2 % at the steep north facing slopes and at the 86.2% flat north facing slopes). Silt shows, not surprisingly, exactly the opposite pattern.
Stones in the top soil can be dominantly found at the south facing slopes and the steep north facing slopes (respectively a stoniness of 23.6 % and 19.2 %). At the sloping areas stoniness is high in the whole profile. The terraces have little stones (4.2 %).
Striking is the high moisture value of the top soil of the smooth west area, an explanation for this high value is that the fieldpoints of the smooth west area were collected after a rainy day.
For the other soil properties the division in the five characterising areas is statistically not important.

Table 13 shows the results of the chi-square test for homogeneity for the differences between the (i) south facing slopes, (iia) the steep north facing slopes, (iib) the flat north facing slopes, (iii) the smooth west area and (iv) the terraces.

For structure and the presence of duff and charcoal in the top horizon, and for the presence of charcoal in the C horizon the differences between the characterising areas are statistically significant ($p < 0.05$). The structure of the top horizon is dominated by weakly granular on the south facing slopes, the steep north facing slopes, the flat north facing slopes and in the smooth west area, single grain is a common structure in these areas as well. In the smooth west area there are also some soils with a moderately granular structure. The terrace soils have a better structure and is dominated by moderately granular. Duff is more present at the north facing slopes, and the smooth west area than at the south facing slopes and the terraces. Duff was most often found at the flat north facing slopes. Charcoal is more present in the top soils of the north facing slopes and the smooth west area than in the top soils of the south facing slopes. An explanation can be that the tree cover of the south facing slopes is less dense (Table 7). If charcoal is present in the terrace soils, than it is present through the whole profile as the terrace soils consist of layer of accumulated materials from the whole area.
For the other soil properties the division in the for characterising areas is statistically not important.

Table 13a: Categorical soil properties of the top horizons, differences between the five characterising areas

		(i) south facing slopes	(iia) steep north facing slopes	(iib) flat north facing slopes	(iii) smooth west area	(iv) ter-races	*Cramer's V*	$p_{(no\ association)}$
top horizon	structure	*n=41*	*n=23*	*n=8*	*n=19*	*n=6*	*0.35*	*$2.91\ 10^{-4}$*
	SG	26.8	26.1	37.5	31.6	0.0		
	WE/GR	70.7	69.6	62.5	57.9	33.3		
	MO/GR	2.4	4.4	0.0	10.5	50.0		
	ST/GR	0.0	0.0	0.0	0.0	16.7		
	duff	*n=41*	*n=24*	*n=9*	*n=20*	*n=6*	*0.31*	*0.0466*
	not present	85.4	79.2	44.4	70.0	100.0		
	present	14.6	26.3	55.6	30.0	0.0		
	charcoal	*n=41*	*n=24*	*n=9*	*n=20*	*n=6*	*0.50*	*$5.65\ 10^{-5}$*
	not present	92.7	41.7	44.4	45.0	66.7		
	present	7.3	58.3	55.6	55.0	33.3		

Table13b: Categorical soil properties of the top horizons, differences between the five characterising areas

		(i) south facing slopes	(iia) steep north facing slopes	(iib) flat north facing slopes	(iii) smooth west area	(iv) ter-races	*Cramer's V*	$p_{(no\ association)}$
mid horizon	structure	*n=21*	*n=14*	*n=6*	*n=10*	*n=5*	*0.36*	*0.0765*
	SG	4.8	0.0	0.0	0.0	20.0		
	WE/GR	80.9	100.0	100.0	60.0	60.0		
	MO/GR	14.3	0.0	0.0	40.0	20.0		
	ST/GR	0.0	0.0	0.0	0.0	0.0		
	charcoal	*n=21*	*n=15*	*n=7*	*n=10*	*n=5*	*0.17*	*0.7957*
	not present	81.0	73.3	71.4	60.0	80.0		
	present	19.0	26.7	28.6	40.0	20.0		
C horizon	structure	*n=25*	*n=18*	*n=7*	*n=16*	*n=2*	*0.25*	*0.4114*
	SG	16.0	0.0	0.0	0.0	0.0		
	WE/GR	80.0	100.0	100.0	93.8	100.0		
	MO/GR	4.0	0.0	0.0	0.0	0.0		
	ST/GR	0.0	0.0	0.0	6.2	0.0		
	charcoal	*n=8*	*n=5*	*n=1*	*n=8*	*n=2*	*1.00*	*0.001*
	not present	100.0	100.0	100.0	100.0	0.0		
	present	0.0	0.0	0.0	0.0	100.0		

The black values indicate that the considered property is statistical significant with $p < 0.05$

4.2.2 Cross tables of the soil properties

To give an indication of the positive or negative correlations between (i) the soil properties and (ii) the soil properties and the landscape characteristics, and the degree of these correlations we made two cross tables. In the tables the Pearsons correlation coefficients (r) are showed, the values of r larger than 0.4 and smaller than -0.4 have been highlighted in grey. Furthermore the significance of these correlations has been checked. Because these cross tables are large, the tables can be found in Appendix (D).

Table D1 shows the correlation between the soil properties of the top horizons and the mid horizons, the C horizon is not included in this table, because too little data were available.
An obvious correlation is the correlation between the sand and silt percentages, this correlation is for both horizons (top vs. top horizon and mid vs. mid horizon) strong and highly significant (p-value < 0.001). An increase of sand will probably result in a decrease of silt. The same applies to a lesser extent for the correlation between the percentages of sand and clay and the opposite applies for the correlation between the percentage of silt and clay (an increase of silt will result in a decrease of clay and the other way around). These correlations are logical as the sum of the three should be 100%, and an increase in sand will automatically result in a decrease in silt and/or clay.
Other strong correlations are the ones between the bulk density and the calculated properties based on bulk density (porosity, water-filled pore space, moisture content, volumetric water content). These correlations are not surprisingly as these properties are all calculated with the measured bulk density.
There is a positive correlation between the top and mid horizon for pH, moisture content, and stoniness. Furthermore there is a strong positive correlation between organic matter of the horizons and the moisture content of the horizons, moisture content (based on bulk density) and water-filled pore space. This means that organic matter increases when the moisture content or water-filled pore space increases and the other way around. Furthermore there is a positive correlation between roots in the top horizon and moisture content and volumetric water content.

Table D2 shows the correlation between the soil properties of the top horizons and the mid horizons and the field characteristics of the study area.
There is a strong correlation between the bulk density related soil properties and aspect, vegetation height, parent material and distance to streams. The vegetation related landscape characteristics (vegetation height, LAI, LAI_{tree}, tree cover and undergrowth cover) correlate strongly with the pH in the top soil and to a lesser extent to the pH in the mid horizon, with only a positive correlation between undergrowth cover and pH. This means that when pH increases in, undergrowth cover decreases and tree cover increases. Plan and profile curvature are negatively correlated to bulk

density and porosity. The stoniness in the mid horizon is correlated to erosion (positively), flow accumulation (negatively) and TWI (negatively). Surprisingly erosion is correlated to sand, silt and clay percentages in the mid horizon.
Other strong correlations are the negative correlation between aspect and charcoal, the positive correlation between root density in the mid horizon and the slope, the negative correlation between organic matter content and elevation, the negative correlation between runoff features and organic matter in the mid horizon, the negative correlation between stoniness in the mid horizon and undergrowth cover, parent material and distance to exposed bedrock.
The characterising areas are correlated to sand, silt and clay in the top horizon and to the presence of charcoal in the top horizon. The aspect north/south is not strongly correlated to any of the soil properties.

4.3 Hydrological analysis

Based on literature, the most important hydrological processes of the Gordon Gulch Valley are described in Appendix (E). In this appendix the dominating hydrological processes identified in the study area are discussed in detail. First a definition of the processes is given, second the soil properties and site characteristics influencing these hydrological processes are discussed and finally a methodology to estimate or calculate the hydrological processes is proposed. Figure 12 shows these hydrological processes in a schematic overview.

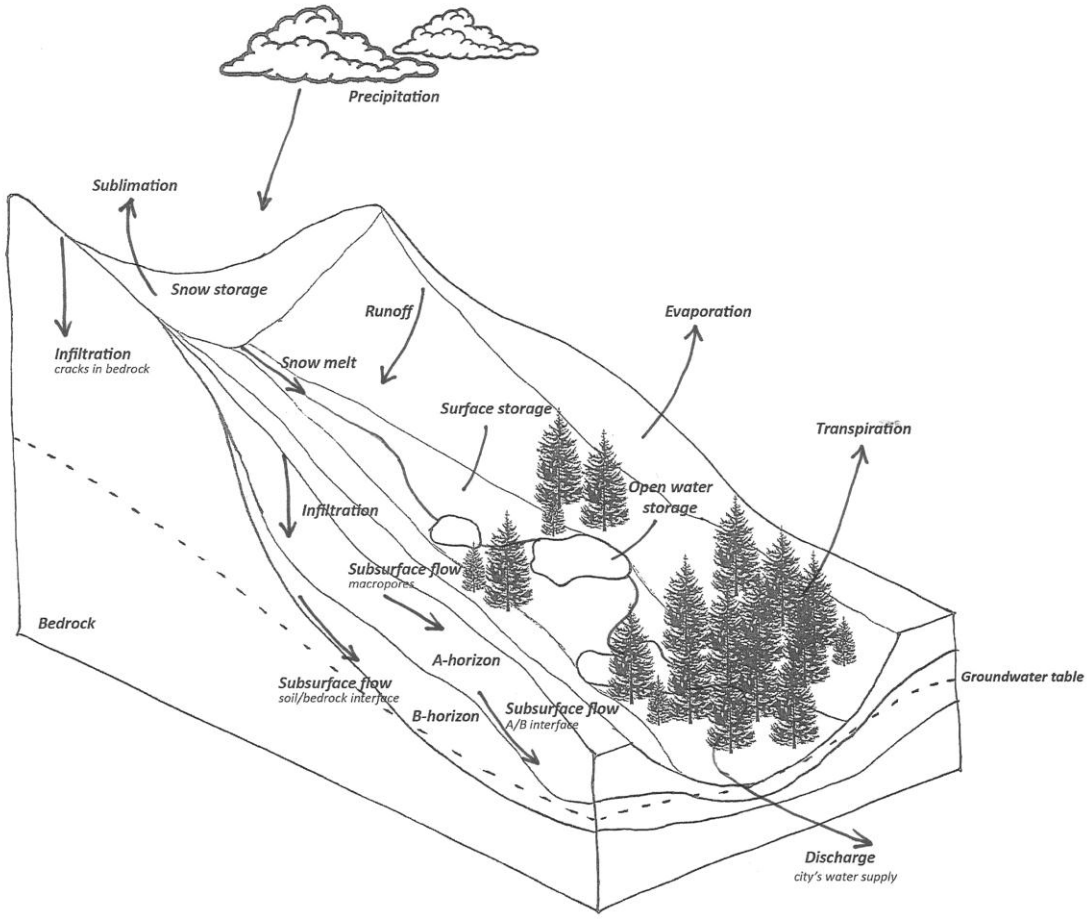

Figure 12: Schematic overview of the most important hydrological processes.

Table 14 summarises the information of Appendix (E). In the first column the hydrological process can be found, the second and third column describes point wise the soil properties and site characteristics influencing these hydrological processes. In the last column the information needed to estimate or calculate these hydrological processes can be found.

Table 14: Hydrological processes (summary of appendix E)

	soil properties	site characteristics	calculation or estimation
precipitation		elevation	
evapotranspiration	soil water content	vegetation characteristics solar radiation air temperature and humidity wind	min. temperature max. temperature humidity wind speed daily global radiation sunshine hours
water storage in snow	-	elevation (precipitation and temperature) topography wind vegetation cover	depth of the snow pack area of the snowpack compaction of the snowpack
snowmelt	-	temperature solar exposure (global daily radiation and vegetation cover) aspect	unknown
sublimation	unknown	wind speed temperature specific humidity net radiation	unknown
runoff	texture soil saturation soil water holding capacity macroporosity organic matter soil depth permeability hydraulic conductivity	steepness of slope vegetation density exposed bedrock precipitation	precipitation evapotransipiration soil saturation soil water holding capacity
infiltration	macropores structure texture fractured nature of bedrock soil saturation organic matter soil depth permeability hydraulic conductivity	vegetation density (soil cover) precipitation steepness of slope	soil water holding capacity pedotransfer functions for soil water content
macropore flow	roots biological activity soil moisture porosity organic matter slickensides	vegetation	unknown
subsurface flow	differences in hydraulic conductivity texture structure soil depth horizon depth permeability	subsoil and bedrock topography	pedotranfer functions for hydraulic conductivity
soil storage capacity and soil saturation	soil depth porosity bulk density redoxomorphic features (mottles and concretions of Fe and Mg)	-	pedotransfer functions for soil water content

4.3.1 Hydrologic modeling – SWAP

Table 15 shows the hydrological fluxes per month for all locations together. Most obvious is that the simulated runoff in the area is zero during the whole year and for all locations. This means that runoff plays no role in the area.
Most precipitation occurs in spring, in the months April, May, June and July. The high standard deviations during these months show that there are large differences between the years, since the variations in rain between the locations is negligible. Snow is falling from October to March and melts from October to May, with a maximum in March (on average 3.04 cm).
Interception values are highest for March, April, May and July. Especially during March and April the standard deviation is high and suggest that the values are highly variable over the locations or over the years. Transpiration is an important process in the area, values are very high. Values are highest from April to July.
The net bottom flux shows several peaks during the year. In the period from March to July net bottom flux is an important process, furthermore there are relatively high peaks in the months September and November. These peaks correspond to the peaks of the precipitation.
Soil moisture reserves are recharged during the spring, with the highest recharge value in April (on average 0.99 cm). During summer, autumn and winter (June to February) water is extracted from the soils, with high values in August and September (respectively -0.22 and -0.20) and even higher values in November and December (respectively -0.64 and -0.77).
In general we can say that the interannual standard deviations are high, indicating a high variation of hydrological properties between the locations and/or between the different years. Figure 16 shows that both are the case.

The figures of rain, snow rate and snowmelt clearly show that the period November 2009 to September 2012 varied in wetness, where the first year (2009-2010) was a really wet year, that 2010-2011 was slightly drier and that the last year (2012-2012) was extremely dry compared to the previous two years.
Peaks in all hydrological properties reflect the water input of rain and snowmelt during the year. Most rain is falling from April to July and snow is melting during March and April in 2010, during January to March in 2011 and in January and March in 2012.
Interception is extremely high during the snowmelt months. This is an artefact of the modelling approach, because snowmelt is modelled as a rain input and therefore 'falls' on top of the vegetation, where it can intercept. The drop of interception in June in Table 15 can be explained by the dry June in 2011 and 2012 when looking at Figure 16. Both transpiration and evaporation approximately reflect the seasonal pattern, with high values in spring and summer and low values in the winter, although there are some sudden drops in this pattern, for example in September 2010, June, August and October 2011, and June 2012 for evaporation and in June and October 2011, and June 2012 for transpiration. Also some peaks can be observed in the transpiration graph for the months September 2011 and July 2012. If we look at the other hydrological properties, these drops and peaks of evaporation and transpiration are clearly reflected by the rainfall in the area.
Rain and snowfall were not allowed to vary spatially. Since the snow rate is temperature dependent and temperature varies over the area, variation appears for rain and snowfall over the area in the month February for all years and for March in 2010.
Groundwater input (net bottom outflux) is important from March to July in 2010, from April to June and September 2011 and in June 2012. Reflecting especially the rainy periods during or just after the snowmelt period. Soil water storage is at first sight not an very important process in the area. Only in a wet year, like 2010, soils will recharge during the snowmelt event. During summer water is extracted until no water remains. Looking at the high number of outliers during the summer of 2010 and the summer of 2012 the results for the soil water storage appears to be variable between the locations. November and December of 2009 show the adaptation of the model to initial moisture settings of the soil.

In general it can be said that variability for all hydrological properties increase when the mean values increase and the processes become more important.

Table 15: Hydrological properties per month for all locations.

		Jan	Feb	Mar	Apr	May	Jun	Jul	Aug	Sep	Oct	Nov	Dec
interception [cm]	min.	0.07	0.01	0.11	0.46	0.62	0.44	0.62	0.00	0.00	0.51	0.28	0.10
	max.	1.52	1.32	3.21	4.05	2.28	1.28	1.63	1.06	0.86	0.91	1.45	0.63
	mean	0.70	0.48	1.68	1.61	1.33	0.75	1.16	0.49	0.32	0.70	0.74	0.32
	sd.	0.37	0.39	0.91	0.94	0.41	0.32	0.34	0.42	0.34	0.11	0.38	0.11
runoff [cm]	min.	0.00	0.00	0.00	0.00	0.00	0.00	0.00	0.00	0.00	0.00	0.00	0.00
	max.	0.00	0.00	0.00	0.00	0.00	0.00	0.00	0.00	0.00	0.00	0.00	0.00
	mean	0.00	0.00	0.00	0.00	0.00	0.00	0.00	0.00	0.00	0.00	0.00	0.00
	sd.	0.00	0.00	0.00	0.00	0.00	0.00	0.00	0.00	0.00	0.00	0.00	0.00
actual transpiration [cm]	min.	0.07	0.00	0.36	1.33	1.45	0.21	1.25	0.00	0.00	0.39	0.14	0.01
	max.	1.86	1.80	4.25	6.11	9.25	11.78	6.83	2.96	3.79	1.37	2.79	1.63
	mean	0.46	0.46	1.85	3.07	3.93	2.62	3.24	0.81	1.04	0.96	1.18	0.27
	sd.	0.37	0.39	0.87	0.88	1.95	2.33	0.70	0.71	1.43	0.22	0.73	0.31
actual evaporation [cm]	min.	0.00	0.01	0.03	0.13	0.13	0.05	0.11	0.00	0.00	0.04	0.01	0.00
	max.	0.33	0.35	0.67	0.95	1.13	1.06	0.88	0.82	0.59	0.37	0.35	0.22
	mean	0.12	0.12	0.30	0.41	0.45	0.25	0.37	0.17	0.11	0.13	0.14	0.07
	sd.	0.06	0.08	0.12	0.15	0.20	0.19	0.16	0.17	0.14	0.06	0.06	0.04
net bottom outflux [cm]	min.	0.00	0.00	0.00	0.00	0.00	0.00	0.00	0.00	0.00	0.00	0.00	0.00
	max.	1.02	0.53	3.60	8.74	6.27	5.84	2.09	0.26	3.09	0.91	1.61	0.21
	mean	0.02	0.03	0.30	1.90	1.56	1.20	0.32	0.00	0.24	0.09	0.20	0.01
	sd.	0.09	0.08	0.67	2.56	1.74	1.68	0.46	0.02	0.59	0.17	0.28	0.03
rain [cm]	min.	0.00	0.00	0.02	3.58	3.29	1.40	4.12	0.00	0.00	1.60	0.00	0.00
	max.	0.10	0.89	4.24	10.49	10.02	8.31	5.72	2.99	4.86	2.01	1.16	0.11
	mean	0.05	0.38	1.57	6.62	6.58	4.41	5.07	1.36	1.74	1.81	0.51	0.04
	sd.	0.04	0.31	1.79	2.89	2.75	2.90	0.69	1.24	2.22	0.21	0.49	0.05
snow rate [cm]	min.	0.58	1.91	0.00	0.00	0.00	0.00	0.00	0.00	0.00	0.00	0.40	0.18
	max.	1.47	3.83	3.99	0.00	0.00	0.00	0.00	0.00	0.00	1.57	1.61	3.35
	mean	0.99	2.72	0.58	0.00	0.00	0.00	0.00	0.00	0.00	0.79	0.95	1.88
	sd.	0.37	0.64	0.86	0.00	0.00	0.00	0.00	0.00	0.00	0.79	0.47	1.31
snowmelt [cm]	min.	0.41	0.03	0.05	0.00	0.00	0.00	0.00	0.00	0.00	0.00	0.31	0.18
	max.	3.20	2.00	5.89	5.91	1.86	0.00	0.00	0.00	0.00	1.20	1.82	1.31
	mean	1.21	0.72	3.04	0.90	0.03	0.00	0.00	0.00	0.00	0.32	1.04	0.50
	sd.	0.63	0.63	1.71	1.58	0.19	0.00	0.00	0.00	0.00	0.33	0.54	0.21
change water storage in soil profile [cm]	min.	-1.72	-3.56	-0.83	-0.87	-0.89	-5.41	-8.96	-9.16	-9.19	-8.91	-9.02	-9.08
	max.	0.51	1.17	3.99	10.89	5.19	0.57	0.38	0.05	1.04	1.26	1.12	0.88
	mean	-0.04	-0.02	0.47	0.99	0.34	-0.09	-0.11	-0.22	-0.20	0.01	-0.64	-0.77
	sd.	0.29	0.51	0.88	1.87	1.01	0.58	0.91	0.93	0.98	1.21	1.36	1.58

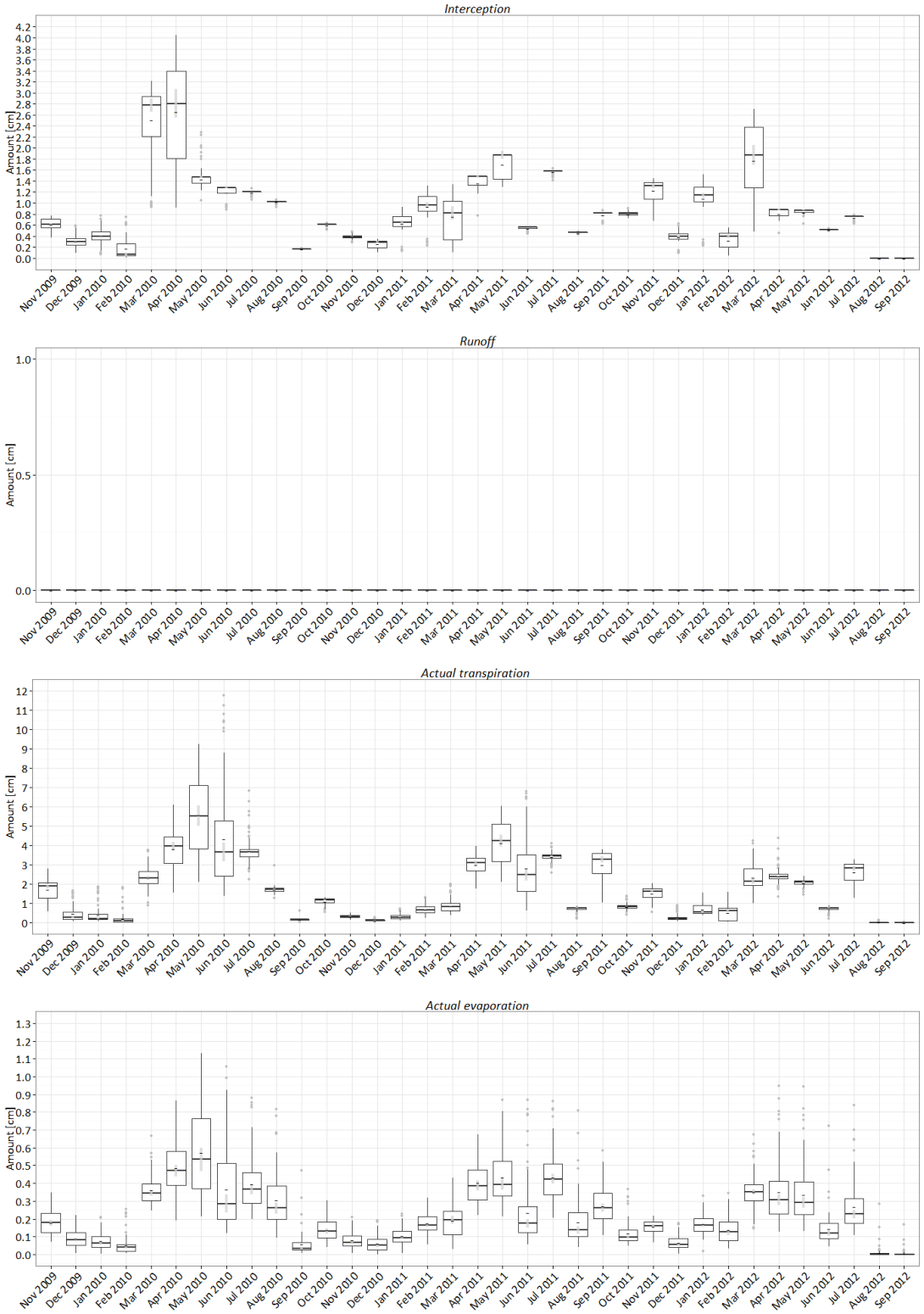

Figure 13a: Boxplots of the monthly evolution of the hydrological fluxes.
The grey dots represent the outliers, the confidence interval is shown with the grey bar and the mean is represented by the black dash.

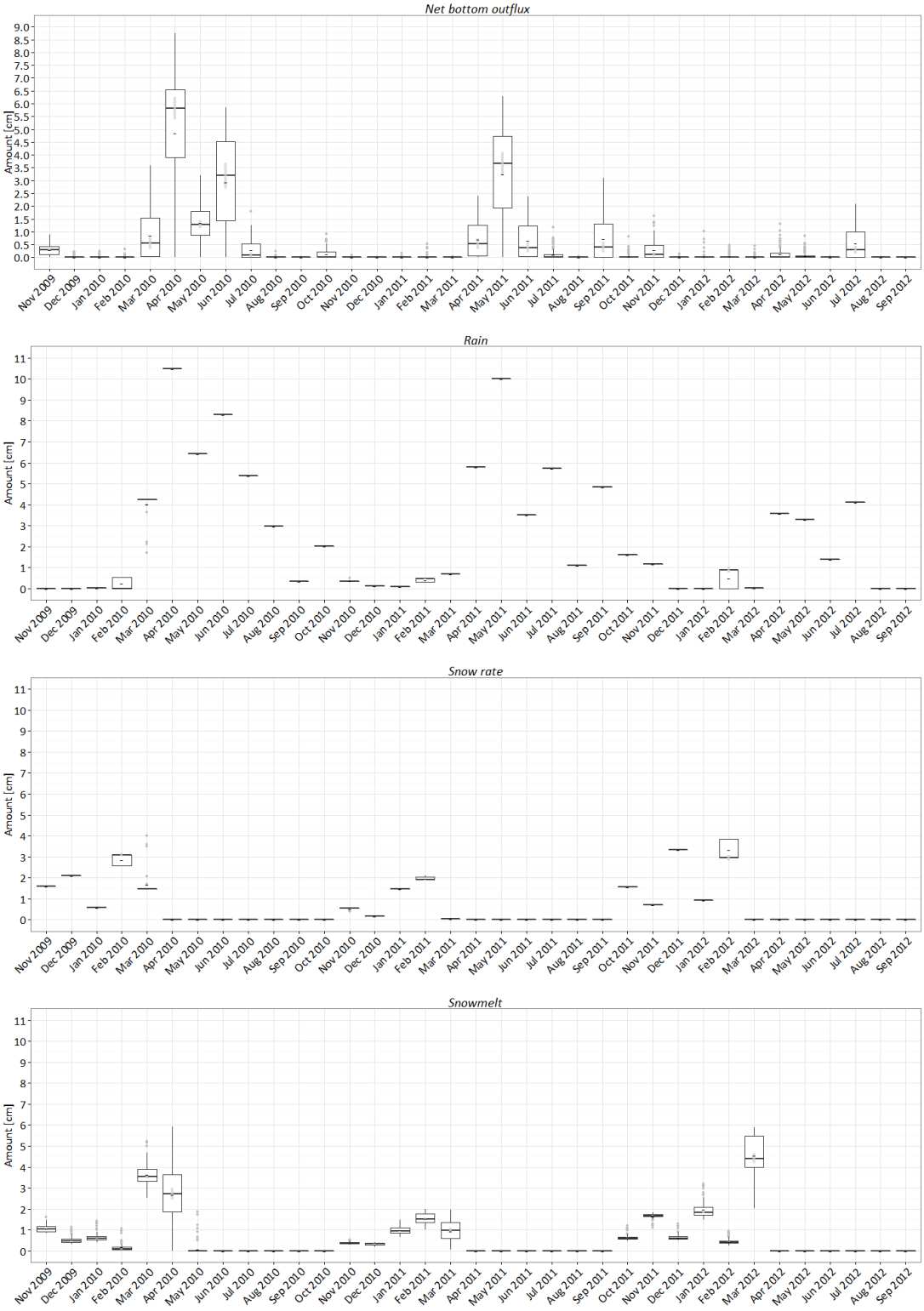

Figure 13b: Boxplots of the monthly evolution of the hydrological fluxes.
The grey dots represent the outliers, the confidence interval is shown with the grey bar and the mean is represented by the black dash.

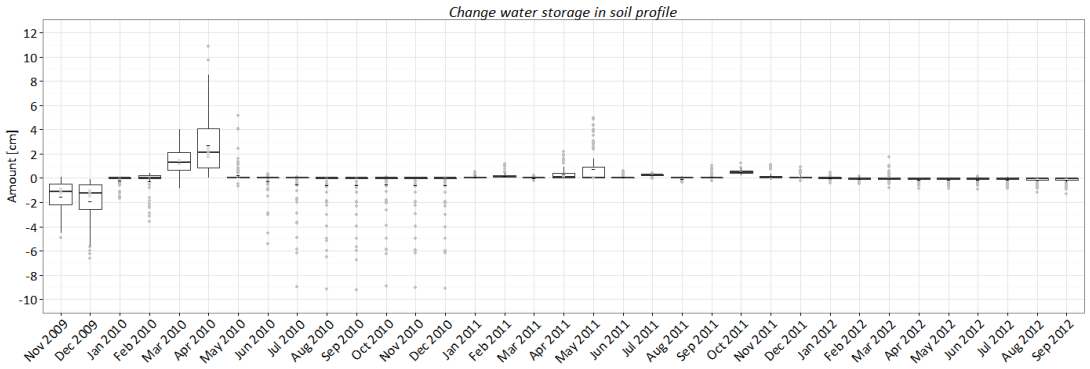

Figure 13c: Boxplots of the monthly evolution of the hydrological fluxes.
The grey dots represent the outliers, the confidence interval is shown with the grey bar and the mean is represented by the black dash.

This high variation between the locations is confirmed by the range of the boxplots of Figure 14, the few statistically significant hydrological properties in Table 16, and the range of the data for each characterising area in Figure 15. Although part of the variation is explained by the subdivision of the area in the five characterising areas it should be noted that there is still a lot of variation within the characterising areas.

Table 16 shows that only the net bottom outflux, rain, snow rate and snowmelt are statistically different. In total the south facing slopes receive most rain (89.5 cm over three years), followed by the flat north facing slopes (88.9 cm) and the terraces (88.8 cm), and by the smooth west area (88.3 cm). The steep north facing slopes receive even less rain (87.4 cm). Snow rate and snowmelt, logically, show the reverse pattern (respectively 22.1, 22.7, 22.7, 23.2 and 24.2 cm). Since all fallen snow will melt at the end of the period it is notable that these values are not equal to each other and can be dedicated to a rounding error by calculating the snow rate and snowmelt.
For the interception, transpiration, evaporation and net bottom flux it is noticeable that the terraces act different compared to the other characterising areas. Also the flat north facing slopes act quite different. Interception is low at the terraces (mean of 25.5 cm), although the variation within this characterising area is large (Figure 14). Means of the other characterising areas are higher (between 29.7 and 31.5 cm). The smooth west area and the south facing slopes show the high variability within the considered area as well. For evaporation and transpiration a reverse pattern can be observed. Terraces and the flat north facing slopes have relatively high transpiration and have little evaporation. For the other areas this is the other way around. The storage change in the soil profile is for all areas around zero. For the flat north facing slopes the three-year total is highly negative (-5.5 cm). Also the terraces show a negative value, but there is a lot of variation within the area, since the range is large.

Table 16: Hydrological properties, cumulative for the whole simulation period (Nov-2009 till Sep-2012)

	(i) south facing slopes	(iia) steep north facing slopes	(iib) flat north facing slopes	(iii) smooth west area	(iv) terraces	$\eta 2$	*p(equal means)*
interception [cm]	30.14	31.51	29.97	29.73	25.50	*0.004*	*0.5019*
actual transpiration [cm]	55.67	57.80	63.97	58.03	79.06	*0.037*	*0.0620*
actual evaporation [cm]	6.98	7.18	9.64	8.38	11.05	*0.027*	*0.1185*
net bottom outflux [cm]	20.79	17.76	11.73	17.95	1.89	*0.049*	*0.0313*
rain [cm]	89.45	87.38	88.88	88.31	88.81	*0.260*	$1.50\ 10^{-7}$
snow rate [cm]	22.08	24.15	22.65	23.22	22.72	*0.260*	$1.50\ 10^{-7}$
snowmelt [cm]	22.09	24.33	22.65	23.25	22.72	*0.254*	$2.30\ 10^{-7}$
change water storage in soil profile [cm]	0.33	-0.48	-5.45	-1.04	-1.62	*0.010*	*0.3498*

The black values indicate that the considered property is statistical significant with $p < 0.05$

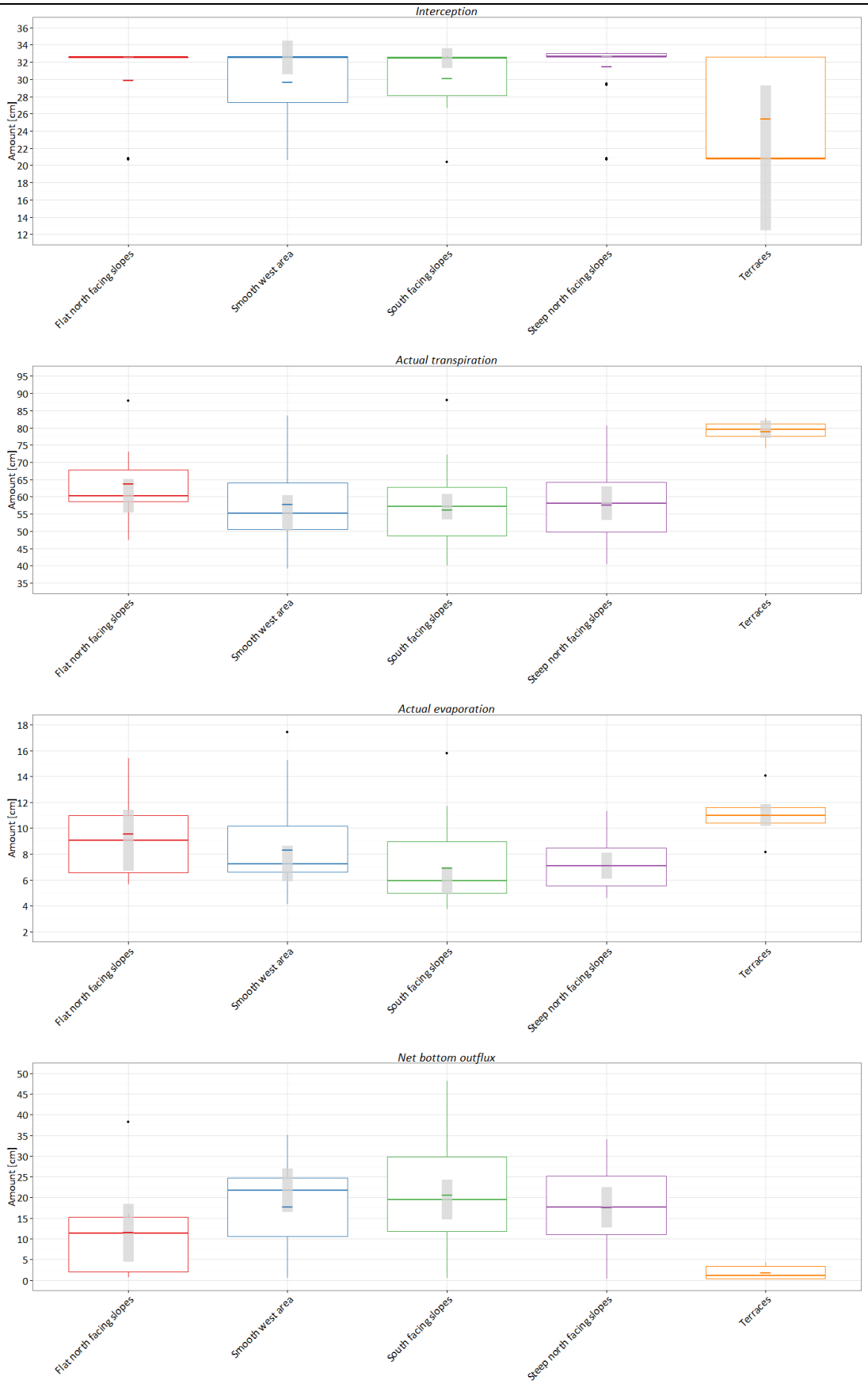

Figure 14a: Boxplot for each characterising area of the three-year total of the hydrological characteristics.
The coloured dashes represent the mean, the lightgrey bar the confidence interval and the black dots the outliers.

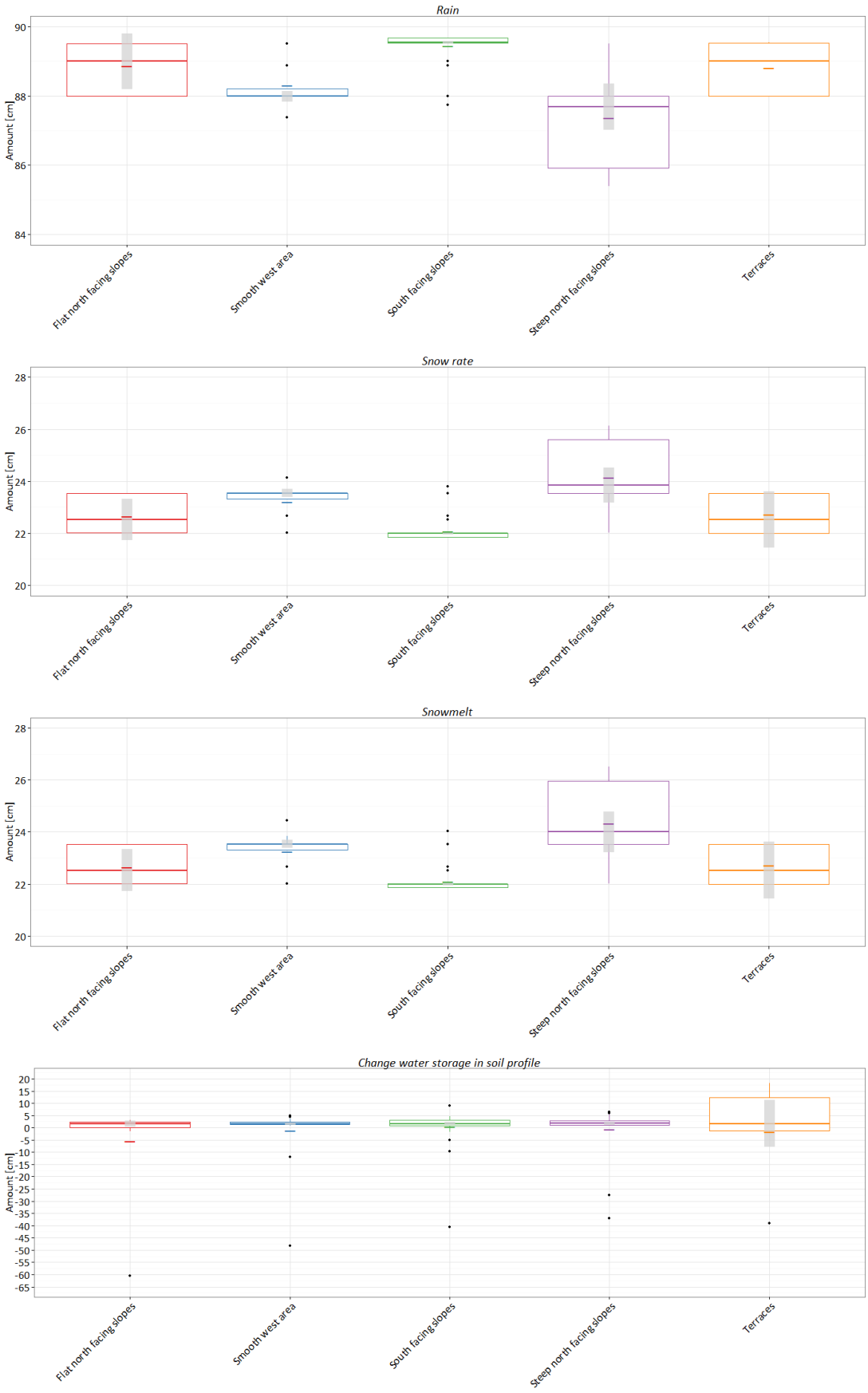

Figure 14b: Boxplot for each characterising area of the three-year total of the hydrological characteristics.
The coloured dashes represent the mean, the lightgrey bar the confidence interval and the black dots the outliers.

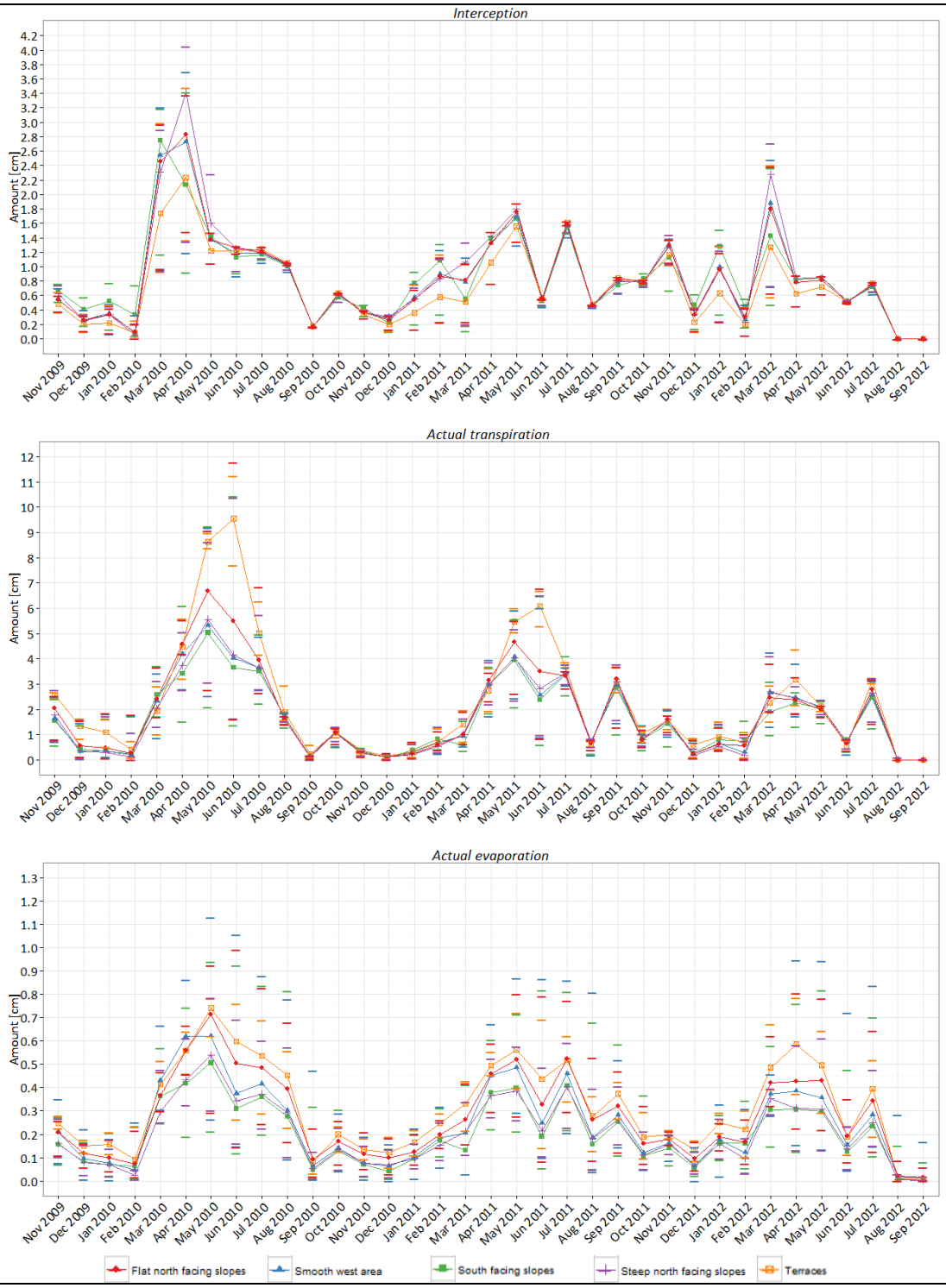

Figure 15a: Monthly evolution of the hydrological characteristics for each characterising area.
The coloured dashes represent the minimum and maximum value in the considered month for the considered characterising area.

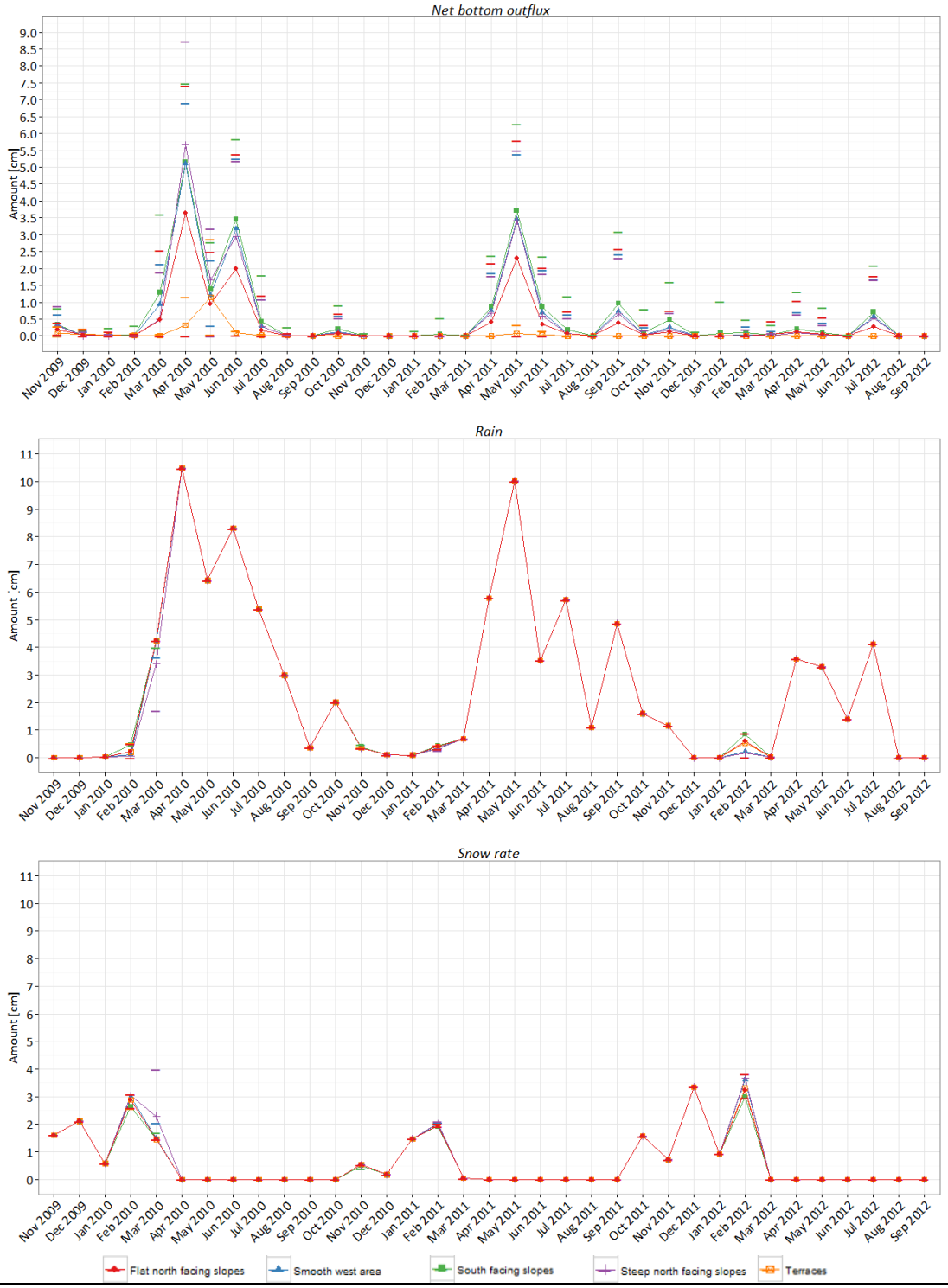

Figure 15b: Monthly evolution of the hydrological characteristics for each characterising area.
The coloured dashes represent the minimum and maximum value in the considered month for the considered characterising area.

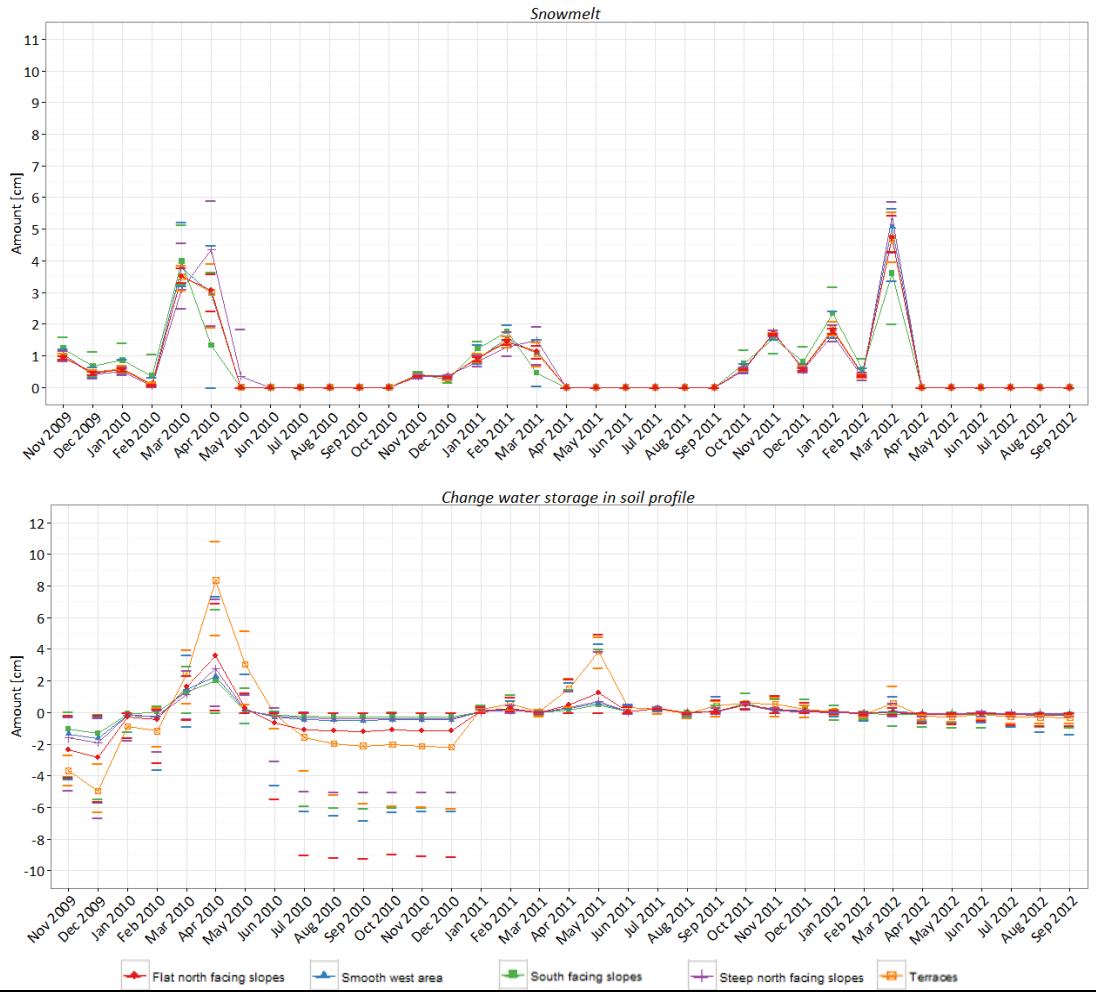

Figure 15c: Monthly evolution of the hydrological characteristics for each characterising area.
The coloured dashes represent the minimum and maximum value in the considered month for the considered characterising area.

Figure 16 shows the evolution of the hydrological properties for each characterising area during the whole simulation period. Differences for the different areas are small for rain and snow rate. Only the steep north facing slopes receive slightly more snow in March 2010, and February 2012.

For snowmelt the differences are larger and show that early in the year snowmelt is highest at the south facing slopes, later in the year snowmelt at the south facing slopes decrease faster than at the other areas. Peaks of the snowmelt at the steep north facing slopes are a bit later than in the other areas for the years 2010 and 2011.

Interception is for the whole period lowest for the terraces, probably because at the terraces transpiration and evaporation are more important processes. Peaks of the interception are in April 2010, May and July 2011, and in March 2012, these peaks reflect the peaks of the water input by rain and snowmelt. The peaks of interception at the south facing slopes are earlier in the year (March 2010, February 2011 and January and March 2012). Especially interception values during the snowmelt period will be overestimated.

During the summer months, transpiration peaks at the terraces. Here the maximum value of transpiration occurs one month later than in the other areas. Striking is that the importance of transpiration at the terraces is much lower during dry years. Especially in the winter months transpiration values are close together, but transpiration values for the other areas are closer together. Transpiration at the flat north facing slopes is, however slightly higher than at the south facing slopes, steep north facing slopes and the smooth west area, this has to do with the differences in tree density, global radiation and profile depth at these slopes.

Evaporation is less variable and less dependent on water inputs from rain and snowmelt than transpiration. This process is most important at the terraces. This can be linked to the amount of

water that is stored in the soil, this is highest at the terraces and so more water is available for evaporation. Peaks reflect the seasonal pattern as well as the input of water by rain and snowmelt.
The south facing slopes and the smooth west area loose most water to the groundwater, also reflected by the little storage of these soils. Terrace soils loose very little water, and more interesting, the pattern of the net bottom flux is different than at the other areas (peak in May 2010 rather than in April and June 2010, Figure 15). This is something that is also recognisable in the storage of the terrace soils, terrace soils are still recharging in May 2010, when water is constant or already extracted from the soils at all other areas. Furthermore terrace soils have more water available for extraction during the summer.

Discussion 5.

5.1 Soil properties

Local soil properties depend on many factors. Soil formation is, according to Jenny (1941) and Völkel et al. (2011), dependent on the soil parent material (p), climate (cl), relief and topographic setting (r), biotic factors (o), time (t), and other factors (...), like human influence:

$$s = f(cl, o, r, p, t, ...) \quad \textit{[8]}$$

Soils in the Gordon Gulch Valley highly reflect the landscape characteristics, such as geology, topography and vegetation. Especially relief and topographic setting and flora were found to be important.

The terraces can be typically categorised as a stable surface, where soils develop in accumulated materials from upslope (Dethier et al., 2012). The soils are deep and moist with few stones, a higher content of sand, and a high pH. The low-lying location, with little global radiation and dense, often deciduous, vegetation results in moist soils and relatively fast soil development.

The flat north facing slopes and the smooth west area have shallow soils and moderate stoniness increasing with depth. Differences between the flat north facing slopes and the smooth west area can be related to landscape differences. The landscape characteristics, especially tree and undergrowth cover and the slopes of the smooth west area, and subsequently the soil properties of the smooth west area show a high variety. On average the smooth west area is less densely covered with deciduous trees and have slightly more undergrowth than the flat north facing slopes which are densely covered with coniferous trees and little undergrowth, furthermore the smooth west area receives more global radiation. As a consequence the smooth west area is warmer and drier, this results in soils lower in organic matter content and with a higher pH.

The soils at the flat north facing slopes contain the highest percentage of fine materials in the top horizon of the study area. These higher contents of fine materials in the top horizon can be explained by the input of aeolian silt and clay (Birkeland et al., 2003; Dethier et al., 2012). The influence of this input of aeolian fine materials was also observed downslope the north facing slopes.

Soils at the south facing slopes and the steep north facing slopes are formed as result of slope processes. The soils are shallow, have a high stoniness in the whole profile but increasing with depth, and increasing contents of clay with depth of the profile. The observation that clay content increases with depth of the profile at the sloping areas contradicts to findings by Dethier et al. (2012). They describe soil profiles with indistinct horizon boundaries with no clay enrichment of the lower horizons, indicating little soil development. That we found clay enrichment in the lower horizons could indicate that the soils are slightly more developed than described by Dethier et al. (2012). However, our methodology to separate clay from silt, based on sieving and sedimentation of the different textures, is relatively simple and not as accurate as the methods used by Dethier et al. (2012). They analysed texture of the <2 mm soil fraction using hydrometer techniques, a more commonly used and more accurate methodology. This could indicate that the clay enrichment we found could be related to the inaccuracy of our methodology and so we have to doubt whether the soils at the south facing slope are slightly more developed than described by Dethier et al. (2012).

Dethier et al. (2012) furthermore found increasing amounts of aeolian silt and clay downslope at both the north and south facing slopes. If we look at the catena flat north facing slopes, steep north facing slopes and terrace soils, we observed a decrease of fine materials downslope instead of an increase. If we look at a catena at the south facing slope (for example fieldpoints 011, 095, 097, and 098), located close to the CZO transect, we do not observe an increase of silt and clay downslope either (respectively 9.8% of silt and 2.2% of clay in fieldpoint 011, 5.6% and 0.6% in fieldpoint 095 6.5% and 0.7% in fieldpoint 097 and 3.7% and 0.0% in fieldpoint 098). Mixing of materials at the slopes and removal by flood events could be an explanation for this, but a more realistic explanation is that also here our methodology for fine materials is not accurate enough.

The clear differences between the steep north facing slopes and the south facing slopes can be related to specific landscape characteristics. Most important is the difference in global radiation

between the two slopes. The steep north facing slopes receive less global radiation, and are moreover more densely vegetated with coniferous trees. The steep north facing slopes are as a result cooler and the soils more moist. The south facing slopes are warm, dry and densely vegetated with herbaceous undergrowth, this results in slightly deeper topsoils, with little organic matter and a higher pH. Hinckley et al. (2012) describe that the north facing slopes have deeper soils than the south facing slopes. Also Anderson et al. (2011) suggest this by looking at the average depth of the mobile regolith (50-75 cm at the north facing slopes versus 20-70 cm at the south facing slopes). Although both south facing slopes and steep north facing slopes are shallow and the differences are small, we found more shallow soils at the north facing slopes. An explanation can be that we excluded mobile regolith as part of the soil, both Hinckley et al. (2012) and Anderson et al. (2011) describe the depth of the soil until the saprolite. In this case it is expected that the steep north facing slopes indeed have deeper soils, because the soils at the steep north facing slopes are more moist and experience more intense weathering. We focused on the upper 40 cm of the soil. For this study this was sufficient, since top soils in combination with the vegetation play a major role in distributing important components of the hydrological cycle (transpiration, evaporation, runoff and groundwater recharge) and in this way, top soils and the vegetation type strongly determine the hydrological response. However differences in depth and structure (dense fracture network) of the mobile regolith and saprolite can be expected. Research into this issue can be interesting and will improve the understanding of the weathering processes in the area, and can improve the knowledge on understanding the subsurface flow paths of infiltrated water.

The factors parent material, biotic factors, climate and human influence were not taken into account as soil forming factors in this research. Nevertheless these soil forming factors are still important factors influencing soil formation, and subsequently hydrology in the study area.
The study area can be categorised in five main categories of parent material, (i) granite, (ii) biotite gneiss, (iii) a mixture of granite and biotite gneiss, with sometimes the presence of schist, (iv) accumulated materials and (v) fluvial materials. Soils differ considerably between the parent materials. Soils within accumulated and fluvial materials are deep and moist, because these soils are formed in materials and with water accumulated from upslope positions. Biotite gneiss and schist are known to weather faster than granite and this probably results in deeper soils.
At totally different positions in the study area (the smooth west area, the flat north facing slopes, and the south facing), we observed several accumulation positions. The soils of these positions developed in accumulated materials. As a consequence the soils are deep and moist and are covered by deciduous undergrowth and trees. The hydrological fluxes of these accumulation positions were modelled by SWAP based on their soil and landscape characteristics. Although these accumulation positions are at different locations in the study area the hydrological response of these three accumulation positions (parent material: accumulated materials) is comparable (Figure 19). This suggests that parent material can have a clear influence on the soils and hydrology in the study area.
Biotic factors are partly included during this research. That vegetation type and density influences soils has already shortly been touched upon. Not only does vegetation affect pH, organic matter content, soil moisture and soil porosity, it also influences soil formation more indirectly, with the shadow effect of trees and the effect on transpiration and interception. The role of roots and treethrows (Gilbert, 2010) in the area are considered to be important in soil stirring and the weathering of rocks. The role of fauna was not taken into account at all. Nevertheless we can expect that both microorganisms (Eilers et al., 2012) and larger soil fauna, such as ants (Gilbert, 2010) and ground squirrels, can effect soil stirring, nutrient cycling, soil compaction and macropore development as well, and subsequently will influence subsurface flow paths.
The effect of climate was taken into account indirectly in this study. The effects of meteorological data were used as input in the hydrological model. Although this does not reflect climate, it include important climatological issues, like the rain-snow transition which result in the importance of snow and snowmelt in the study area.
The effect of human influence in the study area is at this moment negligible, the area is mainly used for recreation purposes. In the past, the study area was used for timber and possibilities for mining were investigated. Relicts of prospect pits are found over the whole area. If the effects of the digging of prospect pits and of intense logging show its relicts in the soils, and subsequently the hydrology as well, we do not know.

5.2 Hydrological properties

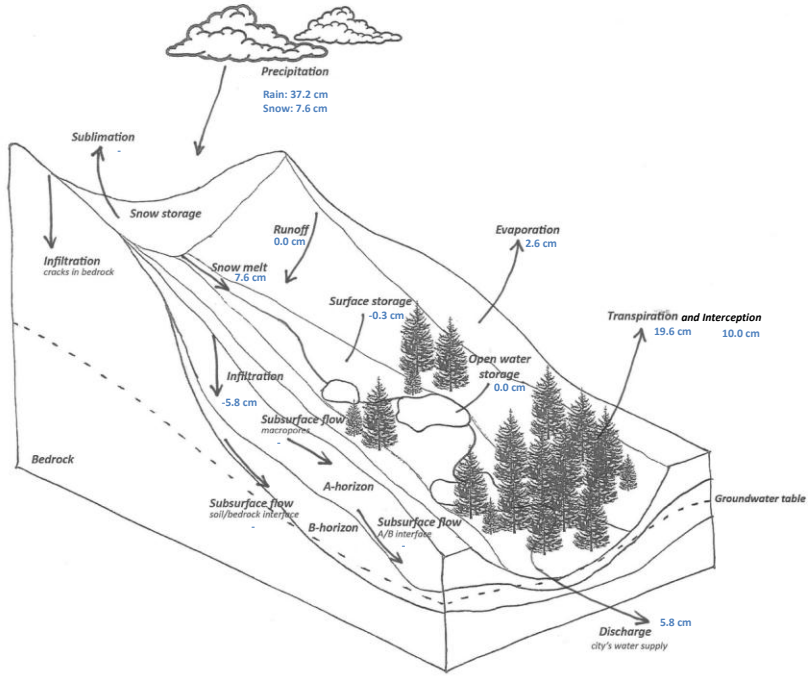

Figure 16: Hydrological properties of the Gordon Gulch Valley.
Water balance is not equal to zero, since we took averaged values of the whole study area to illustrate this figure.

Validation of the model based on measured discharge data (Boulder Creek CZO, 2013b) - daily averaged discharge data can be found in Appendix F - shows that the pattern of our modelled net bottom outflux match the pattern of the discharge quite accurately (Figure 17) and that the performance of the model can be considered fairly well. The early peaks of the modelled hydrological properties in April 2010 could indicate that the snowmelt we modelled is not completely accurate with the actual snowmelt in 2010. This is confirmed Figure 18, which shows little precipitation in May and by Figure 6, which shows that according the measured data snow melts until May in that year. Furthermore the discharge and the net bottom ouflux is not directly comparable, since the discharge is the water outflow of the whole area and the net bottom outflux is the averaged value over all fieldpoints in the area. These will not all effect the total discharge in the same amount.

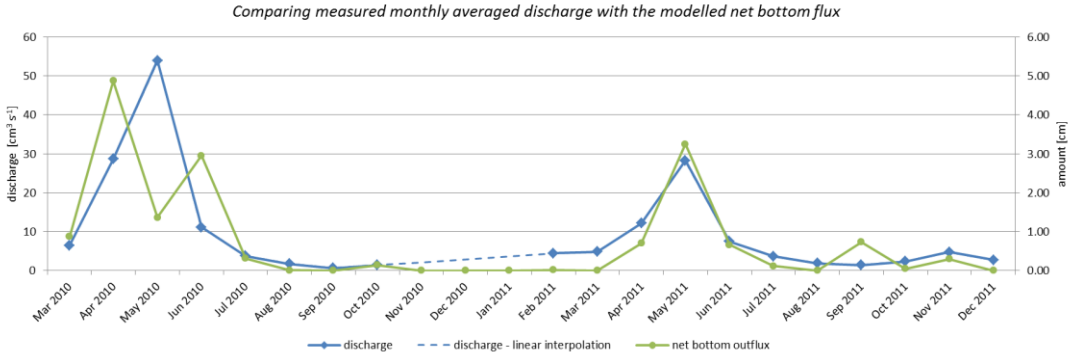

Figure 17: Measured discharge data compared to the net bottom outflux.

Our simulations indicate that when it rains, infiltration dominates in the whole area, caused by the extremely high permeability of the sandy soils in the area. Although runoff features were observed at

the south facing slopes, runoff will not occur due to soil saturation, because of the permeability of the soils and the deep groundwater.
When temperatures drop below zero degrees Celsius, it snows in the watershed. The steep north facing slopes receive most snow, because these areas are low lying and have relatively little global radiation, which result in lower temperatures. When temperatures rise above zero degrees Celsius again, the accumulated snow melts. Temperature differences, caused by differences in global radiation and vegetation density (the north facing slopes receive less global radiation and are denser vegetated with trees than the south facing slopes), result in large differences between the north and south facing slopes. At the steep north facing slopes the seasonal snow melts in a single, sustained melt event and at the south facing slopes snow melts in repeated, small melt events (Langston et al., 2011). These snowmelt events result, just like rain, in infiltration in the whole area.
No or little subsurface flow is expected at the A/B horizon interface, because the soils are extremely permeable in the whole area. Even the mobile regolith and saprolite are expected to be permeable. Subsurface flow at the soil/bedrock interface and macropore flow could be expected. This is consistent with the discussion in Hinckley et al. (2012), they measured the subsurface flow of water during the melt season and discuss that even by refreezing of the subsurface, primarily vertical transport dominates. Langston et al. (2011) support this as well based on their results. They found that lateral water flow along the soil/saprolite interface only becomes dominant when the soil is near saturation, since soils are highly permeable it is not expected that these will saturate. Although not expected in this area, differences in depth and structure (fracture network) of the mobile regolith and saprolite can influence the subsurface flow (Langston et al., 2011). Research into the differences of the mobile regolith and saprolite within the study area and there influence on subsurface flowpath can confirm these expectations.
Finally, water is expected to reach the groundwater or the creek, which will take the water outside the study area (discharge).

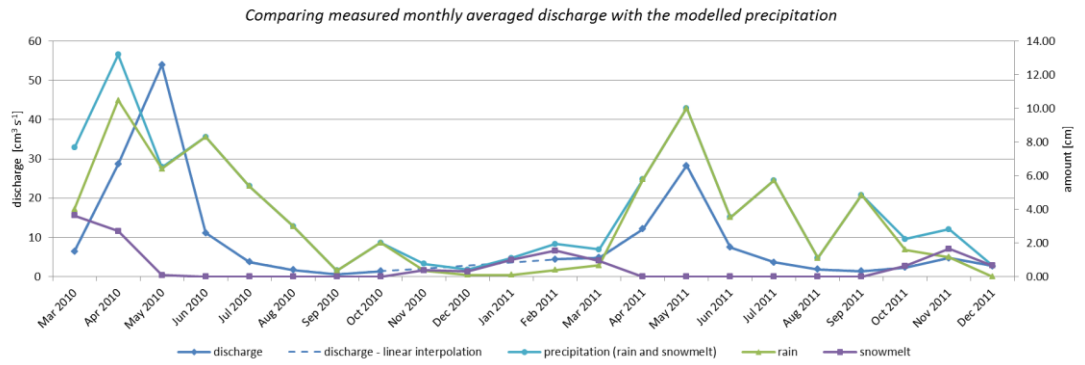

Figure 18: Measured discharge data compared to the precipitation input (rain and snowmelt).

Both transpiration and interception are important processes in the area. Interception is likely overestimated by the model, because rain and snowmelt were both assumed to be similar processes and were modelled lying on top of the vegetation. As a result a large amount of this water will evaporate before it reaches the soil. We expect that if this is modelled correctly, with the snow lying on the surface under the tree canopy it will mainly add to the transpiration and evaporation. Even in the current set of simulations, a lot of the water in the area is transpirated by vegetation. Not surprisingly, vegetation density highly influences the amount of transpiration of the areas. The densely tree covered terraces have much more transpiration than the scarcely tree covered south facing slopes. However, transpiration appears to be high for the flat north facing slopes, while this area is less covered with trees than the steep north facing slopes. A logical explanation for this is that global radiation influence the amount of transpiration, especially during the summer months. This would explain why the transpiration during summer is almost equal for the south facing slopes, the smooth west area and the steep north facing slopes, while differences in vegetation are large. The transpiration at the terraces shows for all years a peak in June (for the other characterising areas this peak is in May). This has to do with the coverage of the terraces by deciduous trees, which result in the highest Leaf Area Index in June. The evaporation peak of the smooth west area in March during

the wet year can be explained in the same way, only the other way around. For the smooth west area the Leaf Area Index is lowest in March, caused by relatively little tree and undergrowth cover. This results in little transpiration and as a result more water will enter the soil and is available for evaporation.
According to Hinckley et al. (2012) the soils at the south facing slopes are drier than the steep north facing slopes, although more water enters the soil. Especially during the drier years we observe the same pattern, although the differences are relatively small. That more water enters the south facing slopes than the steep north facing slopes, and that little of this water will be stored by the soils at the south facing slopes could be explained by the high global radiation and scarcely vegetated warm south facing slopes and the extremely high permeability of the soils at the south facing slopes (Table A3, Appendix A). During the wet year we observe however that in April more water enters the soil at the steep north facing slope, apparently the amount of snow on the steep north facing slopes that much higher, that interception and evaporation of the snow will not result in reducing the snowmelt.
The terrace soils act like a sponge in the study area. Although evaporation of the terrace soils is highest in the whole study area, least of the water is leaching to the groundwater. Storage of the water in the soil is therefore really important and reflects clearly the seasons. Where water is stored by the soils when the snow melts and where water evaporates in wet years till the end of December and in drier years by some terrace soils till September. These soils are thus really important for the water supply of areas outside the study area.

Although comparisons of the modelled hydrological properties with measured data of the study area (discharge and snow) show that the hydrological properties are quite accurately predicted, the accuracy of the hydrological properties can still be improved. First of all snow rate and snowmelt could be modelled more accurately, this includes no modelling of snowmelt on top of the vegetation and calibrate the snow even more to available data of the study area. Secondly vegetation could be modelled more accurately, right now the vegetation is only basically modelled and variation of vegetation is really simplified. Furthermore initial soil moisture conditions obviously influence the first months of the simulation (change water storage in soil profile in Figure 15). This could be improved when available measured data is used for the initial soil moisture conditions.

Although we have determined hydrological properties of the Gordon Gulch watershed based on soil properties, landscape characteristics, and meteorological data, at this moment it is not clear to what extent these inputs influence the resulting hydrological properties. It would be interesting to look in more detail at the contribution of the separate inputs. This can be relatively simply done by running the SWAP model again with keeping certain inputs constant over the whole area and/or the whole simulation period. We expect that soil mainly influence subsurface flow paths, runoff, soil moisture storage and the net bottom outflux.

Moreover, it is clear that there are interactions between landscape characteristics, soil characteristics and hydrological characteristics. However, the sequence of these interactions is indistinct. Are soils formed by hydrology and landscape characteristics or is hydrology influenced by soil and landscape characteristics or can we speak of positive feedback and works the interaction in two directions? We expect that the last is the case, that most interactions between landscape, soil and hydrology work in two directions.
One of the interactions which can substantiate this, is the interaction between vegetation and soils. On the one hand we know that forest is covering the area for a long time and that the vegetation played a role in soil formation, for example increasing weathering as a result of rooting, organic matter input as a result of organic waste and by influencing hydrology directly by increasing transpiration and interception and indirectly by the shadow effects. On the other hand we observed a correlation between vegetation and pH, coniferous trees result in soils with lower pH and deciduous trees result in soils with a higher pH. As a consequence these soils will attract certain types of vegetation, probably vegetation that is already there, suggesting that the interaction between soil and vegetation have a positive feedback.
Another interaction which can show this is the interaction between accumulation positions and soil formation and hydrology. Modelled in SWAP based on soil and landscape characteristics (deep and moist soils, densely covered with deciduous undergrowth and trees). On the one hand the characteristics of the deep and moist soils of these locations result in certain hydrological properties,

such as high transpiration, high water storage of the soils (Figure 19) and little bottom outflux, on the other hand we can expect that water and soil materials from upslope will collect at these positions and will increase the speed of the soil formation of these locations. Subsequently these deeper soils result in even more water collection and reinforce the hydrological response of these locations.

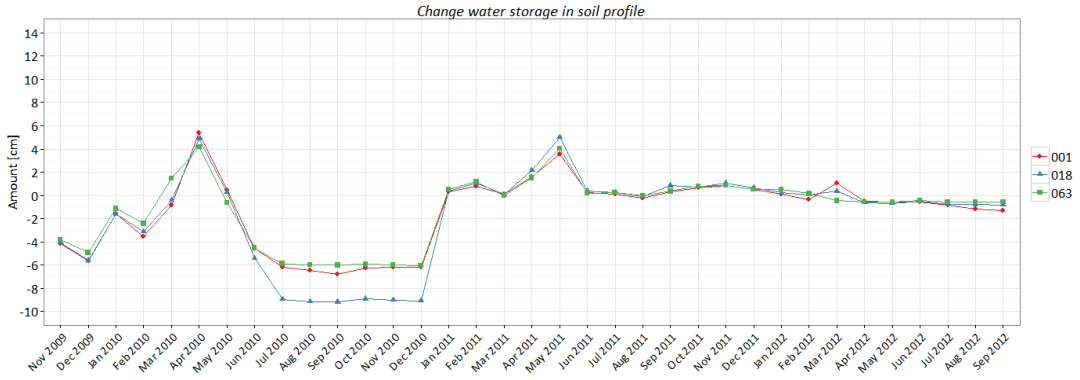

Figure 19: Change of water storage in soil profile for three accumulation positions.
Fieldpoint 001 is location in the smooth west area, 018 at the flat north facing slopes, and 063 at the south facing slopes. SWAP models these accumulation positions only based on the soil and landscape characteristics (deep and moist soil in accumulated materials, densely covered with deciduous undergrowth and trees).

5.3 A complex landscape

Literature shows that present CZO research in the Gordon Gulch Valley focusses on the obvious visual differences between the north and south facing slopes in the watershed (Anderson et al., 2011; Langston et al., 2011; Dethier et al., 2012; Hinckley et al., 2012).

Table 17 and Table 18 show the results for the soil properties when we divide the whole area in north and south facing slopes. The light areas in Figure 20 show the north facing slopes in the study area, the dark areas the south facing slopes.
The differences between soils on the north and south facing slopes proved to be significant ($p < 0.05$) for the thickness of the litter/duff layer, for pH, sand, silt and charcoal in the top horizon, and for OM in the C horizon. All other soil properties did not differ statistically significantly.

When dividing the area in the five characterising areas, more soil properties proved to be statistically significant (Table 12 and Table 13). This indicates that the division of the study area in north and south facing slopes slightly explains the variety of soil properties in the area and that the division of the study area in the five characterising areas explains this variety of soil properties better.

Table 17a: Soil properties of the horizons and general soil properties, differences between the north and south facing slopes

		mean north facing slopes	mean south facing slopes	η^2	*p(equal means)*
general upper 7 cm of the soil	bulk density [g cm^{-3}]	1.14	1.19	*0.008*	*0.3640*
	soil porosity [%]	56.91	55.20	*0.009*	*0.3593*
	soil water-filled pore space [%]	17.81	16.04	*0.009*	*0.3348*
	moisture content [mass%]	9.15	8.86	*0.000*	*0.0198*
	volumetric water content [volume%]	10.13	8.96	*0.010*	*0.3263*
	thickness Oi/Oh [cm]	3.69	2.24	*0.049*	*0.0500*
	thickness top horizon [cm]	8.61	9.84	*0.005*	*0.4782*
	thickness mid horizon [cm]	17.22	17.20	*0.000*	*0.9958*
	starting depth C horizon [cm]	14.00	16.37	*0.010*	*0.3466*

Table 17b: Soil properties of the horizons and general soil properties, differences between the north and south facing slopes

		mean north facing slopes	mean south facing slopes	η^2	p(equal means)
top horizon	OM [%]	8.66	8.09	0.002	0.6608
	pH [-]	5.35	5.59	0.044	0.0355
	sand [%]	87.96	89.79	0.048	0.0302
	silt [%]	11.31	9.48	0.051	0.0248
	clay [%]	0.72	0.72	0.000	0.9974
	moisture content [mass%]	11.06	8.59	0.014	0.2452
	roots [%]	12.18	14.31	0.016	0.2129
	stoniness [%]	17.66	20.13	0.008	0.3650
mid horizon	OM [%]	4.62	3.94	0.023	0.2518
	pH [-]	5.33	5.62	0.044	0.1160
	sand [%]	88.28	88.69	0.003	0.7056
	silt [%]	10.66	10.23	0.003	0.6775
	clay [%]	1.06	0.98	0.004	0.6412
	moisture content [mass%]	6.25	5.03	0.029	0.2026
	roots [%]	12.74	13.38	0.002	0.7270
	stoniness [%]	28.06	23.15	0.029	0.2053
C horizon	OM [%]	5.28	2.63	0.270	0.0227
	pH [-]	5.68	5.12	0.142	0.1227
	sand [%]	88.28	85.71	0.084	0.2284
	silt [%]	10.76	12.90	0.066	0.2877
	clay [%]	0.96	1.39	0.082	0.2336
	moisture content [mass%]	6.56	3.35	0.080	0.2416
	roots [%]	8.79	7.36	0.014	0.3156
	stoniness [%]	37.86	40.70	0.004	0.5455

The black values indicate that the considered property is statistical significant with $p < 0.05$

Table 18: Categorical soil properties of the top horizon, differences between the north and south facing slopes

		observations north facing slope	observations south facing slope	Cramer's V	p(no association)
top horizon	structure	n=31	n=66	0.19	0.320
	SG	19.35	30.30		
	WE/GR	67.74	63.63		
	MO/GR	9.58	6.06		
	ST/GR	3.23	0.00		
	duff	n=33	n=68	0.07	0.518
	not present	81.82	75.00		
	present	18.18	25.00		
	charcoal	n=33	n=67	0.24	0.015
	not present	48.48	73.13		
	present	51.52	26.87		
mid horizon	structure	n=17	n=39	0.31	0.070
	SG	0.00	5.13		
	WE/GR	100.00	74.36		
	MO/GR	0.00	20.51		
	ST/GR	0.00	0.00		
	charcoal	n=19	n=39	0.09	0.488
	not present	68.42	76.92		
	present	31.58	23.08		
C horizon	structure	n=25	n=43	0.24	0.281
	SG	0.00	9.30		
	WE/GR	100.00	86.05		
	MO/GR	0.00	2.33		
	ST/GR	0.00	2.33		
	charcoal	n=5	n=14	0.18	0.421
	not present	80.00	92.86		
	present	20.00	7.14		

The black values indicate that the considered property is statistical significant with $p < 0.05$

Figure 20 shows that present CZO research mainly focusses on a transect starting halfway the north facing slope and ending at the south facing slope, herewith focussing on two dominating areas in the watershed, (i) the steep north facing slopes and (ii) the south facing slopes.
In order to look at how this focus is at odds with the spatial variation that we found, we have selected 6 fieldpoints to correspond to the transect of the CZO. The CZO has 10 points which focus on

snowdepth research (point 1 to 10) and 6 locations which focus on other research elements (3, 4, 5, 6, 9, and 10). We corresponded fieldpoint 048 to location 3, 047 to 4, 046 to 5, 098 to 6, 097 to 9 and 095 to 10. Fieldpoint 094 would actually correspond better to location 9, however, this fieldpoint was excluded for analysis, because the output of SWAP was unreliable as a result of several warnings. Furthermore we should add that fieldpoint 046 is located close to the terrace soils and show a lot of comparable properties to the terrace soils, this, however, corresponds to location 5 of the CZO transect.

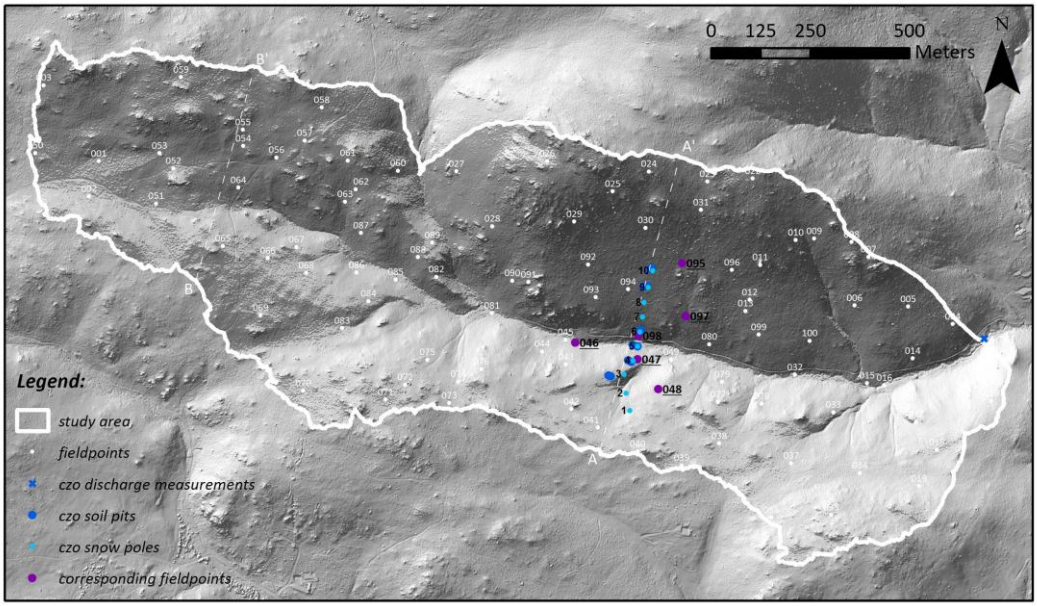

Figure 20: Location of the transect of the CZO and the corresponding fieldpoints from our dataset used as subset to compare our data to the data of the CZO.
Where fieldpoint 046 corresponds to 5, 047 to 1, 2 and 4, 048 to 3, 095 to 10, 097 to 7, 8 and 9, 098 to 6. The profile graph of the CZO transect can be found on p. 22 (A – A').The dark colour shows the south facing slopes and the light colour the north facing slopes.

Figure 21 shows the result of the comparison of our subset with the CZO transect. We excluded rain and snow rate from the figure, because rain was not allowed to vary over the area and because snow rate is more or less equal to the snowmelt when we look at the monthly totals.
Transpiration and evaporation are higher at the north facing slopes than on the south facing slopes. This corresponds to the clear differences in vegetation density between the areas. Interception is highly variable for both the north and the south facing slopes. The pattern of interception clearly reflects the pattern of snowmelt. Furthermore the input of water is clearly influenced by the differences in snowmelt between the slopes. Snow on the south facing slopes melts earlier in the year than at the north facing slopes, resulting in earlier decrease of the snowpack at the south facing slopes. This corresponds to the clear differences in global radiation between the slopes.
All these things influence the amount of water storage and the bottom outflux of the soil. Little water enters the north facing slopes, caused by the high amounts of evaporation and transpiration. Although on the south facing slopes more water enters the soil, most water will end up in the groundwater and little water is stored in the soils. This difference can be explained by the extremely high permeability of the soils at the south facing slopes (Table A3, Appendix A).
If we compare the results of this subset with the steep north facing slopes and the south facing slopes of the complete dataset in Figure 21, we can conclude that for the subset the differences between the north and south facing slopes are, for the net bottom outflux and the soil water storage, magnified.

The present CZO research clearly conveys the important differences between two dominating landscape characteristics of the study area. The choice, however, seems to emphasise differences by looking at an extreme transect through these landscape characteristics. Furthermore this in depth research is done based on a transect with only several fieldpoints, while our research to investigate a

complex landscape needed 100 fieldpoints. Therefore, although present CZO research is very valuable, it could overlook other valuable aspects of a complex landscape, which can have serious consequences for catchment-wide predictions and consequently policy implications. Our research has clearly indicated that there are three other interesting areas, with each their own landscape, soil and hydrological characteristics.

However, even the present study is not yet focussing on the interactions between the areas and between the individual fieldpoints. This could be investigated with research focussing on 3D-modeling of hydrology instead of 1D-modelling used in this research. This could improve the understanding of the catchment-wide hydrology even more.

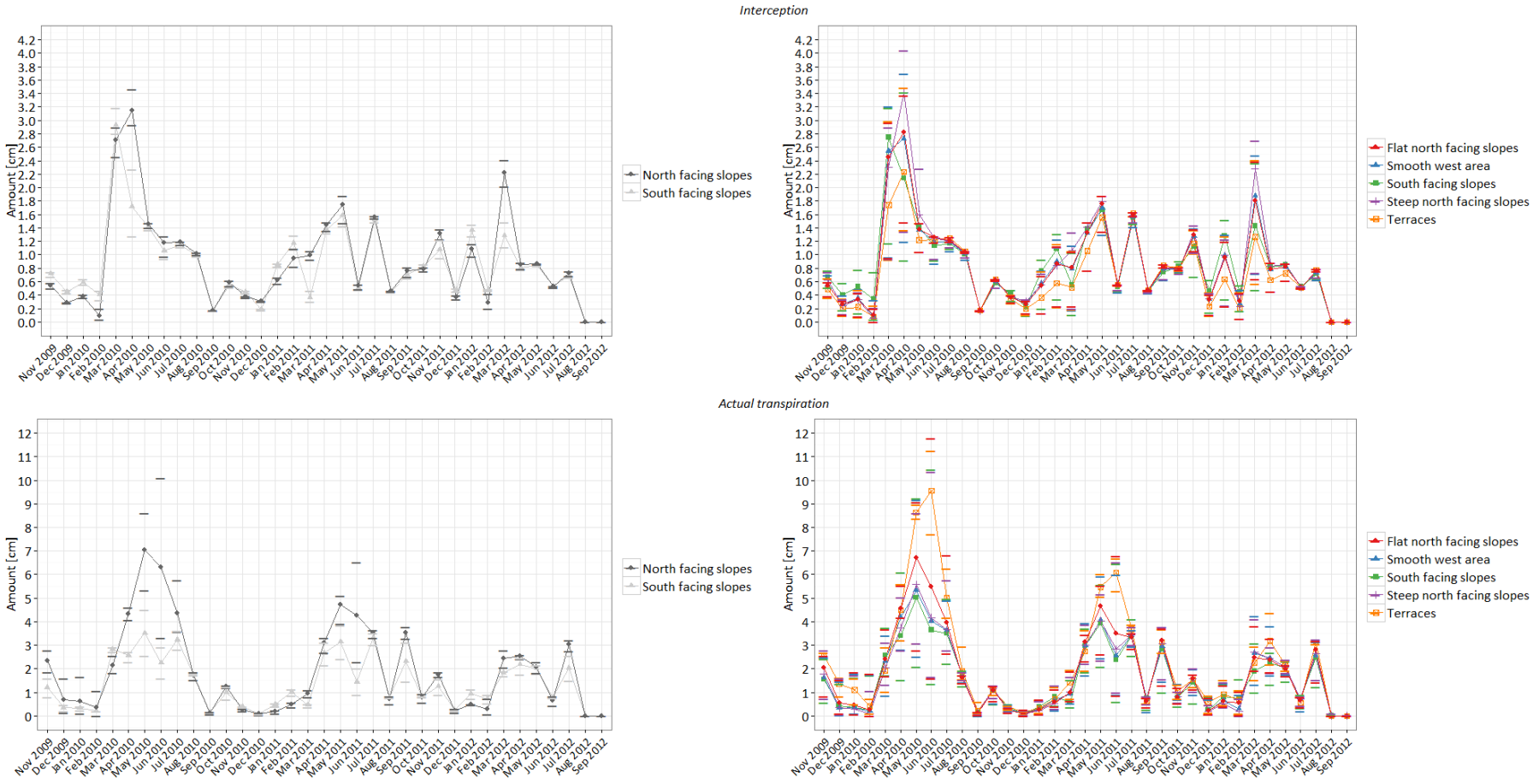

Figure 21a: Hydrological properties of a subset of the field points, corresponding to the location of the CZO transect, compared to the hydrological properties of the whole area subdivided into the five characterising areas.

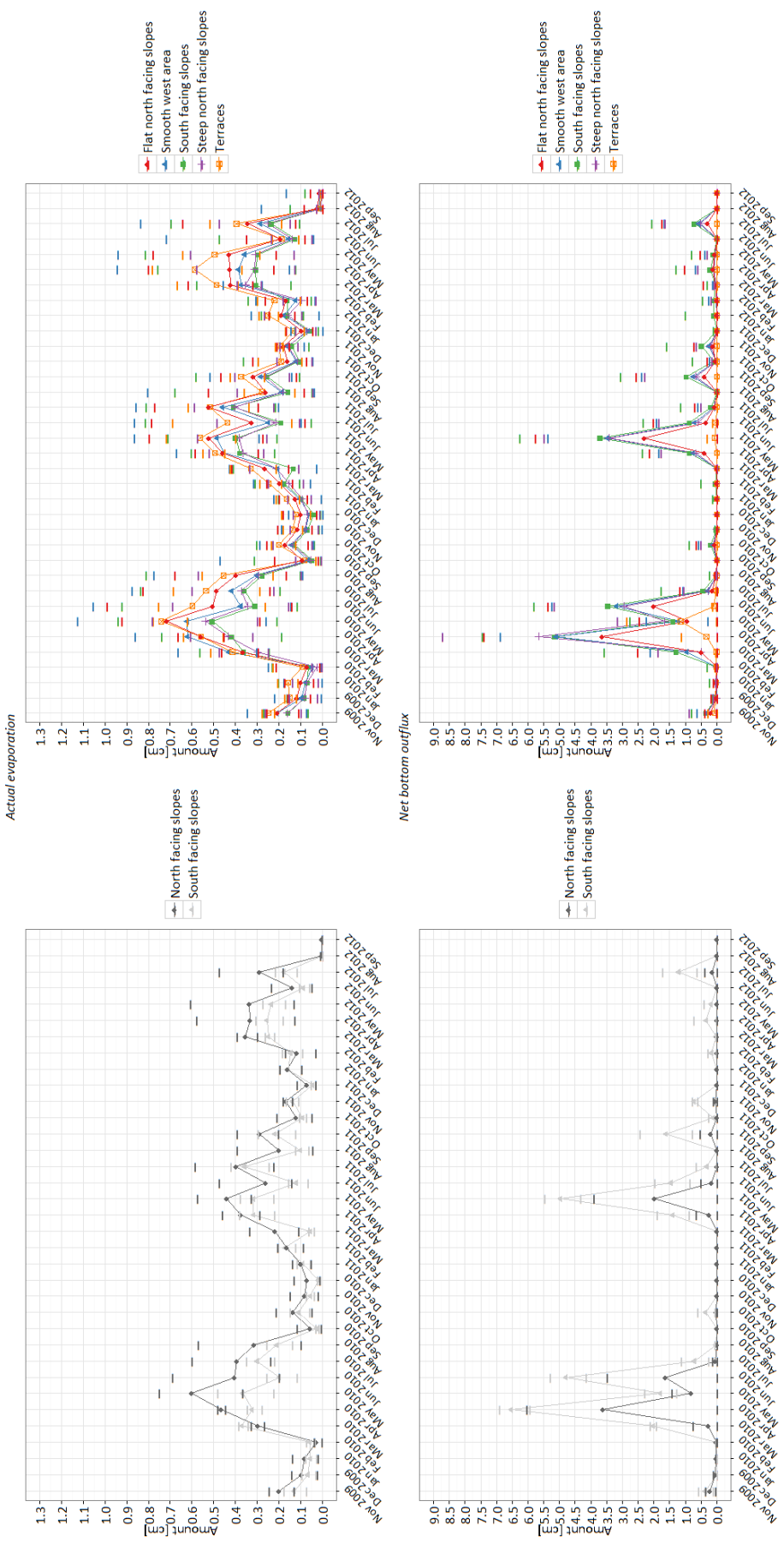

Figure 21b: Hydrological properties of a subset of the field points, corresponding to the location of the CZO transect, compared to the hydrological properties of the whole area subdivided into the five characterising areas.

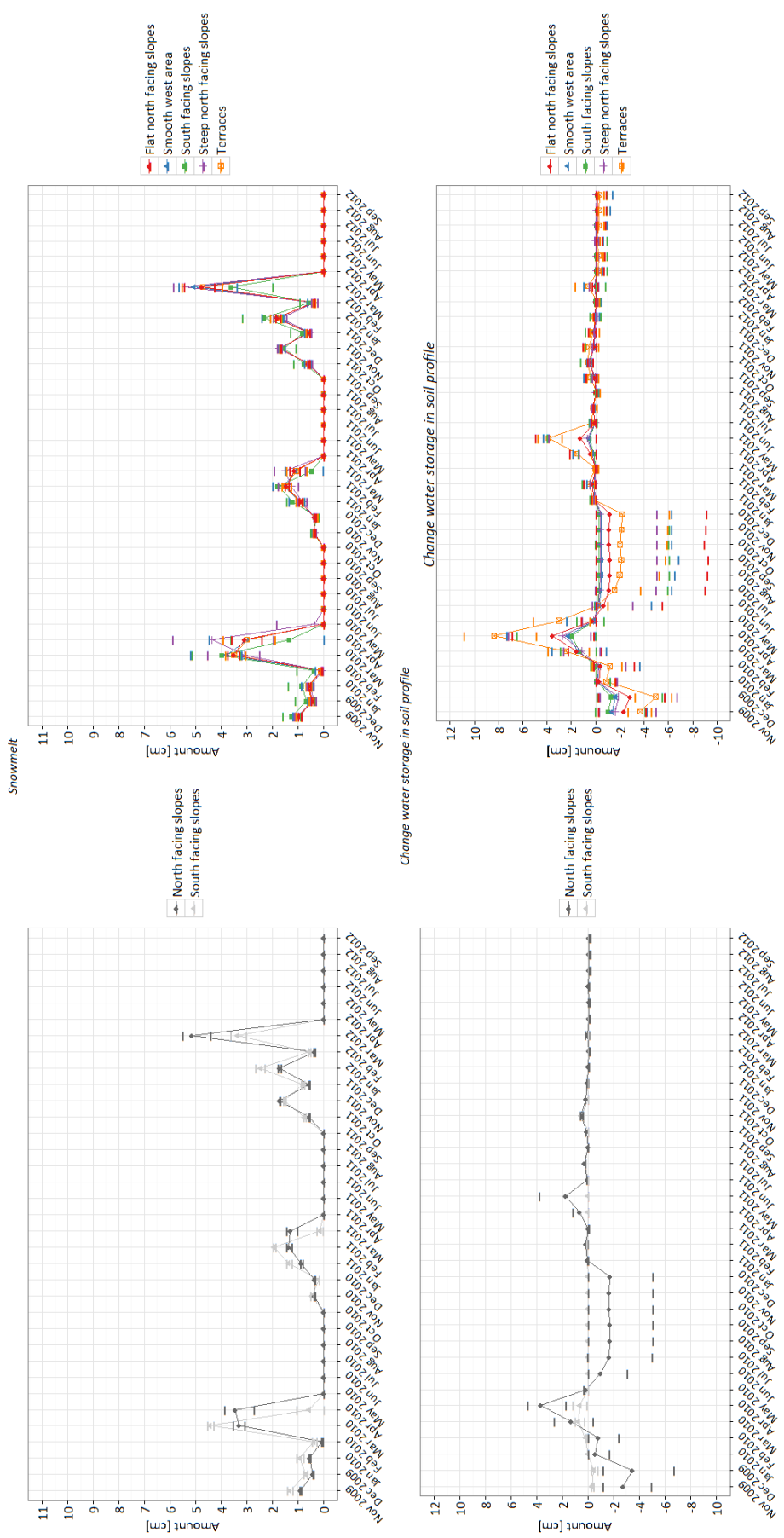

Figure 21c: Hydrological properties of a subset of the field points, corresponding to the location of the CZO transect, compared to the hydrological properties of the whole area subdivided into the five characterising areas.

Conclusion 6.

The Gordon Gulch Valley can be divided in five characterising areas, (i) the south facing slopes, (iia) the steep north facing slopes, (iib) the flat north facing slopes, (iii) the smooth area in the west of the study area and (iv) the Gordon Gulch and its small terraces. Each of these areas has its own landscape characteristics, and subsequently its own soil properties and hydrological behaviour.

The south facing slopes are characterised by steep slopes which are scarcely vegetated with coniferous trees (*Pinus Ponderosa*), and denser vegetated with herbaceous undergrowth. The south facing aspect entails that these slopes receive high amount of global radiation. The sandy soils are shallow, dry and highly permeable. They are characterised by little organic matter and a high stoniness through the whole profile. Despite these steep slopes and the shallow soils, the high permeability is preventing the slopes from runoff (which is the case for the whole area). The combination of high global radiation and a low tree cover result in less water input by snow, the snowpack is melting earlier in the year and is intermittent. Interception is high, while transpiration and evaporation are low as a result of the low tree cover and dry soils respectively. A lot of water enters the soil, most of this water ends up in the groundwater or creek. As a consequence little water is available to store in the soil.

The north facing slopes can be subdivided in two areas, (i) the steep north facing slopes and (ii) the flat north facing slopes. The steep north facing slopes are characterised by steep slopes, little undergrowth and a dense tree cover (*Pinus contorta*). The slopes receive little global radiation caused by the north facing aspect. Inmixing from aeolian inputs of silt and clay result in soils with slightly more fine materials. The soils are further characterised by a high moisture content, high organic matter percentages, a low pH and a high stoniness. Water input by snow is largest at the steep north facing slopes. The snowpack on these slopes is melting in the late spring and is not intermittent. Transpiration is moderately at these slopes. Although an overestimation, a lot of water of the steep north facing slopes is lost to interception. Most of the water which enters the soil will end up in the groundwater or the creek, only little water is evaporated and stored in the soil.
The flat slopes are characterised by relatively flat slopes compared to the south facing slopes and the steep north facing slopes. The tree cover (*Pinus contorta*) is slightly less dense and undergrowth are more common. Although still characterised by an north facing aspect, the flat position and relatively high position in the landscape entails that the slopes receive slightly more global radiation. The soils are characterised by a high organic matter content in the top soils, a slightly lower moisture content than the steep north facing slopes and by a slightly higher percentage of fine materials as a result of aeolian inputs. The soils contain less stones than the steep north facing slopes, since hillslope processes are less important here. At the flat north facing slopes transpiration is a more dominant process, less water is intercepted. As a consequence more water enters the soil. Compared to the steep north facing slope, little of this water ends up in the groundwater or the creek and more water is stored in the soil and evaporated during warm periods.

The smooth west area is characterised by flat slopes, receives relatively much global radiation and is covered by a moderate density of trees and undergrowth. Since the study area is west-east oriented, the smooth west area is located highest in elevation. The shallow, sandy soils of the smooth west area are further characterised by high organic matter percentages in the top soil, a high stoniness in the whole profile. Also here, although to a lesser extent, the influence of aeolian input result in slightly more fine materials. The smooth west area is, caused by its moderate vegetation cover and by receiving moderate global radiation, characterised by moderate transpiration and interception. Water which enters the soil, mainly ends up in the groundwater or creek or evaporates. Only little water is stored in these soils.

The terraces are located at the bottom of the valley. These highly vegetated areas are covered with a mixture of deciduous (*Populus tremuloides*) trees and coniferous (*Pinus ponderosa* and *Pinus contorta*) and a high density of deciduous undergrowth. The terraces are relatively flat and receive

little global radiation. Soil here have developed in accumulated materials from the hillslope and as a result of fluvial processes. This results in deep sandy, often layered, soils, high in organic matter and moisture content. Furthermore these soils contain little stones. The high density of deciduous vegetation result in a lot of transpiration. Interception values are low. The soils of the terraces act like a sponge and store a lot of water when available, in warm periods water is extracted from the soils by evaporation. The terrace soils have water most water available of the study area, in wet years this water is even available during the whole year.

Soil properties can be used to determine hydrological characteristics in a mountainous watershed. Hydrological characteristics, however cannot be determined without the availability of other data, like meteorological data for the water input, landscape characteristics like vegetation properties for transpiration and some hydrological properties for calibration. To which amount soil characteristics influence the hydrological characteristics needs further investigation, what we can conclude is that soil properties directly influence the amount of overland and subsurface flow, the amount of water that is stored by or evaporated out of the soil and subsequently the amount of water that ends up in the groundwater or the creek.

Understanding the hydrological properties in a complex landscape, like the Gordon Gulch watershed, will add to more accurate catchment-wide predictions and consequently helps policy in protecting and managing surface and groundwater resources in order to protect year-round water availability in semi-arid environments, like the Front Range of the Rocky Mountains.

References 7.

Anderson, R. S., Riihimaki, C. A., Safran, E. B. and MacGregor, K. R. 2006. Facing reality: Late Cenozoic evolution of smooth peaks, glacially ornamented valleys, and deep river gorges of Colorado's Front Range. *Geological Society of America, Special Paper,* 398, 397-418.

Anderson, S. P., Anderson, R. S., Hinckley, E.-L. S., Kelly, P. and Blum, A. 2011. Exploring weathering and regolith transport controls on Critical Zone development with models and natural experiments. *Applied Geochemistry,* 26, Supplement, S3-S5.

Anderson, S. P., Bales, R. C. and Duffy, C. J. 2008. Critical Zone Observatories: Building a network to advance interdisciplinary study of Earth surface processes. *Mineralogical Magazine,* 72, 7-10.

Arya, L. M. and Paris, J. F. 1981. A physicoempirical model to predict soil moisture characteristics from particle-size distribution and bulk density data. *Soil Science Society of America Journal,* 45, 1023-1030.

Beniston, M. 2006. Mountain weather and climate: A general overview and a focus on climatic change in the Alps. *Hydrobiologia,* 562, 3-16.

Birkeland, P. W., Shroba, R. R., Burns, S. F., Price, A. B. and Tonkin, P. J. 2003. Integrating soils and geomorphology in mountains - an example from the Front Range of Colorado. *Geomorphology,* 55, 329-344.

Boulder Creek CZO. *Gordon Gulch* [Online]. Available: http://czo.colorado.edu/html/gg.shtml [Accessed December 2012].

Boulder Creek CZO. 2013a. *Boulder Creek Betasso met data query* [Online]. Available: http://czo.colorado.edu/query/betmet1.shtml [Accessed December 2012].

Boulder Creek CZO. 2013b. *Discharge for Lower Gordon Gulch* [Online]. Available: http://czo.colorado.edu/query/disLowerGG.shtml [Accessed February 2013].

Boulder Creek CZO. 2013c. *Hydrology* [Online]. Available: http://czo.colorado.edu/html/data-hydrology.shtml [Accessed February 2013].

Bubel, A. 2008. *Geomorphology of Devlin's Park and the Caribou Creek catchment, Colorado Front Range.* Bachelor of Arts, Williams College. (unpublished undergraduate thesis).

Buraas, E. M. 2009. *Getting water into the ground and to the channel, Gordon Gulch, Colorado.* Bachelor of Arts, Williams College. (unpublished undergraduate thesis).

Clevers, J. and Verhoef, W. 1993. LAI estimation by means of the WDVI: a sensitivity analysis with a combined PROSPECT-SAIL model. *Remote Sensing Reviews,* 7, 43-64.

Condit, H. R. 1970. The spectral reflectance of American soils. *Photogrammetric Engineering,* 36, 955-966.

Dethier, D. P., Birkeland, P. W. and McCarthy, J. A. 2012. Using the accumulation of CBD-extractable iron and clay content to estimate soil age on stable surfaces and nearby slopes, Front Range, Colorado. *Geomorphology,* 173–174, 17-29.

Dethier, E. N. 2011. *Examining knickpoints in the Middle Boulder Creek Catchment, Colorado.* Bachelor of Arts, Williams College. (unpublished undergraduate thesis).

Eilers, K. G., Debenport, S., Anderson, S. and Fierer, N. 2012. Digging deeper to find unique microbial communities: the strong effect of depth on the structure of bacterial and archaeal communities in soil. *Soil Biology and Biochemistry,* 50, 58-65.

FAO 1990. Guidelines for Soil Description. 3 ed. Rome, Italy: FAO.

Gilbert, R. B. 2010. *Regolith stirring by biological processes, Gordon Gulch, Colorado.* Bachelor of Arts, Williams College. (unpublished undergraduate thesis).

Hinckley, E. S., Ebel, B. A., Barnes, R. T., Anderson, R. S., Williams, M. W. and Anderson, S. P. 2012. Aspect control of water movement on hillslopes near the rain–snow transition of the Colorado Front Range. *Hydrological Processes*.

Jenny, H. 1941. *Factors of soil formation.* New York, NY, USA, McGraw-Hill.

Kroes, J. G., Dam, J. C. V., Groenendijk, P., Hendriks, R. F. A. and Jacobs, C. M. J. 2008. SWAP version 3.2. Theory desription and user manual. *Report1649 - SWAP32 Theory description and user manual.* Wageningen, Netherlands: Alterra.

Kustas, W. P., Rango, A. and Uijlenhoet, R. 1994. A simple energy budget algorithm for the snowmelt runoff model. *Water Resourser Research,* 30, 1515-1527.

Langston, A. L., Tucker, G. E., Anderson, R. S. and Anderson, S. P. 2011. Exploring links between vadose zone hydrology and chemical weathering in the Boulder Creek critical zone observatory. *Applied Geochemistry,* 26, Supplement, S70-S71.

Martinec, J. (ed.) 1989. *Hour-to-hour snowmelt rates and lysimeter outflow during an entire ablation period. Proceedings of the Baltimore Symposium.* Baltimore, MD, USA: IAHS Publisher.

McBratney, A. B., Minasny, B., Cattle, S. R. and Vervoort, R. W. 2002. From pedotransfer functions to soil inference systems. *Geoderma,* 109, 41-73.

Meybeck, M., Green, P. and Vörösmarty, C. 2001. A new typology for mountains and other relief classes: an application to global continental water resources and population distribution. *Mountain Research and Development,* 21, 34-45.

Munsell Color 2009. *Geological rock-color chart.* Grand Rapids, MI, USA.

Murphy, S. F. 2006. *State of the watershed: water quality of Boulder Creek, Colorado.* Denver, CO, USA, U.S. Department of the Interior & U.S. Geological Survey.

Murphy, S. F., Verplanck, P. L. and Barber, L. B. 2003. *Comprehensive water quality of the Boulder Creek Watershed, Colorado, during high-flow and low-flow conditions, 2000.* Denver, CO, USA, U.S. Department of the Interior & U.S. Geological Survey.

National Science Foundation, Boulder Creek Critical Zone Observatory and National Center for Airborne Laser Mapping. 2010. *Boulder Creek Critical Zone Observatory August 2010 Snow-Off LiDAR Survey* [Online]. Available: http://opentopo.sdsc.edu/gridsphere/gridsphere?gs_action=lidarDataset&cid=geonlidarframeportlet&opentopoID=OTLAS.032012.26913.1 [Accessed January 2013].

NHI 2008. *Modelrapportage V1.0 - deelrapport gewaskenmerken.* Nationaal Hydrologisch Instrumentarium.

Pachepsky, Y. A., Rawls, W. J. and Lin, H. S. 2006. Hydropedology and pedotransfer functions. *Geoderma,* 131, 308-316.

Richards, L. A. 1931. Capillary conduction of liquids through porous mediums. *Physics,* 1, 318-333.

Schaap, M. G., Leij, F. J. and van Genuchten, M. T. 2001. Rosetta: a computer program for estimating soil hydraulic parameters with hierarchical pedotransfer functions. *Journal of Hydrology,* 251, 163-176.

Schaap, M. G., Pachepsky, Y. and Rawls, W. J. 2005. Graphic user interfaces for pedotransfer functions. *Developments in Soil Science,* 30, 349-356.

Sonneveld, M. P. W., Backx, M. A. H. M. and Bouma, J. 2003. Simulation of soil water regimes including pedotransfer functions and land-use related preferential flow. *Geoderma,* 112, 97-110.

Soulsby, C., Tetzlaff, D., Rodgers, P., Dunn, S. and Waldron, S. 2006. Runoff processes, stream water residence times and controlling landscape characteristics in a mesoscale catchment: an initial evaluation. *Journal of Hydrology,* 325, 197-221.

Stumpp, C., Engelhardt, S., Hofmann, M. and Huwe, B. 2009. Evaluation of pedotransfer functions for estimating soil hydraulic properties of prevalent soils in a catchment of the Bavarian Alps. *European Journal of Forest Research,* 128, 609-620.

Terribile, F., Coppola, A., Langella, G., Martina, M. and Basile, A. 2011. Potential and limitations of using soil mapping information to understand landscape hydrology. *Hydrology and Earth System Sciences,* 15, 3895-3933.

USDA-NCRS. 2008. *Soil Survey Geographic (SSURGO) database*. Fort Worth, TX, USA: USDA-NCRS.

USDA-NCRS. 2011. *GeoSpatialDataGateway* [Online]. Available: http://datagateway.nrcs.usda.gov/ [Accessed June 2012].

USDA-NRCS. 1999. Soil Taxonomy. A Basic System of Soil Classification for Making and Interpreting Soil Surveys. Washington, DC, USA: USDA-NRCS.

USGS. 2005. *State geologic maps*. Reston, VA, USA: USGS.

USGS. 2012. *USGS Global Visualization Viewer* [Online]. Available: http://glovis.usgs.gov/ [Accessed December 2012].

van Dam, J. C. 2000. *Field scale water flow and solute transport. SWAP model concepts, parameter estimation and case studies.* PhD thesis, Wageningen University.

van Tol, J., Le Roux, P. and Hensley, M. 2011. Chapter 12. Soil indicators of hillslope hydrology. *In:* Özkaraova Güngör, E. B. (ed.) *Principles, application and assessment in soil science.* Rijeka, Croatia: InTech.

van Tol, J. J., Le Roux, P., Hensley, M. and Lorentz, S. A. 2010. Soil as indicator of hillslope hydrological behaviour in the Weatherley Catchment, Eastern Cape, South Africa. *Water SA,* 36, 513-520.

Vereecken, H., Maes, J., Van Orshoven, J. and Feyen, J. 1989. Deriving pedotransfer functions of soil hydraulic properties. *Land qualities in space and time. Proc. ISSS symposium, Wageningen, 1988*, 121-124.

Völkel, J., Huber, J. and Leopold, M. 2011. Significance of slope sediments layering on physical characteristics and interflow within the Critical Zone - examples from the Colorado Front Range, USA. *Applied Geochemistry,* 26, Supplement, S143-S145.

Western Regional Climate Center. 2012. *SOD USA Climate Archive, Colorado* [Online]. Available: http://www.wrcc.dri.edu/summary/wyF.html [Accessed February 2013].

Wösten, J. H. M. 1997. Chapter 10. Pedotransfer functions to evaluate soil quality. *In:* Gregorich, E. G. and Carter, M. R. (eds.) *Soil quality for crop production and ecosystem health. Developments in soil science.* Amsterdam, Netherlands: Elsevier.

Wösten, J. H. M., Pachepsky, Y. A. and Rawls, W. J. 2001. Pedotransfer functions: bridging the gap between available basic soil data and missing soil hydraulic characteristics. *Journal of Hydrology,* 251, 123-150.

Appendix A.

Hydraulic properties

i. Hydraulic characteristics (Output pedotransfer functions)

Table A shows a summary of the hydraulic properties. Table A shows the hydraulic properties for each horizon. Although there are seven Van Genuchten parameters, the residual water content, the saturated water content and the saturated hydraulic conductivity are most interesting if we look at the hydraulic properties.

Looking at the residual water content (θ_r), the residual water content decreases with the depth. The saturated water content (θ_s) increases in the mid horizons and decreases in the C horizons. As we look at the saturated hydraulic conductivity (K_{sat}), the top horizons are more permeable than the mid and C horizons.

Table A1: Summary of the hydraulic properties

Soil property	n	mean	min.	max.	sd.
θ_r [cm^3 cm^{-3}]	177	0.043	0.033	0.052	0.003
θ_s [cm^3 cm^{-3}]	177	0.479	0.330	0.726	0.071
α [cm^{-1}]	177	0.050	0.035	0.083	0.009
n [-]	177	2.08	1.36	3.67	0.462
K_s [cm day^{-1})	177	496.67	84.13	1071.57	187.16
K_0 [cm day^{-1}]	177	91.54	28.18	472.35	66.02
L [-]	177	-0.85	-2.22	-0.73	0.204

Table A2: Hydraulic properties per horizon

		θ_r [cm^3 cm^{-3}]	θ_s [cm^3 cm^{-3}]	α [cm^{-1}]	n [-]	K_s [cm day^{-1}]	K_0 [cm day^{-1}]	L [-]
top horizon	n	100	100	100	100	100	100	100
	min.	0.035	0.330	0.035	1.36	84.13	28.18	-2.22
	max.	0.052	0.726	0.083	3.67	1071.57	472.35	-0.73
	mean	0.043	0.478	0.050	2.14	201.27	92.10	-0.85
mid horizon	n	58	58	58	58	58	58	58
	min.	0.036	0.353	0.036	1.37	120.29	29.55	-2.16
	max.	0.050	0.709	0.069	3.22	926.17	264.02	-0.73
	mean	0.043	0.488	0.051	2.02	168.40	62.22	-0.86
C horizon	n	19	19	19	19	19	19	19
	min.	0.032	0.359	0.042	1.52	87.56	38.84	-1.02
	max.	0.045	0.583	0.065	2.38	658.58	206.83	-0.75
	mean	0.041	0.459	0.049	1.94	125.83	76.14	-0.81
η^2		*0.032*	*0.007*	*0.001*	*0.016*	*0.037*	*0.006*	*0.003*
p(equal means)		*$1.69\ 10^{-2}$*	*$2.52\ 10^{-1}$*	*$6.11\ 10^{-1}$*	*$9.79\ 10^{-2}$*	*$1.08\ 10^{-2}$*	*$3.15\ 10^{-1}$*	*$4.40\ 10^{-1}$*

The black values indicate that the considered property is statistical significant with $p < 0.05$

ii. Differences between the landscape characteristics

Table A differentiates the hydraulic properties in the five characterising areas. The saturated water content of the top horizon is smallest at the north facing slopes and largest at the terraces. The residual water content of the top soils of the south facing slopes and the smooth west area are close to the highest residual water content. In general for all characterising areas the residual water content decreases with the depth. The saturated water content is highest at the terraces and the flat north facing slopes. Lowest is the saturated water content at the steep sloping areas. The saturated water content increases with the depth for the south facing slopes, the steep north facing slopes and the terraces and is decreasing for the flat north facing slopes. The smooth west area has a variable saturated water content over the depth. The permeability of the top (saturated hydraulic conductivity) is highest at the south facing slopes, and lowest at the north facing slopes. Saturated hydraulic conductivity increases with the depth for all characterising areas except for the flat north facing slopes.

Table A3: Hydraulic properties, differences between the five characterising areas

	soil property	south facing slopes	steep north facing slopes	flat north facing slopes	smooth west area	terraces	η^2	*p(equal means)*
top horizon	θ_r [cm³ cm^{-3}]	0.045	0.041	0.041	0.044	0.045	*0.180*	*1.08 10^{-5}*
	θ_s [cm³ cm^{-3}]	0.462	0.474	0.500	0.493	0.520	*0.016*	*0.2100*
	α [cm^{-1}]	0.048	0.050	0.053	0.051	0.056	*0.022*	*0.1397*
	n [-]	2.38	1.95	1.82	2.07	2.07	*0.151*	*6.54 10^{-5}*
	K_s [cm day^{-1})	577.07	479.37	378.28	524.34	539.00	*0.079*	*0.0046*
	K_0 [cm day^{-1}]	86.51	78.81	108.99	99.46	133.58	*0.001*	*0.7737*
	L [-]	-0.86	-0.79	-0.92	-0.88	-0.87	*0.002*	*0.6982*
mid horizon	θ_r [cm³ cm^{-3}]	0.044	0.042	0.042	0.044	0.045	*0.048*	*0.1001*
	θ_s [cm³ cm^{-3}]	0.464	0.477	0.499	0.532	0.521	*0.009*	*0.4862*
	α [cm^{-1}]	0.048	0.050	0.052	0.055	0.056	*0.011*	*0.4360*
	n [-]	2.17	1.94	1.90	1.85	2.12	*0.044*	*0.1155*
	K_s [cm day^{-1})	518.23	475.54	392.00	474.94	497.46	*0.038*	*0.1442*
	K_0 [cm day^{-1}]	76.59	79.80	102.34	129.78	145.29	*0.004*	*0.6588*
	L [-]	-0.81	-0.79	-0.96	-0.97	-0.89	*0.008*	*0.5187*
C horizon	θ_r [cm³ cm^{-3}]	0.041	0.041	0.039	0.042	0.045	*0.008*	*0.7151*
	θ_s [cm³ cm^{-3}]	0.428	0.483	0.449	0.430	0.571	*0.213*	*0.0467*
	α [cm^{-1}]	0.045	0.051	0.049	0.045	0.064	*0.233*	*0.3661*
	n [-]	1.99	1.82	1.96	2.15	1.74	*0.111*	*0.1640*
	K_s [cm day^{-1})	351.07	446.87	442.31	415.01	446.87	*0.111*	*0.1640*
	K_0 [cm day^{-1}]	50.08	86.11	64.34	53.57	195.13	*0.169*	*0.0809*
	L [-]	-0.83	-0.77	-0.77	-0.79	-0.92	*0.049*	*0.3636*

The black values indicate that the considered property is statistical significant with $p < 0.05$

iii. Validation of the hydraulic properties

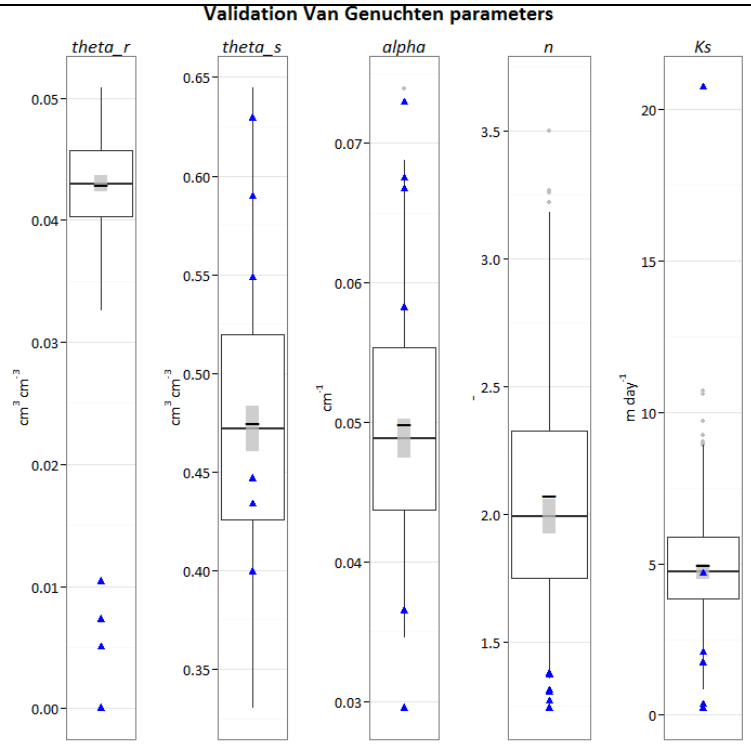

Figure A1: Validation of the Van Genuchten parameters based on the data of Hinckley et al. (2012)
The blue triangles show the observations of Hinckley et al. (2012), the lightgrey points represent the outliers, the lightgrey bar shows the confidence interval and the black dash is the mean.

Based on data of Hinckley et al. (2012) we validated the hydraulic properties. Hinckley et al. (2012) measured for three soils (one on the north facing slope, one on the south facing slope and a terrace soil) the Van Genuchten parameters at two depths (0-10 cm and 10-25 cm). We compared their results with the range of our hydraulic properties. Figure A shows the result of this validation. In most cases the data of Hinckley et al. (2012) are located within the range of our hydraulic properties, only our values of the parameter θ_r are higher than the measurements of Hinckley et al. (2012). The estimated hydraulic properties by rosetta are close to the reality and could be used as realistic input for the SWAP model.

Appendix B.

SWAP input

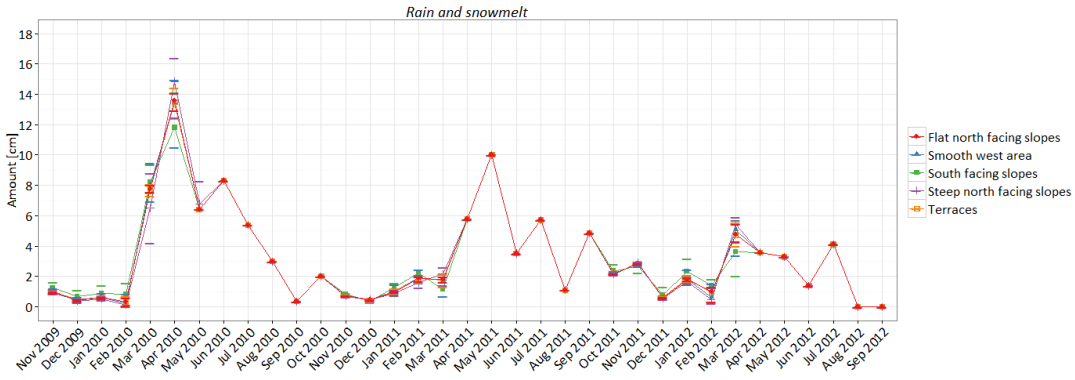

Figure B1: The swap precipitation input, in this case the sum of rain and snowmelt.

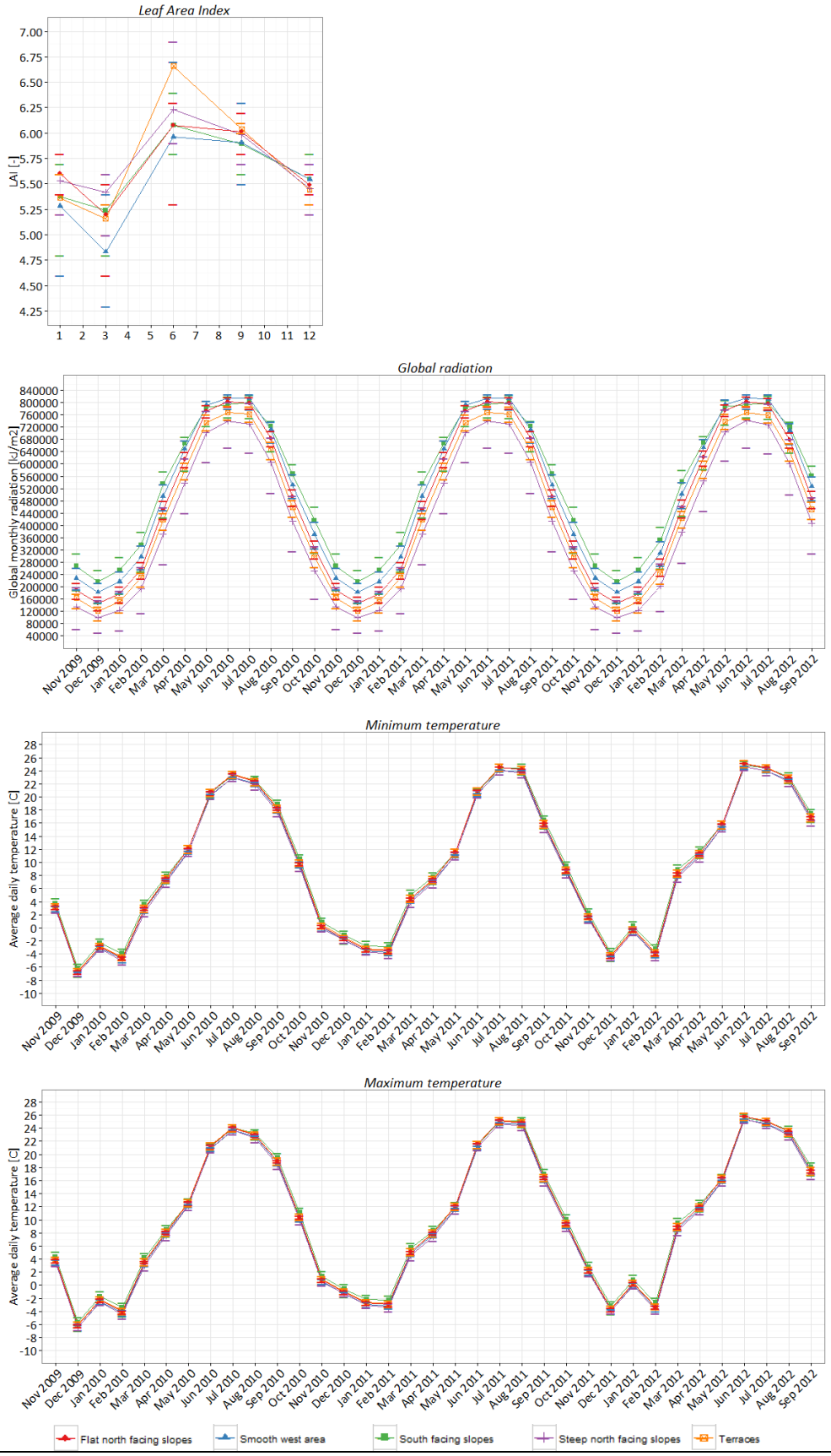

Figure B2: Graphical representation of a selection of the swap input

Cross tables field characteristics

Table C1: Correlation matrix (Pearsons correlation coefficients [-]) field characteristics

	aspect	plan curvature	profile curvature	slope	elevation	global annual radiation	erosion	flow accumu-lation	TWI	vegetation height	LAI	LAI_{tree}	tree cover	undergrowth cover	runoff features	parent material	distance to streams	distance to exposed bedrock	characte-rising areas	aspect N/S
aspect	1.00																			
plan curvature	0.07	1.00																		
profile curvature	0.04	0.39***	1.00																	
slope	0.00	0.09	0.04	1.00																
elevation	-0.02	-0.05	0.00	-0.32**	1.00															
global annual radiation	0.51***	0.05	-0.04	-0.18	0.41***	1.00														
erosion	0.08	0.12	-0.11	-0.07	0.37***	0.07	1.00													
flow accumu-lation	-0.06	-0.01	0.25*	-0.03	-0.40***	-0.12	-0.84***	1.00												
TWI	0.12	-0.28**	0.04	-0.40***	-0.05	0.12	-0.53***	0.50***	1.00											
vegetation height	-0.48***	-0.12	0.02	0.20	-0.24*	-0.56***	-0.10	0.07	-0.12	1.00										
LAI	-0.31**	-0.06	-0.04	0.17	-0.16	-0.31**	-0.01	0.00	-0.09	0.57***	1.00									
LAI_{tree}	-0.23*	0.02	0.02	-0.13	0.04	-0.40***	0.07	0.00	-0.07	0.63***	0.54***	1.00								
tree cover	-0.43***	-0.11	0.04	-0.11	0.21*	-0.40***	0.16	-0.14	0.06	0.64***	0.51***	0.63***	1.00							
undergrowth cover	0.19	-0.04	0.11	0.16	-0.41***	0.31**	-0.53	0.49***	0.30**	-0.22*	-0.12	-0.49***	-0.48***	1.00						
runoff features	0.39***	-0.06	-0.08	0.17	0.11	0.36***	0.05	-0.12	-0.13	-0.17	0.03	-0.01	-0.28**	-0.01	1.00					
parent material	0.05	-0.14	0.26*	-0.20	-0.10	0.09	-0.48***	0.50***	0.44***	0.02	-0.04	-0.03	-0.01	0.50***	-0.12	1.00				
distance to streams	0.22*	0.10	0.11	-0.31**	0.56***	0.42***	0.41***	-0.35***	-0.11	-0.42***	-0.07	-0.04	-0.06	-0.20	0.28**	-0.18	1.00			
distance to exposed bedrock	-0.09	-0.16	-0.08	-0.01	-0.24*	-0.13	-0.26*	0.20	0.31**	0.12	0.11	-0.03	0.01	0.19	0.03	0.17	-0.23*	1.00		
characte-rising areas	-0.32**	0.06	0.05	-0.33**	-0.24*	-0.67***	0.04	0.07	0.04	0.30**	0.28**	0.39***	0.38***	-0.34**	-0.29**	-0.02	-0.05	0.10	1.00	
aspect N/S	0.61***	0.07	0.18	-0.08	0.24*	0.75***	-0.01	0.04	0.20	-0.47***	-0.35***	-0.37***	-0.40***	0.35***	0.31**	0.09	0.33**	-0.12	-0.56***	1.00

Significance codes: 0.001 '***'; 0.01 '**'; 0.05 '*'
The grey areas indicate a Pearsons correlation coefficient of -0.4 > r > 0.4

Cross tables soil properties (top and mid horizon)

Table D1: Correlation matrix (Pearsons correlation coefficients [-]) soil properties (top and mid horizon)

		general (upper 7 cm of the soil)					top horizon										mid horizon								
		bulk density	porosity	water-filled pore space	moisture content	volumetric water content	OM	pH	sand	silt	clay	moisture	roots	stoniness	duff	charcoal	OM	pH	sand	silt	clay	moisture	roots	stoniness	charcoal
general (upper 7 cm of the soil)	bulk density	1.00																							
	porosity	-1.00***	1.00																						
	water-filled pore space	0.02	-0.02	1.00																					
	moisture content	-0.57***	0.57***	0.76***	1.00																				
	volumetric water content	-0.25*	0.25*	0.95***	0.90***	1.00																			
top horizon	OM	-0.16	0.16	-0.12	0.01	-0.06	1.00																		
	pH	0.13	-0.13	0.04	0.02	0.03	-0.26*	1.00																	
	sand	-0.09	0.09	0.04	0.08	0.06	0.17	0.14	1.00																
	silt	0.10	-0.10	-0.02	-0.06	-0.04	-0.17	-0.13	-0.99***	1.00															
	clay	-0.04	0.04	-0.20	-0.14	-0.18	0.00	-0.16	-0.31**	0.21*	1.00														
	moisture	-0.30**	0.30**	0.30**	0.40***	0.39***	0.34**	-0.07	-0.05	0.06	-0.10	1.00													
	roots	-0.12	0.12	0.36***	0.40***	0.41***	-0.05	0.13	0.05	-0.04	-0.14	0.34***	1.00												
	stoniness	-0.18	0.18	-0.11	-0.04	-0.11	-0.22*	-0.01	0.04	-0.05	0.06	-0.19	-0.09	1.00											
	duff	-0.12	0.12	-0.16	-0.11	-0.14	0.21*	-0.23*	0.13	-0.14	0.03	0.05	-0.30**	-0.06	1.00										
	charcoal	-0.19	0.19	0.16	0.20	0.20	0.19	-0.19	-0.17	0.18	-0.05	0.21*	-0.05	-0.26*	0.10	1.00									
mid horizon	OM	-0.31*	0.31*	0.33*	0.44**	0.40**	0.16	0.09	0.00	0.02	-0.12	0.24	0.07	-0.26	0.02	0.21	1.00								
	pH	-0.08	0.08	0.07	0.18	0.12	-0.02	0.54***	0.15	-0.14	-0.13	0.09	0.32*	-0.40**	-0.32*	-0.06	0.17	1.00							
	sand	-0.12	0.12	-0.05	0.05	0.00	0.03	0.17	0.22	-0.22	-0.02	0.16	0.26	-0.08	-0.30*	-0.25	0.00	0.35*	1.00						
	silt	0.12	-0.12	0.11	0.00	0.06	-0.02	-0.16	-0.24	0.24	0.01	-0.15	-0.26	0.02	0.30*	0.26	0.01	-0.30*	-0.99***	1.00					
	clay	0.02	-0.02	-0.34*	-0.30*	-0.34*	-0.03	-0.11	0.03	-0.04	0.02	-0.11	-0.09	0.38**	0.07	0.01	-0.07	-0.38**	-0.39**	0.24	1.00				
	moisture	-0.35*	0.35*	0.33*	0.47***	0.42**	0.14	0.10	0.16	-0.15	-0.13	0.53***	0.20	-0.09	-0.07	0.22	0.49***	0.08	-0.08	0.05	0.18	1.00			
	roots	0.03	-0.03	-0.03	-0.04	-0.04	-0.03	0.07	0.06	-0.07	0.07	-0.03	0.23	0.18	-0.19	-0.07	-0.02	0.09	0.16	-0.19	0.12	-0.16	1.00		
	stoniness	0.08	-0.08	-0.15	-0.25	-0.20	-0.05	-0.08	-0.13	0.11	0.21	-0.23	-0.27	0.76***	-0.12	-0.05	-0.24	-0.37**	-0.13	0.06	0.45***	-0.05	0.27	1.00	
	charcoal	-0.21	0.21	0.23	0.32*	0.28	0.09	-0.05	0.07	-0.09	0.11	0.18	0.11	-0.11	-0.04	0.17	0.28*	0.20	0.14	-0.12	-0.19	0.15	0.11	-0.18	1.00

Significance codes: 0.001 '***'; 0.01 '**'; 0.05 '*'
The grey areas indicate a Pearsons correlation coefficient of -0.4 > r > 0.4

Table D2: Correlation matrix (Pearsons correlation coefficients [-]) field characteristics and soil properties (top and mid horizon)

		aspect	plan curvature	profile curvature	slope	elevation	global annual radiation	erosion	flow accumu-lation	TWI	vegetation height	LAI	LAI_{tree}	tree cover	undergrowth cover	runoff features	parent material	distance to streams	distance to exposed bedrock	characte-rising areas	aspect N/S
general upper 7 cm of the soil	bulk density	0.27**	-0.31**	-0.35***	-0.02	0.09	0.22*	0.17	-0.11	-0.05	-0.38***	-0.19	-0.24*	-0.30**	0.00	0.17	-0.22*	0.14	-0.01	-0.18	0.12
	porosity	-0.27**	0.31**	0.35***	0.02	-0.09	-0.22*	-0.17	0.11	0.05	0.38***	0.19	0.24*	0.30**	0.00	-0.17	0.22*	-0.14	0.01	0.18	-0.12
	water-filled pore space	-0.22*	-0.13	-0.11	-0.12	-0.05	-0.11	-0.09	0.13	0.10	0.25*	0.19	0.18	0.21*	0.12	-0.14	0.30**	-0.35***	0.08	0.07	-0.16
	moisture content	-0.28**	0.16	0.22*	-0.07	-0.10	-0.18	-0.24*	0.23*	0.17	0.34**	0.23*	0.21*	0.28**	0.20	-0.26*	0.46***	-0.37***	0.08	0.12	-0.17
	volumetric water content	-0.28**	-0.07	-0.01	-0.13	-0.07	-0.17	-0.17	0.18	0.15	0.33**	0.22*	0.21	0.27**	0.16	-0.21*	0.39***	-0.40***	0.10	0.11	-0.19
top horizon	OM	-0.10	-0.10	0.09	-0.12	-0.14	-0.12	-0.07	0.00	0.10	0.05	0.06	0.02	0.17	-0.09	-0.22*	0.04	-0.04	0.05	0.18	-0.06
	pH	0.11	-0.01	-0.06	0.09	-0.11	0.26*	-0.28**	0.24*	0.19	-0.28**	-0.21*	-0.39***	-0.43***	0.49***	0.13	0.18	-0.05	-0.02	-0.26*	0.22*
	sand	0.13	-0.11	-0.03	0.13	-0.04	0.29**	-0.28**	0.18	0.17	0.06	0.03	-0.12	-0.08	0.33**	0.13	0.14	-0.05	0.03	-0.43***	0.23*
	silt	-0.15	0.12	0.02	-0.14	0.04	-0.28**	0.27**	-0.17	-0.16	-0.08	-0.02	0.11	0.07	-0.32**	-0.13	-0.15	0.05	-0.01	0.43***	-0.23*
	clay	0.11	-0.09	0.07	0.07	0.04	-0.20	0.15	-0.10	-0.06	0.11	-0.05	0.11	0.13	-0.20	0.00	-0.02	-0.02	-0.16	0.10	-0.07
	moisture content	-0.37***	-0.05	-0.05	-0.17	0.03	-0.19	-0.19	0.10	0.19	0.27*	0.15	0.21*	0.27*	-0.07	-0.22*	0.31**	-0.26*	0.23*	0.15	-0.24*
	root density	-0.05	-0.08	0.11	-0.04	-0.01	0.12	-0.31**	0.27*	0.28**	0.09	0.07	-0.06	0.00	0.34***	0.04	0.38***	-0.14	0.13	-0.20	0.16
	stoniness	0.14	0.37***	-0.09	0.28**	0.09	0.14	0.24*	-0.24*	-0.32**	-0.04	-0.06	0.02	-0.15	-0.21*	0.31**	-0.39***	-0.01	-0.19	-0.26*	0.13
	duff	0.00	-0.18	-0.10	-0.27*	0.18	0.04	0.13	-0.13	0.12	0.07	0.01	0.17	0.18	-0.27*	-0.02	-0.10	0.17	0.09	0.13	0.15
	charcoal	-0.42***	-0.07	0.10	-0.24*	0.15	-0.36***	0.02	-0.04	-0.04	0.22	0.05	0.23*	0.38***	-0.23*	-0.38***	0.02	0.01	0.00	0.42***	-0.24*
mid horizon	OM	-0.34*	0.15	0.02	-0.11	-0.45**	-0.33*	-0.31*	0.32*	0.19	0.27*	0.20	0.17	0.27	0.25	-0.49***	0.11	-0.38**	0.22	0.34*	-0.29*
	pH	-0.02	0.00	0.11	0.14	-0.07	0.28	-0.42**	0.29*	0.24	-0.19	0.02	-0.43**	-0.19	0.67***	0.01	0.39**	-0.05	0.15	-0.21	0.27
	sand	0.12	-0.12	-0.02	0.33*	-0.21	0.04	-0.45**	0.28	0.20	0.03	0.08	-0.08	-0.15	0.39**	0.06	0.29*	-0.22	0.05	-0.20	0.00
	silt	-0.13	0.12	0.00	-0.35*	0.22	-0.03	0.43**	-0.25	-0.16	-0.04	-0.07	0.09	0.17	-0.36*	-0.07	-0.23	0.22	-0.03	0.22	0.01
	clay	0.00	0.02	0.14	0.05	0.03	-0.09	0.29*	-0.26	-0.27	0.06	-0.07	-0.03	-0.06	-0.31*	0.04	-0.42**	0.03	-0.14	-0.06	-0.03
	moisture content	-0.33	-0.17	-0.02	-0.12	-0.25	-0.20	-0.32*	0.15	0.32*	0.28	0.06	-0.05	0.19	0.16	-0.25	0.22	-0.43**	0.26	0.14	-0.19
	root density	-0.11	0.26	0.14	0.45**	0.19	0.07	0.03	-0.08	-0.39**	0.22	0.13	0.04	0.02	-0.04	0.16	-0.14	0.06	-0.26	-0.27	0.11
	stoniness	0.09	-0.04	-0.35*	0.39**	0.13	-0.12	0.51***	-0.48***	-0.54***	0.16	0.06	0.04	0.09	-0.54***	0.22	-0.52***	-0.01	-0.41*	-0.07	-0.11
	charcoal	-0.21	0.19	0.07	0.08	-0.24	-0.23	-0.24	0.05	0.08	0.28	0.16	0.13	0.13	0.10	-0.01	0.00	-0.31*	0.40*	0.12	-0.22

Significance codes: 0.001 '***'; 0.01 '**'; 0.05 '*'
The grey areas indicate a Pearsons correlation coefficient of -0.4 > r > 0.4

Appendix E.

Hydrological processes

In general hydrologic movement is strongly influenced by soil characteristics and surface and subsurface topography (Sidle et al., 2001). The degree of their influence varies with the moisture content of the soil. According to Lin et al. (2006) the influence of soil characteristics is dominating in drier periods, whereas in wetter periods topography becomes the controlling factor of the hydrological movement.

In this appendix the dominating hydrological processes identified in the study area are discussed in more detail. First a definition of the processes is given, second the soil properties and site characteristics influencing these hydrological processes are discussed and finally a methodology to estimate or calculate the hydrological processes is proposed.

i. Precipitation

Precipitation [mm] is all liquid or solid phase product of the condensated water vapour in the atmosphere that falls to the earth's surface under gravity.

Estimation and calculation
Precipitation data for the study area can be collected from nearby meteorological stations. The annual average is 550 mm precipitation a year, with a peak from March to May. In winter the main form of precipitation is snow, which accumulates from September to May.

ii. Evaporation and transpiration

Evapotranspiration [mm] is the sum of evaporation and transpiration. Evaporation is defined, by Allen et al. (1998), as the process whereby liquid water is converted to water vapour and the movement of this water vapour to the air from sources such as the soil, vegetation, water bodies, and other surfaces. Transpiration is defined, by Allen et al. (1998) as well, as the vaporisation of liquid water contained in plant tissues (mainly through the stomata of the plant) and the movement of this water vapour to the atmosphere. Both transpiration and evaporation depends on energy supply (solar radiation and air temperature), vapour pressure (air humidity) and wind, furthermore the amount of evaporation and transpiration is influenced by the available water (soil water content and crop characteristics). Since evaporation and transpiration occur simultaneously and it is difficult to distinguish both processes, evapotranspiration was introduced.

Site characteristics
Aspect influences the amount of evapotranspiration, due to differences in the amount of direct sunlight (van Tol et al., 2011). South facing (northern hemisphere) slopes receive more direct sunlight and as a result these slopes are generally drier compared to north facing slopes.

Estimation and calculation
Evapotranspiration is influenced by three factors, (i) weather parameters, (ii) crop characteristics, and (iii) management and environmental aspects. Therefore a distinction is made between reference crop evapotranspiration (ET_0, based on a reference crop and climate), crop evapotranspiration under standard conditions (ET_c), and crop evapotranspiration under non-standard conditions ($ET_{c\ adj}$). In this study we will focus on ET_0, since this parameter is only affected by climatic data. According to Allen et al. (1998) the best method to calculate ET_0 is the FAO Penman-Monteith method. The Penman-Monteith equation is as follows:

$$\lambda ET = \frac{\Delta(R_n - G) + \rho_a c_p \dfrac{(e_s - e_a)}{r_a}}{\Delta + \gamma\left(1 + \dfrac{r_s}{r_a}\right)} \qquad \textit{[1]}$$

where ET is the evapotranspiration [mm day^{-1}], λ is the latent heat of vaporisation [MJ kg^{-1}], R_n is the net radiation [MJ m^{-2} day^{-1}], G is the soil heat flux [MJ m^{-2} day^{-1}], (e_s-e_a) is the vapour pressure deficit of the air [kPa], ρ_a is the mean air density at constant pressure [kg m^{-3}], c_p is the specific heat of the air [MJ kg^{-1} °C^{-1}], Δ represents the slope of the saturation vapour pressure temperature relationship [kPa °C^{-1}], γ is the psychrometric constant [kPa °C^{-1}] and r_s is the (bulk) surface resistance [s m^{-1}] and r_a is the (bulk) aerodynamic resistance [s m^{-1}].

Based on a reference crop (assuming a crop height of 0.12 m, a fixed surface resistance of 70 s m^{-1} and an albedo of 0.23) the FAO Penman-Monteith can be derived from the original Penman-Monteith equation:

$$ET_0 = \frac{0.408\Delta(R_n - G) + \gamma \dfrac{900}{T + 273} u_2 (e_s - e_a)}{\Delta + \gamma(1 + 0.34u_2)} \qquad \textit{[2]}$$

where ET_0 is the reference evapotranspiration [mm day^{-1}], R_n is the net radiation at the crop surface [MJ m^{-2} day^{-1}], G is the soil heat flux density [MJ m^{-2} day^{-1}], T is the air temperature at 2 m height [°C], u_2 is the wind speed at 2 m height [m s^{-1}], e_s is the saturation vapour pressure [kPa], e_a is the actual vapour pressure [kPa], e_s-e_a is the saturation vapour pressure deficit [kPa], Δ is slope vapour pressure curve [kPa °C^{-1}], and γ is the psychrometric constant [kPa °C^{-1}].

The value of ET_0 can be calculated based on available climate data, i.e. minimum and maximum temperature, humidity, wind speed, global radiation, sunshine hours. Values for G, e_s, e_a, Δ, and γ can be calculated based on the functions in Allen et al. (1998).

iii. Open water storage

Open water storage accounts for all water storage in open water.

Estimation and calculation

Except for the Gordon Gulch Creek, which drains water out of the area, no open water is present in the Gordon Gulch Valley.

iv. Discharge

Discharge [m^3 s^{-1}] is the volume rate of water (including any suspended solids, dissolved chemical species and/or biologic material) transported out of the area. In this study the discharge is defined by the water volume draining out of the study areas through the creek (i.e. Gordon Gulch Creek).

Estimation and calculation

Discharge of water can be measured at the location were Gordon Gulch Creek is flowing out of the study area. For Gordon Gulch Valley these data are available (Boulder Creek CZO, 2013a).

v. Water storage in snow

Water storage in snow [m^3] is defined as the amount of water that is locked up in the form of snow and ice.

Soil properties and site characteristics

Snow deposition is influenced by *elevation*, due to its relation to *temperature* and *precipitation*, therefore generally greater amounts of snow are deposited at higher *elevations* (Erickson et al., 2005; Farinotti et al., 2010). After deposition snow is redistributed by wind, avalanching and sloughing (Erickson et al., 2005). From this moment *topography*, *wind* and *vegetation cover* become important factors controlling snow accumulation en distribution in the catchment (Marks and Winstral, 2001; Winstral et al., 2002; Seyfried et al., 2009). This results in scour sites with little snow accumulation on wind-exposed areas and to drift zones with a lot of snow accumulation at the sheltered areas (Marks and Winstral, 2001)

Estimation and calculation

The amount of water stored in snow can be estimated by the depth of the snow pack and the area of the snow pack. A description of the estimation of these parameters is discussed in the next section.

vi. Snowmelt

Snowmelt is the water movement created by the water produced from melting snow. Snowmelt can be seen as a protracted process because it releases months of accumulated precipitation in a relative short time period (Seyfried et al., 2009). The water movement can be divided in (i) surface runoff and (ii) infiltration into the underlying soil or bedrock[1].

Site characteristics

According to Seyfried et al. (2009) snowmelt is strongly affected by *solar exposure*. As a consequence *aspect* influences the amount of snowmelt as well, due to differences in the amount of direct sunlight, south facing slopes (northern hemisphere) receive more direct sunlight and as a result these slopes generally have a larger amount of snowmelt compared to north facing slopes.

Infiltration of snowmelt result in wet conditions as the amount of snowmelt often is large, this can result in a reversed catena, where the wettest soils are found at the topographic higher points (Seyfried et al., 2009).

Estimation and calculation

Data on snow distribution, accumulation, snow water equivalence and runoff could be collected from available data (e.g. U.S. Snowpack Telemetry (SNOTEL) network or CZO data (Boulder Creek CZO, 2013b)), or simulations of the patterns of snow deposition, distribution and melt can be made based on modelling (for example (I)SNOBAL (Marks et al., 1999), SWETREE (Elder et al., 1995) and ALPINE3D (Lehning et al., 2006)).

vii. Sublimation

Sublimation is the process where water in its solid phase is transformed to the gaseous phase without passing through an intermediate liquid phase.

Soil properties

Which soil properties affect sublimation is unknown.

Site characteristics and

According to Hood et al. (1999) sublimation is strongly influenced by *wind speed*, *temperature*, *specific* humidity and *net radiation*. During periods with a lot of sublimation *wind speed* will dominantly influence sublimation, in periods with little sublimation, *temperature* and *net radiation* will be more important driving factors of sublimation.

Estimation and calculation

Methods to estimate sublimation are described by Hood et al. (1999).

[1] According to Seyfried et al. (2009) and others frozen soils are generally limited under deep snow cover and forested ecosystems, therefore the effects of frozen soils on runoff and infiltration does not have to be considered.

viii. Runoff

Runoff (or (Horton's) overland flow) is the horizontal flow across land surfaces when precipitation has exceeded infiltration capacity or storage capacity (soil saturation).

Soil properties and site characteristics

Overland flow is triggered on soils with low *infiltration rates*, shallow soils with a low *water storage capacity*, *saturated* soils, and soils prone to crust forming (resulting in low infiltration rates) (van Tol et al., 2011).

The amount of overland flow is highly affected by *texture*, especially by the sand and clay contents (van Tol et al., 2011). Sandy soils are more *permeable* and have a *higher hydraulic conductivity* then clayey soils, therefore runoff is occurring more often on clayey soils.

The *soil thickness* also effects the amount of runoff, as a thicker soil needs a greater volume of water to be saturated.

Furthermore runoff is, according to Van Tol et al. (2011), affected by the *steepness of the slopes*, in general a steeper slope generates larger volumes of runoff. Beside this, the amount of overland flow is influenced by *vegetation density*, due to the positive relation of vegetation to macroporosity and organic matter. As a result a higher vegetation density decreases the amount of overland flow. Beside the slope gradients Ticehurst et al. (2007) indicate two other factors which increase the probability of overland flow, (i) *exposed bedrock*, and (ii), *erosion features* (i.e. thin or no top soil horizons (A horizon), the absence of aeolian materials).

Estimation and calculation

Both Ibrahim and Cordery (1995) and Wolock and McCabe (1999) describe a very simplistic method to estimate the mean monthly runoff. This method is based on precipitation, evapotranspiration and the storage capacity of the soil. This results in the following equation (Wolock and McCabe, 1999):

$$S_i = P_i - ET_i - SMR_i$$
$$SMR_i = \min[(SM_{cap} - SM_i) or (P_i - ET_i)] \qquad \textit{[3]}$$

where S_i is the mean runoff [mm] for month i, P_i is the precipitation [mm] for month i, ET_i is the potential evapotranspiration [mm] for month i, SMR_i is the soil moisture recharge [mm] for month i, SM_i is the *soil moisture storage* [mm] for month i, and SM_{cap} is the *soil moisture storage capacity* [mm].

ix. Infiltration

Infiltration can be divided in (i) soil infiltration, and (ii) rock infiltration.

Soil infiltration is the process by which water on the ground surface enter the soil. Infiltration rate [mm h^{-1}] is a measure of the rate at which soil is able to absorb precipitation. If the precipitation rate exceeds the infiltration rate, runoff will occur. The rate of infiltration is affected by soil characteristics including *ease of entry*, *soil storage capacity*, and the *transmission rate through the soil*.

Bedrock infiltration is the process of water moving through the cracks in the bedrock or on solid bedrock within saprolite. According to Ticehurst et al. (2007) this flowpath is extremely important for recharge of lower slopes, groundwater levels and generating baseflow.

Soil properties and site characteristics

Soil infiltration

Soil infiltration is affected by *macropores* in the soil (Neary et al., 2009), which make the soil more permeable. Infiltration rates are influenced by *soil cover*, because infiltration rates reduce when the impact of raindrops has resulted in aggregate breakdown and crust forming (Neary et al., 2009). A rapid infiltration into and movement within soils is characterised by a soil with a massive *structure* and a light *texture* (Ticehurst et al., 2007).

Furthermore soil infiltration is favoured by small *topographic gradients* (Ticehurst et al., 2007).

Rock infiltration
Rock infiltration is mainly influenced by the fractured nature of the bedrock (Ticehurst et al., 2007). A more fractured nature will result in more rock infiltration, because the permeability is higher.

Estimation and calculation
If assuming that overland flow occurs when the soil is totally saturated, like is done in the previous section, than it is possible to assume that the mean monthly infiltration can be estimated based on the following equation:

$$I_i = SM_{cap} - SM_i \quad \textbf{[4]}$$

where I_i is the mean infiltration [mm] for month i, SM_i is the *soil moisture storage* [mm] for month i, and SM_{cap} is the *soil moisture storage capacity* [mm].

x. Soil storage capacity

The soil storage capacity is defined as the volume of the soil which can be saturated with water. A high storage capacity facilitates more infiltration, a greater water holding capacity and a longer residence time (van Tol et al., 2011). This results in more subsurface flow, more water contributing to the groundwater bodies, a longer duration of streamflow, and less overland flow.

Soil properties and site characteristics
Soil depth together with *porosity* determines the storage capacity of the soil (van Tol et al., 2011).

Van Tol et al. (2011) and Ticehurst et al. (2007) mention that *soil colour* (like the grey colour of gleyed soil horizons), *mottles* and *redoxomorphic features* (like iron and manganese) can indicate poor drainage conditions and periodic saturation. *Redoxomorphic features* in soils involve localities where there is deoxidation of Fe and Mn and localities where there is oxidation of Fe and Mn. Deoxidation is associated with low chroma values (grey colours) and oxidation is associated with high chroma colours (yellow, red and black colours), often in the form of mottles and concretions (van Tol et al., 2011). The presence of Fe concretions indicate a fluctuating water table, the presence of manganese coating is an indication of soils high in soil moisture (Terribile et al., 2011). Van Tol et al. (2011) and Ticehurst et al. (2007) state that an increase in *amount and size of the mottles and concretions* correlate to a longer saturation period. In general, the sequence of soil colours from red-brown-yellow-grey, resemble to an increase in degree of saturation (Ticehurst et al., 2007). Terribile et al. (2011) add to this that the *outline* of the Fe concretions gives additional information. A diffuse outline of the Fe concretions indicate a wet period and a fluctuating water table. An abrupt outline of the Fe concretions indicate a dry period and a fluctuating water table.

Estimation and calculation
Soil depth together with *porosity* determines the storage capacity of the soil (van Tol et al., 2011). Porosity (*f*)is a measure of the total void space in a porous material and is defined by:

$$f = 1 - \frac{\rho_d}{\rho_s} \quad \textbf{[5]}$$

where ρ_d is the *bulk density* [mg m^{-3}] and ρ_s is the *particle density* [mg m^{-3}], generally taken 2.65 mg m^{-3} for soils low in organic matter.
Based on the porosity the water saturation (*s*)of the soil [%] (the volume of water relative to the porosity) can be calculated:

$$s = \frac{V_w}{V_f} \quad \textbf{[6]}$$

where V_w is the *water content* [mm^3 mm^{-3}] and V_f is the *total pore volume* [mm^3 mm^{-3}]. Complete saturation is impossible, since there is always some air trapped in the pores by the water (Hillel, 1980).

xi. Macropore flow

Macropore flow is the subsurface flow through macropores, it contributes a significant amount of subsurface water to the streamflow and responds usually quick to rainfall (van Tol et al., 2011). Macropores are created by roots, soil fauna, shrinking/drying (cracks), soil aggregate development, and by subsurface erosion forming soil pipes (Neary et al., 2009).The size of the macropores, the accessibility and the continuity of the pores determine the contribution of macropore flow to the subsurface water flow (van Tol et al., 2011).

Soil properties and site characteristics
First of all macropore flow is directly influenced by *vegetation* (resulting in roots), *biological activity*, and the occurence of *slickensides*, as these factors are responsible for the creation of macropores (Neary et al., 2009; Terribile et al., 2011).
The continuity of macropores is influenced by *soil moisture*, an increase of *soil moisture* results in an increase of the continuity (Nieber et al., 2000). On the contrary the influence of macropore flow is lower in soils with a high *soil porosity*, because of the storage potential of the soil (Uchida et al., 2006). According to van Tol et al. (2011) topsoil horizons high in *organic matter* have a positive influence on the macropore flow, as organic matter increases the macroporosity.

Estimation and calculation
How macropore flow can be estimated or calculated is unknown.

xii. Subsurface flow

Subsurface flow can be divided in (i) subsurface flow at the A/B interface, and (ii) subsurface flow at the soil/bedrock interface.
Due to differences in structures, densities, and hydraulic conductivities vertical flow is hindered and water will tend to move laterally at the A/B interface or soil/bedrock interface if the upper layer is more permeable than the lower layer (van Tol et al., 2011).

Soil properties and site characteristics
Subsurface flow is characterised by differences in *hydraulic conductivity*. Soil horizons or bedrock with low hydraulic conductivity under soil horizons with a higher hydraulic conductivity are indicators of subsurface flow (Neary et al., 2009). According to Van Tol et al. (2011) the amount of water moving laterally is furthermore influenced by *soil and horizon depth*, the *permeability* and differentiation between the horizons (i.e. differences in *structure*, and *density*).
The *eluviation* (leaching) and *illuviation* (accumulation) of soil materials (i.e. fine materials like silt and clay, minerals, etc.) can be an indication of the presence of subsurface flow (van Tol et al., 2011).

Beside this the variation in *subsoil* and *bedrock topography* (or *subsurface topography*) at small scales has proven to be important for subsurface flow. This variation can cause zones of subsurface accumulation, which results in faster saturation and initiate macropore flow (Neary et al., 2009). Furthermore subsurface flow is only possible when *slope* is favouring lateral movement down the slope (van Tol et al., 2011).

Estimation and calculation
Water flow in soils can be described based on a combination of Darcy's law and the Richards' (1931) partial differential equation for water flow in saturated soils:

$$\frac{\partial \theta}{\partial t} = \frac{\partial}{\partial x}\left[K(h)\left(\frac{\partial h}{\partial z} - 1 \right) \right] \qquad \textbf{[7]}$$

where h is the soil water pressure head [hPa], θ is the volumetric water content [m^3 m^{-3}], K is the hydraulic conductivity [m s^{-1}], t is time [s], and z is soil depth [m].

Appendix F.

Discharge

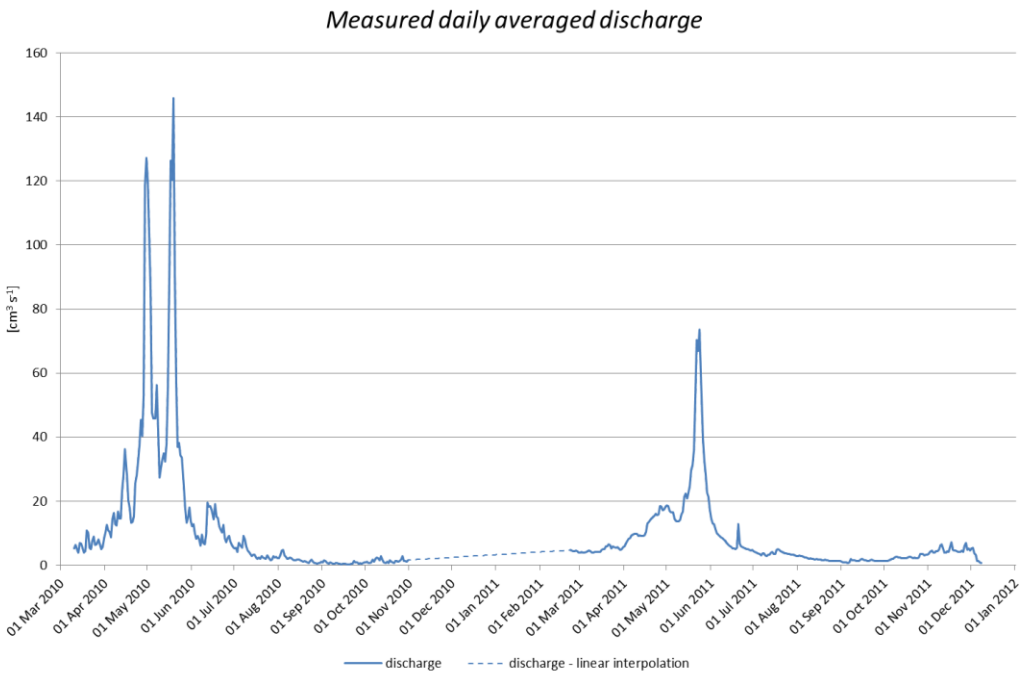

Figure F1: Daily averaged discharge data [$cm^3 s^{-1}$].

References X.

Allen, R. G., Pereira, L. S. and Raes, D. 1998. Crop evapotranspiration : guidelines for computing crop water requirements. Rome, FAO.

Boulder Creek CZO. 2013a. Discharge for Lower Gordon Gulch [Online]. Available: http://czo.colorado.edu/query/disLowerGG.shtml [Accessed February 2013].

Boulder Creek CZO. 2013b. Hydrology [Online]. Available: http://czo.colorado.edu/html/data-hydrology.shtml [Accessed February 2013].

Elder, K., Michaelsen, J. and Dozier, J. 1995. Small basin modeling of snow water equivalence using binary regression tree methods. IAHS Publications-Series of Proceedings and Reports-Intern Assoc Hydrological Sciences, 228, 129-140.

Erickson, T. A., Williams, M. W. and Winstral, A. 2005. Persistence of topographic controls on the spatial distribution of snow in rugged mountain terrain, Colorado, United States. Water Resources Research, 41, 1-17.

Farinotti, D., Magnusson, J., Huss, M. and Bauder, A. 2010. Snow accumulation distribution inferred from time-lapse photography and simple modelling. Hydrological Processes, 24, 2087-2097.

Hillel, D. 1980. Applications of soil physics. New York, Academic Press.

Hinckley, E. S., Ebel, B. A., Barnes, R. T., Anderson, R. S., Williams, M. W. and Anderson, S. P. 2012. Aspect control of water movement on hillslopes near the rain–snow transition of the Colorado Front Range. Hydrological Processes.

Hood, E., Williams, M. and Cline, D. 1999. Sublimation from a seasonal snowpack at a continental, mid-latitude alpine site. Hydrological Processes, 13, 1781-1797.

Ibrahim, A. B. and Cordery, I. 1995. Estimation of recharge and runoff volumes from ungauged catchments in eastern Australia. Hydrological sciences journal, 40, 499-515.

Lehning, M., Völksch, I., Gustafsson, D., Nguyen, T. A., Stähli, M. and Zappa, M. 2006. ALPINE3D: a detailed model of mountain surface processes and its application to snow hydrology. Hydrological Processes, 20, 2111-2128.

Marks, D., Domingo, J., Susong, D., Link, T. and Garen, D. 1999. A spatially distributed energy balance snowmelt model for application in mountain basins. Hydrological Processes, 13, 1935-1959.

Marks, D. and Winstral, A. 2001. Comparison of Snow Deposition, the Snow Cover Energy Balance, and Snowmelt at Two Sites in a Semiarid Mountain Basin. Journal of Hydrometeorology, 2, 213-227.

Neary, D. G., Ice, G. G. and Jackson, C. R. 2009. Linkages between forest soils and water quality and quantity. Forest Ecology and Management, 258, 2269-2281.

Nieber, J. L., Bauters, T. W. J., Steenhuis, T. S. and Parlange, J.-Y. 2000. Numerical simulation of experimental gravity-driven unstable flow in water repellent sand. Journal of Hydrology, 231-232, 295-307.

Seyfried, M., Grant, L., Marks, D., Winstral, A. and McNamara, J. 2009. Simulated soil water storage effects on streamflow generation in a mountainous snowmelt environment, Idaho, USA. Hydrological Processes, 23, 858-873.

Terribile, F., Coppola, A., Langella, G., Martina, M. and Basile, A. 2011. Potential and limitations of using soil mapping information to understand landscape hydrology. Hydrology and Earth System Sciences, 15, 3895-3933.

Ticehurst, J. L., Cresswell, H. P., McKenzie, N. J. and Glover, M. R. 2007. Interpreting soil and topographic properties to conceptualise hillslope hydrology. Geoderma, 137, 279-292.

Uchida, T., McDonnell, J. J. and Asano, Y. 2006. Functional intercomparison of hillslope and small catchments by examining water source, flowpath and mean residence time. Journal of Hydrology, 327, 627-642.

van Tol, J., Le Roux, P. and Hensley, M. 2011. Chapter 12. Soil indicators of hillslope hydrology. In: Özkaraova Güngör, E. B. (ed.) Principles, application and assessment in soil science. Rijeka, Croatia: InTech.

Winstral, A., Elder, K. and Davis, R. E. 2002. Spatial snow modeling of wind-redistributed snow using terrain-based parameters. Journal of Hydrometeorology, 3, 524-538.

Wolock, D. M. and McCabe, G. J. 1999. Explaining spatial variability in mean annual runoff in the conterminous United States. Climate Research, 11, 149-159.